Z_N symmetry and confinement-deconfinement transition in $SU(N)$+Higgs theory

By

Minati Biswal

PHYS10201204004

The Institute of Mathematical Sciences, Chennai

A thesis submitted to the

Board of Studies in Physical Sciences

In partial fulfillment of requirements

For the Degree of

DOCTOR OF PHILOSOPHY

of

HOMI BHABHA NATIONAL INSTITUTE

January, 2018

Homi Bhabha National Institute

Recommendations of the Viva Voce Board

As members of the Viva Voce Board, we certify that we have read the dissertation prepared by *Minati Biswal* entitled "Z_N *symmetry and confinement-deconfinement transition in* $SU(N)$*+Higgs theory*" and recommend that it maybe accepted as fulfilling the dissertation requirement for the Degree of Doctor of Philosophy.

D. Indumathi — Date: 19.9.18

Prof. Indumathi D (Chair)

Sanatan Digal — Date: 19.9.18

Prof. Sanatan Digal (Guide/Convener)

Date: 19/9/18

Prof. Rajesh Ravindran

Date: 19/9/18

Prof. Shrihari Gopalakrishna

S.R. Hassan — Date: 19/9/18

Prof. Syed R. Hassan

Saumen Datta — Date: 19/9/2018

External Examiner (SAUMEN DATTA)

Final approval and acceptance of this dissertation is contingent upon the candidate's submission of the final copies of the dissertation to HBNI.

I hereby certify that I have read this dissertation prepared under my direction and recommend that it may be accepted as fulfilling the dissertation requirement.

Date: 19.9.18

Place: Chennai

Sanatan Digal

Guide

STATEMENT BY AUTHOR

This dissertation has been submitted in partial fulfillment of requirements for an advanced degree at Homi Bhabha National Institute (HBNI) and is deposited in the Library to be made available to borrowers under rules of the HBNI.

Brief quotations from this dissertation are allowable without special permission, provided that accurate acknowledgment of source is made. Requests for permission for extended quotation from or reproduction of this manuscript whole or in part may be granted by the Competent Authority of HBNI when in his or her judgment the proposed use of the material is in the interests of scholarship. In all other instances, however, permission must be obtained from the author.

Minati Biswal

Minati Biswal

DECLARATION

I, hereby declare that the investigation presented in the thesis has been carried out by me. The work is original and has not been submitted earlier as a whole or in part for a degree / diploma at this or any other Institution / University.

Minati Biswal

Minati Biswal

Dedicated to

My parents and my teachers

ACKNOWLEDGMENTS

First of all, I would like to express gratitude to my supervisor Prof. Sanatan Digal for his continuous support and encouragement throughout the years. It's been a great opportunity to work with him and learn physics. I am very thankful to my first year course work teachers, Prof. Rajesh, Prof. Nemani, Prof. Anishetty, Prof. Murty, Prof. Shrihari, and Prof. Sinha. I would also like to thank my DC members Prof. Indumati, Prof. Rajesh, Prof. Shrihari and Prof. Hassan for their encouragement throughout the years. I have greatly benefitted from interactions with Prof. Satyavani Vemparala. I would also like to thank Prof. Ajit M. Srivastava of Institute of Physics for very insightful physics discussions.

I have greatly benefitted from working with Dr. Deka. I am very thankful to him for teaching me lattice QCD numerical techniques. It was fun working with Dr. Saumia, and I am thankful for her cooperative behavior and encouragement during the years. It was helpful for me learning physics from my friends Rusa, Atanu, Pavan, Rajesh, Renjan and Prosenjit during the course work days. I am thankful to my friends Jilmy and Anvy for being there. I am also grateful to Tanmay and Rekha, they have been terrific friends and always available for me whenever I needed to talk. I wish to thank Mr. Mangalapandi for helping me out in the cluster related issues. I would like to thank G. Srinivasan and M. Hussain for helping me in the system related issues and mainly they were anytime ready to help me. It was pleasant being with Ranjana and Dipu bhai on weekends. I am indebted to them for inviting me for delicious foods. Ranjana was always being there for me and listening to me. She has helped me a lot in many ways building my confidence. I am lucky to be child of my parents. Without the support of my family members my father, mother, peisi, sisters, brother-in-laws and brothers nothing could have been possible. Today whoever I am its a result of my brother Debakanta's constant encouragement and supportive nature.

List of publications (included in this thesis)

1. **"Dynamical Restoration of Z_N Symmetry in $SU(N)$+Higgs Theories"**
   Minati Biswal, Sanatan Digal and P. S. Saumia
   Nucl. Phys. B **910**, 30 (2016)
   arXiv:1511.08295 [hep-lat]

2. **"Confinement-deconfinement transition in an $SU(2)$ Higgs theory"**
   Minati Biswal,Mridupawan Deka, Sanatan Digal and P. S. Saumia
   Phys. Rev. D **96**, 014503 (2017)
   arXiv:1610.08265 [hep-lat]

List of publications (not included in this thesis)

1 **"Free energy of a baryon at finite temperatures and its implications to the heavy-ion collisions"**
   Minati Biswal, Sanatan Digal and P. S. Saumia
   Mod. Phys. Lett. A **30**, 1550130 (2015)
   10.1142/S0217732315501308

Sign: Minati Biswal
MINATI BISWAL

Seminars/Posters presented

1. **"Baryons in heavy ion collisions"**, poster presented at "7^{th} International Conference On Physics And Astrophysics Of Quark Gluon Plasma ", VECC Kolkata, India held during 1st to 6th February 2015.

2. **"Dynamical restoration of Z_N symmetry in $SU(N)$+Higgs theory"**, talk was given at "CNT QGP Meet 2015", VECC Kolkata, India held during 16th to 20th November 2015.

3. **"Dynamical restoration of Z_N symmetry in $SU(N)$+Higgs theory"**, talk was given at "Institute of Physics" Bhubaneswar, India on 8th August 2016.

4. **"Z_N symmetry and Confinement-Deconfinement transition in $SU(N)$+Higgs theory"**, talk was given at "Theory Divison, PRL" Ahmedabad, India on 22nd June 2017.

5. **"Z_N symmetry and confinement-deconfinement transition in $SU(N)$+Higgs theory"**, poster presented at "Helmholtz International Summer School on Hadron Structure,Hadronic Matter, Lattice QCD" BLPT, Joint Institute for Nuclear Research, Dubna, Russia held during 20th August to 2nd September 2017.

Conferences and workshops attended

1. **School on Quantum Field Theories on Lattice** held at SINP Kolkata, India from 2nd – 6th December 2013.

2. **International Workshop on Frontiers of QCD** held at IIT Bombay, Powai, Mumbai, India from 2nd – 5th December 2014.

3. **XXIX SERC Main School-2014 on Theoretical High Energy Physics** held at BITS Pilani, K K Birla Goa Campus, India from 20th December 2014 to 8th January 2015.

ABSTRACT

In this thesis, we study the Z_N symmetry and confinement-deconfinement (CD) transition in SU(N) Higgs theory. In the absence of the Higgs field, the Euclidean action is invariant under the Z_N gauge transformation. This symmetry is spontaneously broken in the deconfinement phase as the Polyakov loop acquires non-zero thermal average value. This gives rise to N degenerate states in the deconfinement phase. In the presence of matter fields, the Euclidean action is not invariant under the Z_N symmetry. This explicit symmetry breaking affects the CD transition. We carry out non-perturbative simulations of this theory to understand how the strength of the explicit symmetry breaking depends on the parameters of the theory.

Our results show that in the Higgs phase, where the Higgs condensate is non zero, the Z_N symmetry is explicitly broken. In the Higgs symmetric phase where the Higgs condensate is expected to vanish, the strength of the Z_N symmetry breaking depends on the lattice cut-off, i.e. the number of points along the temporal direction (N_τ) of the Euclidean lattice. For vanishing bare Higgs mass and Higgs quartic coupling, the $N = 2$ CD transition is found to be a crossover with finite explicit symmetry breaking for $N_\tau = 4$. For the same bare parameters, this transition turns out to be second order, accompanied by the realization of the Z_2 symmetry for $N_\tau = 8$. We observe that for $N_\tau = 4$, the Z_N symmetry is restored in parts of the Higgs symmetric phase. In the $\lambda - \kappa$ plane (λ Higgs quartic coupling, κ the gauge-Higgs interaction strength), the Z_N symmetry is restored for $\kappa > \kappa(\lambda)$. This $\kappa(\lambda)$ line moves closer to the Higgs transition line with the increase in the number of temporal lattice points (N_τ). For $N_\tau = 8$ this line coincides with the Higgs transition line. Since for $N_\tau = 8$ with vanishing bare Higgs mass and Higgs quartic coupling the Z_2 symmetry is realized, it will also be the case for all non-zero values of

the bare Higgs mass. In contrast, in QCD, where the explicit symmetry breaking grows stronger with the decrease in the quark mass.

Contents

1 Introduction **1**

2 Z_N symmetry in SU(N) gauge theories **9**

2.1 Partition function for pure SU(N) gauge theory 9

2.2 Partition function in the presence of fundamental matter fields 15

2.3 Z_N symmetry in pure SU(N) gauge theory 18

2.4 Z_N symmetry in the presence of fundamental matter fields 20

3 Polyakov loop effective potential calculations **23**

3.1 Effective potential for pure SU(N) gauge theory 23

3.2 Effective potential for SU(2)+Higgs theory 30

4 Strong coupling methods **35**

4.1 Discretization of continuum SU(N)+Higgs action on the lattice 36

4.2 Strong coupling expansion in SU(2)+Higgs theory 40

5 Numerical Methods **47**

5.1 Monte carlo techniques 48

5.2 Heat bath algorithm 50

5.3 Pseudo-heat bath algorithm 53

6 Dynamical symmetry restoration in SU(N)+Higgs theory: Simulations - I 59

6.1 Lattice action and parameters 59

6.2 Sketch of Higgs phase diagram 60

6.3 Numerical simulations: Explicit breaking of Z_N symmetry 62

6.4 Numerical simulations: Realization of Z_N symmetry 64

6.5 Phase diagram related to Z_N symmetry for $N_\tau = 4$ 71

7 N_τ dependence of Z_N symmetry and CD transition: Simulations-II . . . 73

7.1 The CD transition for $N_\tau = 2$ and 4 75

7.2 The CD transition for $N_\tau = 8$ 79

7.3 N_τ dependence of explicit Z_2 breaking 82

7.4 Interaction between gauge and Higgs field 84

7.5 Phase diagram of Z_2 breaking for higher N_τ 86

8 Discussions and Conclusions 87

Synopsis

At very high temperature, around ~150MeV, hadrons melt to form the quark-gluon plasma (QGP). Such extreme thermal conditions existed in the early Universe and currently are being created in heavy-ion collision experiments. Theoretical studies using quantum chromodynamics (QCD) show that the melting of hadrons to QGP proceeds via the confinement-deconfinement (C-D) transition. The nature of this transition depends on the presence of fermionic matter fields, i.e Quarks. Interestingly this transition occurs in all $SU(N)(N > 2)$ gauge theories like QCD, for example in the Electroweak theory. As in QCD, presence of bosonic matter fields also affects the nature of C-D transition. Therefore, it is important to study in detail the effect of bosonic and fermionic matter fields on this transition.

The C-D transition is studied by writing the partition function of the theory in the path integral form. At finite temperatures, the pure gauge sector of these theries have the Z_N symmetry [1, 2]. This can be argued as follows: since the excitations of the gauge fields(gluons) are bosonic, the gauge fields in the Euclidean space must be periodic along the temporal direction. This boundary condition allows for gauge transformations to be periodic in the temporal direction upto a factor z, where $z \in Z_N$ and $Z_N \subset SU(N)$. All possible gauge transformations therefore can be classified by the Z_N group. Since the action remains invariant, the Z_N group is a symmetry group of the pure gauge part. In such a gauge transformation, the Polyakov loop (L) (which is the trace of path order product

of links in the temporal direction) transforms like a Z_N spin under the Z_N transformation, i.e $L \rightarrow zL$. When only gauge fields are considered, the Z_N symmetry is spontaneously broken at high temperatures in the deconfinement phase where $\langle L \rangle \neq 0$. It is restored below the C-D transition temperature (T_d) in the confinement phase where $\langle L \rangle = 0$ [3,4]. Because of this unique property the Polyakov loop serves as an order parameter for the C-D phase transition. Bosonic (Fermionic) statistics requires that the bosonic (fermionic) fields of the above theories are periodic (antiperiodic) in the temporal direction. Since the matter fields are in the fundamental representation, the Z_N gauge transformed matter fields do not have periodic boundary conditions anymore. Therefore the gauge transformations corresponding to $z \neq I$ (where I is the identity element of Z_N) cannot act on the matter fields. Only the periodic gauge transformations ($z = I$) act on both the gauge and matter fields, hence keep the total action invariant. Though the $z \neq I$ gauge transformation cannot act on the matter fields, one can consider them acting only on the gauge fields. In such cases the action will not remain invariant. So, at the classical level, the Z_N symmetry is explicitly broken in the presence of matter fields. This situation is similar to introducing an external field in spin systems [5]. The effect of matter fields is equivalent to having an external ordering field for the Polyakov loop. The actual effect of the matter fields on the Z_N symmetry can only be known when fluctuations, perturbative and/or non-perturbative in nature, are considered. Previous perturbative calculations upto 1-loop have shown that the Z_N symmetry is explicitly broken when matter fields are coupled to the pure gauge theory [6,7]. The 1-loop effective potential for the Polyakov loop also shows that, there are meta-stable states corresponding to the local minima with negative entropy [7]. In these calculations only the zeroth mode of the temporal gauge field is coupled to the matter fields. Furthermore these studies are limited to very high temperatures where the coupling and fluctuations are small. It is important that the effect of fluctuations on the Z_N symmetry be considered near the C-D transition region. Effects of matter fields on the Z_N symmetry are expected to be large near the transition region and are likely to affect the nature of the C-D transition [8,9]. So in this study, we compute the effect of the

fundamental Higgs field on the Z_N symmetry for $N = 2$ and 3 [10]. We focus on the properties of the Polyakov loop and other observables to study the Z_N symmetry.

For the simulation study, the continuum action is discretized on a four-dimensional $N_\tau \times N_s^3$ Euclidean lattice. In the simulation process, the Higgs field Φ_n and the gauge link $U_{n,\mu}$ are repeatedly updated to generate the Monte Carlo history. The field variable Φ_n is updated using pseudo heat-bath algorithm [11, 12] and $U_{n,\mu}$ is updated using the standard heat-bath algorithm [13]. In the update method, the new configuration is generated from the old one using the Boltzmann factor (e^{-S}) and taking care of the principle of detailed balance. Since the new configuration is generated from the old one, there will be auto-correlation between the consecutive configurations. To reduce this auto-correlation, we use the over-relaxation method [14].

The distributions of the Polyakov loop show that the Z_N symmetry is explicitly broken in the Higgs broken phase ($\langle\Phi\rangle \neq 0$) for large κ. For small enough explicit symmetry breaking, there exist meta-stable states 1(a). The explicit symmetry breaking decreases with κ . For small κ the symmetry is restored which leads to symmetric distribution of the Polyakov loop 1(b).

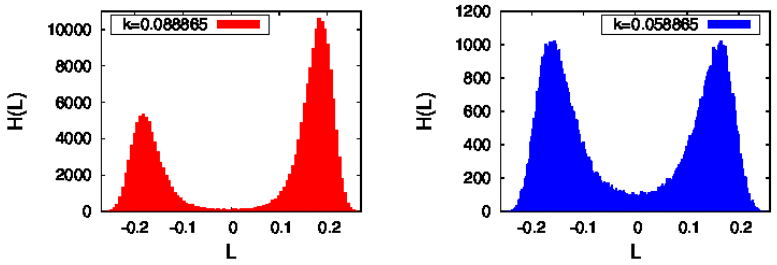

Figure 1. The histogram of the Polyakov loop ($H(L)$) *vs* Polyakov loop(L) in Higgs symmetric phase for (a)far from Higgs transition line and (b)near Higgs transition line.

For $N = 2$, the restoration of the Z_N symmetry gives rise to critical behavior which is shown by computing the Binder cumulant of the Polyakov loop and its finite size scaling. The Binder cumulant scales with volume and its value at the crossing point for different volumes is consistent with the 3D-Ising universality class. We believe the

restoration of the Z_N symmetry is driving the critical behavior of the C-D transition. Previously it was thought that the symmetry is restored only when the mass of the matter field is infinitely heavy [15]. Previous studies have found that the Polyakov loop has large cutoff effects [6]. It is possible that the region in the Higgs symmetric phase where the Z_N symmetry is restored may depened on number of temporal lattice site (N_τ). Therefore, we study the Z_N symmetry and the behavior of C-D transition in $SU(2)$ Higgs theory for different N_τ. To simplify this study, we consider the bare mass and bare Higgs quartic coupling to be zero [16]. We find that the C-D transition is a cross-over for $N_\tau = 2, 4$. In the following, figure: 2(a) shows that the C-D transition is a cross-over for $N_\tau = 2$. For $N_\tau = 8$, in figure: 2(b) the average of the Polyakov loop shows spatial volume dependence and it scales with volume like the magnetization in 3D-Ising modelindicating a critical behavior. Similarly the susceptibility, Binder cumulant of the Polyakov loop and their scalings show a critical behavior belonging to 3D-Ising universality class. We believe that in this case the restoration of the Z_N symmetry gives rise to the critical behavior of the C-D transition.

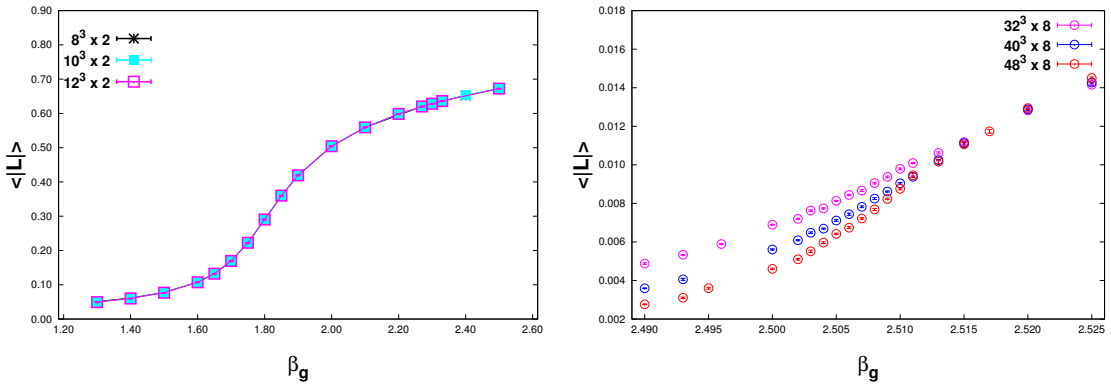

Figure 2. The Polyakov loop average ($\langle|L|\rangle$) vs gauge coupling (β_g) for (a) $N_\tau = 2$, and (b) $N_\tau = 8$.

Further we compute the average of the gauge and Higgs field interaction for different N_τ. As interaction increases with increase in N_τ, it is clear that the symmetry restoration is not due to decoupling of the gauge and Higgs fields for large N_τ. We argue

that the increase in phase space with N_τ is responsible for the Z_N symmetry restoration. These results contradict 1-loop perturbative prediction and suggest that calculations beyond 1-loop perturbation theory are necessary. Our results for $N_\tau = 8$ suggest that the Z_N symmetry is restored in all of the Higgs symmetric phase ($\langle \Phi \rangle = 0$).

Bibliography

[1] B. Svetitsky, Phys. Rept. **132**, 1 (1986).

[2] B. Svetitsky and L. G. Yaffe, Nucl. Phys. B **210**, 423 (1982).

[3] J. Kuti, J. Polonyi and K. Szlachanyi, Phys. Lett. B **98**, 199 (1981).

[4] L. D. McLerran and B. Svetitsky, Phys. Lett. B **98**, 195 (1981).

[5] F. Karsch, C. Schmidt and S. Stickan, Comput. Phys. Commun. **147**, 451 (2002)

[6] N. Weiss, Phys. Rev. D **25**, 2667 (1982).

[7] V. Dixit and M. C. Ogilvie, Phys. Lett. B **269**, 353 (1991).

[8] V. M. Belyaev, I. I. Kogan, G. W. Semenoff and N. Weiss, Phys. Lett. B **277**, 331 (1992).

[9] F. Karsch, E. Laermann, A. Peikert, C. Schmidt and S. Stickan, Nucl. Phys. Proc. Suppl. **94**, 411 (2001)

[10] F. Karsch, E. Laermann and C. Schmidt, Phys. Lett. B **520**, 41 (2001)

[11] M. Biswal, S. Digal and P. S. Saumia, Nucl. Phys. B **910**, 30 (2016)

[12] M. Creutz, Phys. Rev. D **21**, 2308 (1980).

[13] N. Cabibbo and E. Marinari, Phys. Lett. B **119**, 387 (1982).

[14] B. Bunk, Nucl. Phys. Proc. Suppl. **42**, 566 (1995).

[15] C. Whitmer, Phys. Rev. D **29**, 306 (1984).

[16] F. Green and F. Karsch, Nucl. Phys. B **238**, 297 (1984).

[17] M. Biswal, M. Deka, S. Digal and P. S. Saumia, Phys. Rev. D **96**, 014503 (2017).

List of Figures

1 The histogram of the Polyakov loop ($H(L)$) *vs* Polyakov loop(L) in Higgs symmetric phase for (a)far from Higgs transition line and (b)near Higgs transition line. xxi

2 The Polyakov loop average ($\langle|L|\rangle$) vs gauge coupling (β_g) for (a) $N_\tau = 2$, and (b) $N_\tau = 8$. xxii

1.1 Energy density curve in QCD showing phase transition [21]. 2

1.2 Sketch of (a) Polyakov loop average (L) vs. T for pure SU(2) gauge theory, (b) Magnetization (average of spins) vs. T for $Z(2)$ Ising model . . 3

3.1 $\frac{6\beta^4 V_{eff}}{\pi^2}$ vs $\frac{\beta C}{2\pi}$ is plotted for SU(2). 29

3.2 $\frac{6\beta^4 V_h}{\pi^2}$ vs $\frac{\beta C}{2\pi}$ is plotted for SU(2)+Higgs when $m_H = 0$. 33

4.1 Sketch of an elementary plaquette U_P 37

4.2 Polyakov loop plotted as a function of β_g for $N_\tau = 2$ and $h = 0$. 44

4.3 Polyakov loop plotted as a function of β_g for $N_\tau = 2$ and $h = 0.0225$. . . . 45

4.4 Polyakov loop plotted as a function of β_g for $N_\tau = 2$ and $h = 0.1$. 45

5.1 Monte Carlo history of the Polyakov loop for $16^3 \times 4$ lattice with $\lambda = 0.005$, $\kappa = 0.058865$ and $\beta_g = 2.35$ in SU(2)+Higgs theory. 56

5.2 Monte Carlo history of $\sum_n \Phi_n^\dagger \Phi_n$ for $16^3 \times 4$ lattice with $\lambda = 0.005$, $\kappa = 0.058865$ and $\beta_g = 2.35$ in SU(2)+Higgs theory. 57

5.3 Monte Carlo history of $\sum_n \Phi_{n+\mu}^\dagger U_{n,\mu} \Phi_n$ for $16^3 \times 4$ lattice with $\lambda = 0.005$, $\kappa = 0.058865$ and $\beta_g = 2.35$ in SU(2)+Higgs theory. 58

6.1 Theoretical expectations of explicit symmetry breaking on $(\lambda - \kappa)$ plane for SU(2) Higgs theory. 61

6.2 Distribution of Polyakov loop for SU(2), $16^3 \times 4$ lattice with $\kappa = 0.088865$, $\lambda = 0.005$ and $\beta_g = 2.31$ 62

6.3 Distribution of Polyakov loop for SU(3), $8^3 \times 4$ lattice with $\kappa = 0.29$, $\lambda = 0.1$ and $\beta_g = 2.50$ 63

6.4 Histogram of Polyakov loop in the confinement phase for SU(2), $32^3 \times 4$ lattice with $\kappa = 0.058865$, $\lambda = 0.005$ and $\beta_g = 2.26$ 64

6.5 Distribution of Polyakov loop for SU(2), $16^3 \times 4$ lattice with with $\kappa = 0.058865$, $\lambda = 0.005$ and $\beta_g = 2.31$ 65

6.6 Distribution of Polyakov loop for SU(3), $8^3 \times 4$ lattice with with $\kappa = 0.05$, $\lambda = 0.1$ and $\beta_g = 1.90$ 66

6.7 Histogram of the +ve and rotated −ve Polyakov loop with $\kappa = 0.058865$, $\lambda = 0.005$ for SU(2)+Higgs. 67

6.8 Average of gauge action for the +ve and −ve Polyakov loop with $\kappa = 0.058865$, $\lambda = 0.005$ for SU(2)+Higgs 68

6.9 (a) Binder cumulant around transition point for different N_s (b) scaling of the Binder cumulant with $t = (\frac{\beta_g - \beta_{gc}}{\beta_{gc}})$, when $\kappa = 0.058865$, $\lambda = 0.005$ for SU(2)+Higgs respectively. 69

6.10 Higgs phase diagram showing Z_N symmetry for $16^3 \times 4$ lattice with $\beta_g = 2.30$ for SU(2)+Higgs theory. 71

7.1 The Polyakov loop average vs β_g for $N_\tau = 2$ 75

7.2 The Susceptibility vs β_g for $N_\tau = 2$ 75

7.3 U_L vs β_g for different volumes for $N_\tau = 2$ 76

7.4 The Polyakov loop average vs β_g for $N_\tau = 4$ 76

7.5 The Susceptibility vs β_g for $N_\tau = 4$ 77

7.6 U_L vs β_g for different volumes for $N_\tau = 4$ 78

7.7 $N_\tau = 8$. (a) The Polyakov loop vs β_g for different volumes, and (b) Scaled Polyakov loop vs β_g for different volumes. 79

7.8 $N_\tau = 8$. (a) Susceptibility vs β_g for different volumes, and (b) Scaled Susceptibility vs β_g for different volumes. 80

7.9 $N_\tau = 8$. (a) The Binder cumulant U_L vs β_g for different volumes, and (b) Scaled U_L vs β_g for different volumes. 80

7.10 $N_\tau = 8$. (a) The values of χ^c_{max} as a function of L for $L = 32, 40$ and 48. The slope of fitted line provides the value of γ/ν. (b) The values of U_c^{eff} obtained from the crossing points of Binder cumulant between two different volumes as a function of ϵ'. The intercept provides the value of U_c. 81

7.11 $H(L)$ vs $|L|$. $H(L)$ is normalized to 2. (a) $16^3 \times 2$ lattice with $\beta_g = 2.2$, (b) $32^3 \times 4$ lattice with $\beta_g = 2.35$, (c) $24^3 \times 6$ lattice with $\beta_g = 2.50$, and (d) $32^3 \times 8$ lattice with $\beta_g = 3.20$ 82

7.12 Monte Carlo history of $\sum_n \Phi^\dagger_{n+\mu} U_{n,\mu} \Phi_n$ for $32^3 \times 8$ lattice with $\lambda = 0$, $\kappa = 0.125$ and $\beta_g = 2.508$ in SU(2)+Higgs theory. 84

7.13 The avg. of $Ka^4 = \frac{1}{8} \sum_{\mu,\nu} \mathrm{Re}(\Phi^\dagger_{n+\mu} U_{n,\mu} \Phi_n)$ for different N_τ near transition point. 85

7.14 Higgs phase diagram showing Z_N symmetry restoration in all over the region of Higgs symmetric phase for $N_\tau = 8$ with $\beta_g = 2.30$ for SU(2)+Higgs theory. 86

8.1 Higgs phase diagram showing Higgs condensate acts like an external symmetry breaking field. 92

1 Introduction

SU(N) gauge theories have been successful in describing the fundamental interactions of nature. The gauge theory of quarks and gluons, (quantum chromodynamics (QCD)) describes the strong interactions of hadrons. When a hadron gas is heated to high temperatures or compressed to high densities, quarks and gluons get deconfined and form the quark-gluon plasma (QGP) [17–20]. The transition to QGP happens around 150 – 170 MeV and proceeds via the confinement-deconfinement (CD) transition. For infinitely heavy quarks, the Z_N symmetry of the gauge theory plays important role in the CD transition. On the other hand in the chiral limit, when the quarks are massless, the CD transition is dominated by the spontaneous breaking of the chiral symmetry. The Polyakov loop in this limit does show behaviour similar to the chiral condensate. Here we will restrict our study mostly to the behaviour of the Polyakov loop. The transition to QGP at finite T and $\mu = 0$ is a crossover. With increase in μ, the transition becomes second order at some critical value ($\mu = \mu_c$) and first order for larger μ values. Fig. 1.1 shows energy density in QCD rises rapidly. This is a signature of CD phase transition around the critical temperature (T_c) [21]. The nature of this transition depends on the presence of fermionic matter fields, i.e. quarks [22–31]. Interestingly this CD transition occurs in all SU(N > 2) gauge theories like QCD, for example in the Electroweak (EW) theory. As in QCD, the presence of bosonic matter fields in fundamental representation also affects the nature of the CD transition. Therefore, it is important to study in detail the effect of bosonic and fermionic matter fields on this transition. Even without the matter fields, pure SU(N) gauge theories undergo the CD transition. For $N = 2$ this transition is second order [3, 4] and for $N \geq 3$

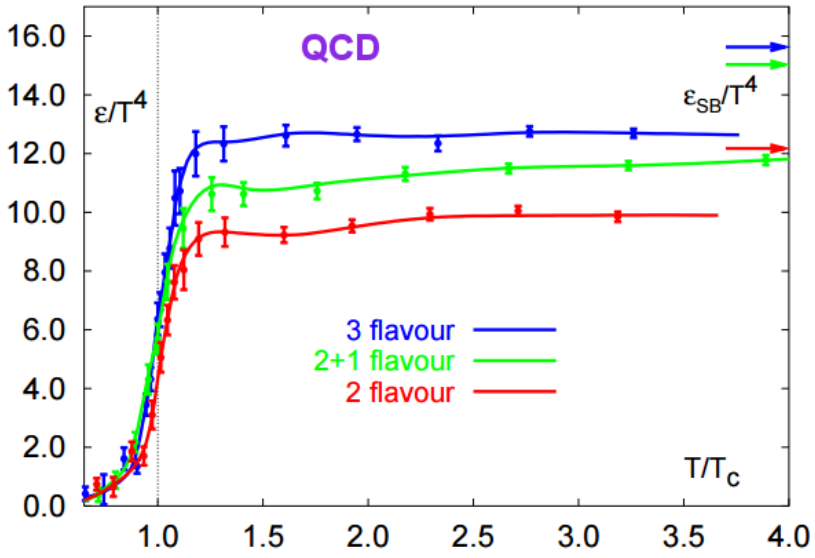

Figure 1.1. Energy density curve in QCD showing phase transition [21].

first order [32–34]. In pure SU(N) gauge theory, the phase transition is described by the Polyakov loop [2],

$$P(\mathbf{x}) = \frac{1}{N}\mathrm{Tr\ P}\exp\left[\int_0^\beta d\tau\ (igA_0(\mathbf{x},\tau))\right]. \tag{1.0.1}$$

Here $\beta = \frac{1}{T}$, T is the temperature. $A_0(\mathbf{x},\tau)$ is a traceless $N \times N$ matrix, temporal gauge field configuration in the Euclidean space. The thermal and volume average of $P(\mathbf{x})$ in eqn (1.0.1), is found to behave like magnetization in ferromagnetic Z_N spins with ferromagnetic nearest neighbor interactions [34–36],

$$L = \langle P(\mathbf{x})\rangle \tag{1.0.2}$$

Where L is the thermal and volume average of the Polyakov loop. L is non-zero above the critical temperature while the magnetization of Z_N spins is non-zero below the critical temperature. A sketch of the temperature dependence of L for pure SU(2) gauge theory and magnetization for Z_2 spin system are shown in the Fig. 1.2. The order of pure SU(N) transition is found to be same as the magnetization transition of ferromagnetic Z_N-spins. For SU(N), the deconfined phase is characterized by N degenerate states, associated with the spontaneous breaking of the Z_N symmetry. The Z_N symmetry arises from the invari-

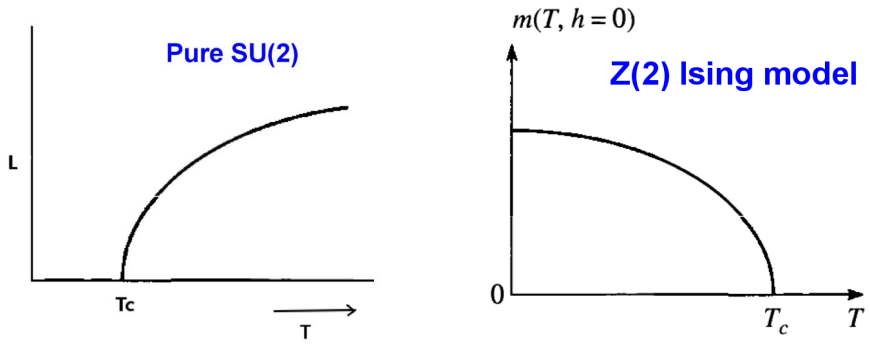

Figure 1.2. Sketch of (a) Polyakov loop average (L) vs. T for pure SU(2) gauge theory, (b) Magnetization (average of spins) vs. T for $Z(2)$ Ising model

ance of the Euclidean gauge action under gauge transformations which are periodic to an element $z \in Z_N$, where Z_N is the center of SU(N). In such a gauge transformation, the Polyakov loop (L) transforms like a Z_N spin under the Z_N transformation, i.e $L \rightarrow zL$. Since $L = 0$ in the confinement phase and $L \neq 0$ in the deconfinement phase, it serves as the order parameter for the CD transition.

The presence of bosonic and fermionic matter fields spoil the Z_N symmetry of the action. Bosonic (Fermionic) statistics requires that the bosonic (fermionic) fields SU(N) theories are periodic (anti-periodic) in the temporal direction. Since the matter fields are in the fundamental representation, the Z_N gauge transformed matter fields do not satisfy the periodic boundary conditions anymore. These gauge transformations therefore can not act on the matter fields. However, it still makes sense to consider these Z_N gauge transformations by restricting their actions only to the gauge fields. These transformations are not like the conventional gauge transformations which act both on the gauge and the matter fields, will not leave the action of the full theory invariant. Even though the action is not invariant, a configuration and its Z_N gauge transformed configuration both will contribute to the partition function. Their individual contribution to the partition function will decide the relative Boltzmann probability of these two configurations in a thermal ensemble. Even though the classical action does not have the Z_N symmetry ultimately the fluctuations of the fields will decide if the Z_N symmetry is relevant in the

presence of matter fields. Hereby Z_N symmetry gauge transformation we imply that the gauge transformations are acting only on the gauge fields. The matter fields can be gauge transformed only when the gauge transformations correspond to the identity of Z_N group.

The issue of Z_N symmetry in the presence of fundamental matter fields has been extensively studied in the literature [6–8]. Perturbative calculations which are limited to very high temperatures away from the transition point, consider fluctuations up to second order around the minimum of the Euclidean action. In pure SU(N) gauge theory, there is no spontaneous breaking of the Z_N symmetry without these fluctuations. These Gaussian fluctuations lead to an effective potential for the Polyakov loop, with the spontaneous breaking of Z_N symmetry [37]. The matter field effects are calculated by considering an ideal gas which couples only to the Polyakov loop or only to the zero mode of the gauge field fluctuations [6]. This results in explicit breaking of the Z_N symmetry, the strength of which depends on the masses and the number of the matter fields. For some cases the explicit symmetry breaking is so large that there are no local minima in the effective potential. For some choice of parameter, the Polyakov loop effective potential has local minima, meta-stable states, with unphysical behavior such as negative pressure and negative entropy [7] . It is not known whether these unphysical behavior persist when fluctuations beyond Gaussian approximation are considered.

The issue of matter fields on the CD transition has been studied in SU(N) gauge theories on the lattice using mean field approximation. These calculations consider strong gauge coupling limit, in which it is possible to reduce the partition function to a form only in terms of the Polyakov loop degrees of freedom [15, 38]. Except for the integration measure (Haar measure), the partition function turns out to be similar to that of Z_N spins with nearest neighbor ferromagnetic coupling. The effect of matter field lead to a determinant, which can be expanded in terms of hopping (parameter) of the matter fields in closed loops on the lattice. The hopping parameter is small for heavy matter fields. In this limit and for small N_τ (N_τ is the number of lattice points in the temporal

direction of the Euclidean lattice) the leading order approximation leads to a term in the effective action which breaks the Z_N symmetry explicitly. The resulting partition function is studied in the mean field approximation for the CD transition. The CD transition becomes weaker with the increase the hopping parameter. For SU(2) with matter fields, the transition becomes a crossover for non-zero hopping parameter. For SU(3) the transition becomes a weak first order , second order and crossover with the increase in the hopping parameter. These results are in the qualitative argument with non-perturbative lattice studies for small N_τ. The CD transition has been studied extensively in QCD using non-perturbative lattice simulations [5]. These studies find that in the heavy quark mass region, the explicit breaking of the Z_N symmetry decreases with mass. This explicit symmetry breaking gives rise to meta-stable states in the deconfined phase [39]. In the chiral limit, however, the behavior of the Polyakov loop cannot be understood in terms explicit symmetry breaking by a uniform external field. Along with the chiral condensate, the Polyakov loop exhibit critical behavior [9]. But the distribution of the Polyakov loop does not show any Z_N symmetry. This suggests that, in the chiral limit, the effective external field is a fluctuating and nonuniform dynamical field instead of a constant uniform field [40]. The behaviors of the chiral transition and the chiral condensate are, however, well described by a uniform/static field in the chiral limit [41].

As in QCD, in SU(N) theory with Higgs in the fundamental representation, the fundamental charges will experience similar force/potential. Previous studies have shown that in the confined phase there will be colorless composite particles of Gluons and the Higgs. In the deconfined phase, there charges experience coulombic interactions (with screening). Although there have been a lot of non-perturbative studies on the CD transition of SU(N) gauge theories coupled to fundamental bosonic fields, very few, have addressed the issue of the Z_N symmetry in these theories. Most of these studies are for small number of temporal lattice site $N_\tau = 2$ with a few for $N_\tau = 4$ [38, 42]. In these studies, the Z_N symmetry is explicitly broken, and the CD transition is different from the pure gauge case once the interaction between gauge and matter switch on. More

studies are necessary to address how the strength of explicit symmetry breaking depends on the various parameters of the theory. More importantly study of the explicit symmetry breaking and the nature of CD transition in the continuum limit, i.e large N_τ. Both in the presence of bosonic and fermionic fields (in fundamental representation) the Euclidean action is not invariant under the Z_N transformation. It is not clear how fluctuations affect the Z_N symmetry in both cases. Studying the Z_N symmetry in the SU(N) Higgs theory will give a better overal picture of the effect of fundamental matter fields. It is possible that such a study may complement the studies done in QCD, also uncover new aspects not yet seen in QCD. In this thesis work, we carry out non-perturbative studies to address these issues by considering temporal lattice points up to $N_\tau = 8$. We compute the distribution of the Polyakov loop and other observables which are relevant for the Z_N symmetry and the CD transition. Most of our simulation studies are for $N = 2$ and $N = 3$. We find that the distribution of the Polyakov loop is similar to the distribution of the magnetization in ferromagnetic N-state Potts model in the presence of the external field [5]. The external field causes asymmetry in the distributions of the magnetization which otherwise has the Z_N symmetry. The larger the external field, larger is the asymmetry in the distribution of the magnetization. In the present case the asymmetry of the Polyakov loop distribution is found to vary with the Higgs quartic coupling (λ) and the gauge-Higgs interaction strength (κ). It is observed that the distribution has large (small) asymmetry when the condensate is large (small). Conventionally It is never expected that the explicit symmetry breaking of Z_N vanish as long as there is a non-zero interaction between the gauge and the Higgs fields. Surprisingly it is found that for $N_\tau = 4$ in the $\lambda - \kappa$ plane, in a region of the Higgs symmetric phase, the Polyakov loop distribution exhibits the Z_N symmetry. The simulation results also show that the different Z_N states in the deconfined phase have the same free energy. This implies that the effective external field is vanishingly small and there is realization of the Z_N symmetry. In the effective potential calculations, the Z_N symmetry is realized only in the limit of infinitely heavy Higgs mass, i.e basically when the Higgs field decouples from the gauge fields. In the present case, this occurs

even though there is a non-zero interaction (correlation) between the gauge and the Higgs fields. The nature of the CD transition is almost same as in the pure gauge theory. It has been argued previously that in a lattice theory of SU(N)+Higgs with frozen radial mode of the Higgs, the presence of Higgs field does not change the pure gauge CD transition for small coupling between the gauge and Higgs fields [43]. The explanation for this was that the Higgs field does not couple to any global order parameter. The presence of Higgs field only modifies the critical "temperature" for the CD transition. Though present results cannot be extrapolated to the continuum limit. The Z_N explicit breaking symmetry results for $N_\tau = 4$ and $N_\tau = 2$ are different, this suggests there are finite cut-off effect on the Z_N symmetry and the CD transition. It is well known that the thermal average of the Polyakov loop has a strong cut-off dependence. The Polyakov loop expectation value decreases with the number of temporal sites (N_τ) of the Euclidean lattice, though the nature of the pure gauge CD transition does not change with N_τ. We mention here that the renormalized Polyakov loop turns out to be cut-off independent [44].

In our simulations of the N_τ dependence study is only for $SU(2)$+Higgs. We believe similar results will hold for higher SU(N)+Higgs. A detailed study of the N_τ dependence was carried out for vanishing bare Higgs mass and the quartic coupling. For these values of the parameters, the CD transition is a crossover for $N_\tau = 2$ and 4. For $N_\tau = 8$ the transition turned out to be second order with the realization of the Z_2 symmetry. This is in contrast to the effective potential calculations which suggest that the explicit symmetry breaking will be maximal in the massless limit. We show that the restoration of Z_2 for higher N_τ is not due increase of the renormalized Higgs mass which can lead to decrease in the correlation between the Higgs and the gauge fields. We find that interaction energy between the Higgs and the gauge fields in a given physical volume increase with N_τ when we use the one loop beta-function. It is important to study if similar N_τ dependence exists for other values of λ and Higgs mass. So in this thesis, we also study the Z_2 symmetry on the $\lambda - \kappa$ plane for $N_\tau = 8$. We find that for small λ, the Z_2 symmetry is restored in all of the Higgs symmetric phase. There is a clear pattern observed

in the variation of the explicit symmetry breaking on the $\lambda - \kappa$ plane. For large κ the explicit symmetry breaking is large at the same time the system is found to be in the Higgs phase. On the other hand for small κ the explicit symmetry breaking is vanishingly small with vanishing Higgs condensate (Higgs symmetric phase). So we believe that the Higgs condensate may play the role of the effective ordering field for the Polyakov loop. More work is needed to establish the connection between the Higgs condensate and the explicit breaking. Our results suggest that since the Z_2 symmetry is realized in the Higgs symmetric phase, it is conceivable that Z_2 domain walls may be present above electroweak transition temperature in the early Universe. This domain walls will disappear once the universe cools down with possible physically observable consequences. Note that with $\lambda = 0$, the Z_2 symmetry is realized already for vanishing Higgs mass. For higher mass, the interaction between the Higgs and the gauge fields will only decrease, so it expected that the Z_2 symmetry would persist for any non-zero Higgs mass. In contrast QCD the Z_N symmetry is there only for infinite quark mass and the explicit symmetry breaking only increases with the decrease in the quark mass.

The thesis is organized as follows. In chapter-2 we derive the partition function in the path integral form and discuss the Z_N symmetry. In chapter-3 we briefly review the Polyakov loop effective potential calculations. Mean field approximation studies of CD transition in the strong coupling limit will be discussed in chapter-4. In chapter-5, we discuss numerical techniques used for our Monte Carlo simulations. In chapter-6 we present our simulation studies for $N_\tau = 4$ and describe N_τ dependence studies in chapter-7. In chapter-8 we present discussions, conclusions, and outlook.

2 Z_N symmetry in SU(N) gauge theories

In this chapter we derive the path-integral form of the partition function for SU(N)+Higgs theories. Afterwards we discuss how this Z_N symmetry arises in the partition function and its breaking in the presence of matter fields in the fundamental representation.

2.1 Partition function for pure SU(N) gauge theory

The classical action for a pure SU(N) gauge theory is given by,

$$S[A] = \int dt\, L = -\frac{1}{2}\int d^4x\, \mathrm{Tr}[F_{\mu\nu}(x)F^{\mu\nu}(x)] \tag{2.1.1}$$

This Lagrangian(L) describes the dynamics and interactions of (N^2-1) spin-1 bosons, called gluons. Here x stands for the four space time vector x_μ (with $\mu = 0,1,2,3$), the gauge field strength $F_{\mu\nu}(x) = \partial_\mu A_\nu(x) - \partial_\nu A_\mu(x) + ig[A_\mu(x), A_\nu(x)]$. Gauge fields are expressed as $A_\mu(x) = \sum_a A^a_\mu(x)T^a$ (with $a = 1,2,...N^2-1$), T^a's are the generators of SU(N) group, which are $N\times N$ traceless matrices in the fundamental representation of the gauge group.

$$\mathrm{Tr}(T_aT_b) = \frac{1}{2}\delta_{ab}, \quad [T_a, T_b] = if_{abc}T_c.$$

The trace in the gauge action (2.1.1) is over color indices. g appearing in $F_{\mu\nu}$ is the gauge

coupling constant. The gauge action (2.1.1) is invariant under the following local SU(N) gauge transformations of the gauge fields.

$$A_\mu(x) \longrightarrow V(x)A_\mu(x)V^{-1}(x) - \frac{i}{g}\left(\partial_\mu V^{-1}(x)\right)V(x) \tag{2.1.2}$$

Here $V(x) = e^{i\Lambda^a(x)T^a}$, $\Lambda^a(x)$'s are space time dependent functions. To study the thermodynamic properties of the system we need the Hamiltonian operator. We will follow the standard procedure to derive the Hamiltonian operator [45]. The conjugate momentum fields $\Pi_{A_\mu(x)}$ for the gauge fields $A_\mu(x)$ are defined as,

$$\Pi_{A_\mu(x)} = \frac{\partial L}{\partial \dot{A}_\mu(x)}. \tag{2.1.3}$$

Since $\dot{A}_0(x)$ doesn't appear in the Lagrangian the corresponding conjugate field $\Pi_{A_0} = 0$. Thus $A_0(x)$ is not a dynamical field. The electric field $E_i(x) = F_{0i}(x)$ turns out to be the conjugate momentum fields for $A_i(x)'$s as,

$$\Pi_{A_i(x)} = \frac{\partial L}{\partial \dot{A}_i(x)} = -E_i(x). \tag{2.1.4}$$

The Hamiltonian is given by the following Legendre transformation of the Lagrangian L,

$$H = \int d^3x\, \mathrm{Tr}[\dot{A}_\mu(x)\Pi_{A_\mu(x)}] - L = \int d^3x\, \frac{1}{2}\mathrm{Tr}\left[E_i(x)E_i(x) + B_i(x)B_i(x) - A_0(x)(D.E(\mathbf{x}))\right]. \tag{2.1.5}$$

Here $B_i(x) = \epsilon^{ijk}F_{jk}(x)$ are the magnetic fields. Note that in the above convention E_i and B_i are $N \times N$ traceless matrices. Appearing in the last term $A_0(x)$ acts as a Lagrange multiplier which makes sure that $D.E = D_iE_i$ is independent of time.

The canonical quantization of this theory requires gauge fixing. The $A_0 = 0$ gauge is found to be suitable for finite temperature studies [46]. The quantization is carried out by setting up the equal time commutation relation between the dynamical

gauge fields A_i and the conjugate momentum fields $\Pi_{A_i} = -E_i$ as,

$$[E_i(\mathbf{x}), A_j(\mathbf{y})] = -i\delta_{ij}\delta^3(\mathbf{x}-\mathbf{y}) \tag{2.1.6}$$

In terms of the gauge and momentum field operators the Hamiltonian operator for the pure SU(N) gauge theory is given by,

$$\hat{H} = \int d^3x \left[\frac{1}{2}(E_i^a)^2 + \frac{1}{4}(B_i^a)^2\right] \tag{2.1.7}$$

The partition function of the theory in the $\{|A(\mathbf{x})\rangle\}$ basis is given by,

$$\mathcal{Z} = \mathrm{Tr}[e^{-\beta\hat{H}}] = \int DA(\mathbf{x})\langle A(\mathbf{x})|e^{-\beta\hat{H}}|A(\mathbf{x})\rangle \tag{2.1.8}$$

Here $\beta = \frac{1}{T}$. Thermal average of any operator (O) is given by,

$$\langle O\rangle = \frac{\mathrm{Tr}(Oe^{-\beta\hat{H}})}{\mathcal{Z}} = \int DA(\mathbf{x})\frac{\langle A(\mathbf{x})|Oe^{-\beta\hat{H}}|A(\mathbf{x})\rangle}{\mathcal{Z}} \tag{2.1.9}$$

In the above 'Tr' is trace over all physical states of the system. Note that setting $A_0(x) = 0$ does not remove unphysical degrees of freedom from the theory completely. Therefore the full Hilbert space of the states spanned by $\{|A(\mathbf{x})\rangle\}$ has which are physically equivalent states. For example, two states $|A(\mathbf{x})\rangle$ and $|A'(\mathbf{x})\rangle$ are physically same/equivalent if $A'_i(\mathbf{x})$ and $A_i(\mathbf{x})$ are related by a time independent gauge transformation. As the states that lie along a gauge orbit are physically equivalent, care must be taken so that only one state from each gauge orbit (gauge field configurations related to one another by gauge transformations) will contribute to the partition function. This is achieved by imposing the Gauss law on the states of the Hilbert space. In the absence of any external charges, the physical states $\{|A_{phys}\rangle\}$ are required to satisfy the Gauss's law,

$$D.E(\mathbf{x})|A_{phys}\rangle = 0 \tag{2.1.10}$$

The Gauss law constraint can also be taken into account by requiring that the physical states are invariant under the operator $\hat{P}$

$$\hat{P} = \int D\Lambda(\mathbf{x}) \exp\left(-i \int d^3x \, \mathrm{Tr}[\Lambda(\mathbf{x})(D.E(\mathbf{x}))]\right) \tag{2.1.11}$$

, i.e $\hat{P}|A_{phys}\rangle = |A_{phys}\rangle$. $\Lambda(\mathbf{x}) = T^a\Lambda^a(\mathbf{x})$, where Λ^a's are $N^2 - 1$ scalar functions vanishing at spatial infinity and $D\Lambda(\mathbf{x})$ is the integral over all possible gauge functions $\Lambda(\mathbf{x})$. The operator $\hat{P}$ generates the time independent gauge transformations which are still allowed in the $A_0 = 0$ gauge. Essentially $\hat{P}$ projects out one state from each gauge orbit. It can be shown that the projection operator $\hat{P}$ commutes with the Hamiltonian, i.e $[\hat{P}, \hat{H}] = 0$. Therefore one can write,

$$e^{-\beta\hat{H}}\hat{P} = e^{-\beta\hat{H}_p} \tag{2.1.12}$$

Where

$$\hat{H}_p = \hat{H} + i \int d^3x \, \mathrm{Tr}(E.D\Lambda(\mathbf{x})/\beta). \tag{2.1.13}$$

Note that in equation (2.1.11) the operators E and Λ can be interchanged by introducing a minus sign. The Gauss law constraint leads to a new term in the Hamiltonian operator. So the partition function the physical degrees of freedom is given by,

$$\mathcal{Z} = \int DA(\mathbf{x})\langle A(\mathbf{x})|e^{-\beta\hat{H}_p}|A(\mathbf{x})\rangle \tag{2.1.14}$$

The momentum operator $E_i(\mathbf{x})$ in the Hamiltonian $\hat{H}_p$ does not commute with the operator $A_i(\mathbf{x})$. Hence the states $|A(\mathbf{x})\rangle$ are not eigen states of $E_i(\mathbf{x})$. The only way to evaluate the above integrand/expectation value is by writing,

$$e^{-\beta\hat{H}_p} = \left(e^{-\epsilon\hat{H}_p}\right)^{\mathcal{N}}. \tag{2.1.15}$$

Here $\epsilon = \frac{\beta}{\mathcal{N}}$. Further $\mathcal{N}-1$ identity operators,

$$\int DA_i(\mathbf{x}, j)\ |A_i(\mathbf{x}, j\epsilon)\rangle\langle A_i(\mathbf{x}, j\epsilon)|, \quad j = 1, ...\mathcal{N}-1, \tag{2.1.16}$$

$$\int DE_i(\mathbf{x}, j)\ |E_i(\mathbf{x}, j\epsilon)\rangle\langle E_i(\mathbf{x}, j\epsilon)|, \quad j = 1, ...\mathcal{N}-1 \tag{2.1.17}$$

are inserted between each consecutive factors of $e^{-\epsilon\hat{H}_p}$ in equation (2.1.14). In the partition function, this leads to factors like the following in the,

$$\langle A_i(\mathbf{x}, (j+1)\epsilon)|E_i(\mathbf{x}, (j+1)\epsilon)\rangle\langle E_i(\mathbf{x}, (j+1)\epsilon)|e^{-\epsilon\hat{H}_p}|A_i(\mathbf{x}, j\epsilon)\rangle \tag{2.1.18}$$

The first factor is

$$\langle A_i(\mathbf{x}, (j+1)\epsilon)|E_i(\mathbf{x}, (j+1)\epsilon)\rangle\ \propto\ \exp[i\int E_i(\mathbf{x}, (j+1)\epsilon).A_i(\mathbf{x}, (j+1)\epsilon)] \tag{2.1.19}$$

apart from a normalization constant. For large $\mathcal{N}$, ϵ is small. The other factor in the above amplitude can be calculated by expanding $e^{-\epsilon\hat{H}_p}$ to first order in epsilon (as $\epsilon << 1$).

$$\langle E_i(\mathbf{x}, (j+1)\epsilon)|[1-\epsilon\hat{H}_p]|A_i(\mathbf{x}, j\epsilon)\rangle. \tag{2.1.20}$$

This can be evaluated easily, by using

$$\begin{aligned}\hat{A}_i|A_i(\mathbf{x}, j\epsilon)\rangle &= A_i(\mathbf{x}, j\epsilon)|A_i(\mathbf{x}, j\epsilon)\rangle \\ \hat{E}_i|E_i(\mathbf{x}, j\epsilon)\rangle &= E_i(\mathbf{x}, j\epsilon)|E_i(\mathbf{x}, j\epsilon)\rangle\end{aligned} \tag{2.1.21}$$

The result is,

$$(1-\epsilon\hat{H}_p)(E_i(\mathbf{x}, (j+1)\epsilon, A_i(\mathbf{x}, j\epsilon)) \times \langle E_i(\mathbf{x}, (j+1)\epsilon)|A_i(\mathbf{x}, j\epsilon)\rangle \tag{2.1.22}$$

$$\simeq e^{-\epsilon\hat{H}_p}(E_i(\mathbf{x}, (j+1)\epsilon, A_i(\mathbf{x}, j\epsilon)) \times \langle E_i(\mathbf{x}, (j+1)\epsilon)|A_i(\mathbf{x}, j\epsilon)\rangle \tag{2.1.23}$$

Another equation like (2.1.19)

$$\langle E_i(\mathbf{x},(j+1)\epsilon)|A_i(\mathbf{x},j\epsilon)\rangle \propto \exp(-i\int E_i(\mathbf{x},(j+1)\epsilon).A_i(\mathbf{x},j\epsilon)). \tag{2.1.24}$$

Through the above steps by inserting the complete set of states, we have converted the partition function into integral over functions $E_i(\mathbf{x}, j\epsilon = \tau_j)$ and $A_i(\mathbf{x}, j\epsilon = \tau_j)$. In the integral the functions $E_i(\mathbf{x},\tau_j)$'s appear in the exponential with linear and quadratic powers. The Gaussian integration of these momentum functions can be carried out exactly, resulting in the following path integral form of the partition function,

$$\mathcal{Z} \propto \int D\Lambda(\mathbf{x}) \prod_j dA_i(\mathbf{x}, j\epsilon)\, \exp[-S(\Lambda(\mathbf{x}), A_i(\mathbf{x}, j\epsilon))] \tag{2.1.25}$$

Where

$$S(\Lambda(\mathbf{x}), A_i(\mathbf{x}, j\epsilon)) = \int d^3x\, \epsilon\, \frac{1}{2}\left[\left(\frac{(A_i(\mathbf{x},(j+1)\epsilon) - A_i(\mathbf{x}, j\epsilon))}{\epsilon} - d_i\left(\frac{\Lambda}{g\beta}\right) + \left(\frac{\Lambda}{\beta}\right) \times A_i(\mathbf{x}, j\epsilon)\right)^2 + B^2\right] \tag{2.1.26}$$

Note that $A_i(\mathbf{x}) = A_i(\mathbf{x}, 0) = A_i(\mathbf{x},\beta)$. In the limit $\mathcal{N} \to \infty$, the path integral is written as

$$\mathcal{Z} = \lim_{\mathcal{N}\to\infty} \mathrm{Tr}(\hat{P}e^{-\epsilon\hat{H}})^{\mathcal{N}} = \int_{A_i(\mathbf{x},0)=A_i(\mathbf{x},\beta)} [D\Lambda][DA_i]e^{-S[\Lambda,A_i]} \tag{2.1.27}$$

Here $\int [DA_i] = \int \prod_i dA_i$ is the functional integral over all possible paths between $A_i(\mathbf{x}, 0)$ and $A_i(\mathbf{x},\beta)$. Λ field depends only on $\mathbf{x}$. However one can consider it dependent on time by enhancing the gauge symmetry to include time dependent gauge transformations. With now $\Lambda = \Lambda(\mathbf{x},\tau)$, it can be thought of as the $A_0(\mathbf{x},\tau)$ field which was set to zero to quantize the theory. In (2.1.27), $\Lambda(\mathbf{x},\tau)$ is replaced by $\beta g A_0(\mathbf{x},\tau)$, the partition function is given by

$$\mathcal{Z} = \int [DA]e^{-S_E[A]} \tag{2.1.28}$$

The Euclidean gauge action in (2.1.28) is given by,

$$S_E[A] = \int_V d^3x \int_0^\beta d\tau \left[\frac{1}{2}\mathrm{Tr}[F_{\mu\nu}(\mathbf{x},\tau)F_{\mu\nu}(\mathbf{x},\tau)]\right]. \tag{2.1.29}$$

Here $F_{\mu\nu} = \partial_\mu A_\nu - \partial_\nu A_\mu + ig[A_\mu \times A_\nu]$. It is interesting to note that after fixing the gauge and implementing the Gauss law the final form of the path integral partition function has all the gauge symmetries present at the classical level. In the following, we derive the partition function for the SU(N)+Higgs theory.

2.2 Partition function in the presence of fundamental matter fields

The classical action SU(N) gauge theory with fundamental Higgs field is given by,

$$S[A,\Phi] = \int d^4x \left[-\frac{1}{2}\mathrm{Tr}[F_{\mu\nu}F^{\mu\nu}] + \frac{1}{2}(D_\mu\Phi)^\dagger(D_\mu\Phi) - \frac{\bar{m}^2}{2}\Phi^\dagger\Phi - \frac{\bar{\lambda}}{4}(\Phi^\dagger\Phi)^2\right] \tag{2.2.1}$$

This action describes the dynamics and interactions of (N^2-1) gluons and $2N$ scaler bosons. The Higgs fields Φ is in the fundamental representation of SU(N). The covariant derivative $D_\mu\Phi$ is defined as $D_\mu\Phi = \partial_\mu\Phi + igA_\mu\Phi$, where g is the gauge coupling constant, The action (2.2.1) is invariant under the following local SU(N) gauge transformations of the gauge and Higgs fields,

$$\begin{aligned} A_\mu(x) &\longrightarrow V(x)A_\mu(x)V^{-1}(x) - \frac{i}{g}\left(\partial_\mu V^{-1}(x)\right)V(x) \\ \Phi(x) &\longrightarrow V(x)\Phi(x). \end{aligned} \tag{2.2.2}$$

Here $V(x) \in$ SU(N). To write the partition function of the system, we will follow the same approach as in the pure SU(N) gauge case. In the $A_0 = 0$ gauge, the conjugate momentum

fields for the Higgs fields are,

$$\Pi_\Phi = \frac{\partial L}{\partial \dot{\Phi}} = \dot{\Phi}^\dagger. \tag{2.2.3}$$

$$\Pi_{\Phi^\dagger} = \frac{\partial L}{\partial \dot{\Phi}^\dagger} = \dot{\Phi}. \tag{2.2.4}$$

The total Hamiltonian in terms of the conjugate momentum fields for gauge and Higgs fields are given by,

$$\begin{aligned} H &= \int d^3x \, \mathrm{Tr}[\dot{A}_i \Pi_{A_i} + \dot{\Phi}\Pi_\Phi + \dot{\Phi}^\dagger \Pi_{\Phi^\dagger} - L] \\ &= \int d^3x \, \mathrm{Tr}[F^2 + \frac{1}{2}(\Pi_\Phi \Pi_{\Phi^\dagger}) - \frac{1}{2}(\vec{\nabla}\Phi - ig\vec{A}\Phi)^\dagger(\vec{\nabla}\Phi - ig\vec{A}\Phi) + \frac{1}{2}\bar{m}^2\Phi^\dagger\Phi + \frac{1}{4}\bar{\lambda}(\Phi^\dagger\Phi)^2] \end{aligned} \tag{2.2.5}$$

Here L is the Lagrangian for SU(N)+Higgs theory. The commutation relations between the Higgs fields and their conjugate momentum fields are taken to be,

$$\begin{aligned} [\Pi_\Phi(\mathbf{x}), \Phi(\mathbf{y})] &= -i\delta^3(\mathbf{x}-\mathbf{y}) \\ [\Pi_{\Phi^\dagger}(\mathbf{x}), \Phi^\dagger(\mathbf{y})] &= -i\delta^3(\mathbf{x}-\mathbf{y}) \end{aligned} \tag{2.2.6}$$

The Hamiltonian operator with gauge field, Higgs field and their corresponding momentum operators are given by,

$$\begin{aligned} \hat{H} = \hat{H}_g + \int d^3x \, \mathrm{Tr}[&\Pi_\Phi \Pi_{\Phi^\dagger} - |(\nabla\Phi)|^2 - ig\partial_i\Phi^\dagger A_i\Phi + igA_i\Phi^\dagger\partial_i\Phi \\ &-g^2 A_i\Phi^\dagger A_i\Phi + \bar{m}^2\Phi^\dagger\Phi + \bar{\lambda}(\Phi^\dagger\Phi)^2] \end{aligned} \tag{2.2.7}$$

Here $\hat{H}_g$ is the Hamiltonian operator for the pure gauge theory (2.1.7). Given total Hamiltonian operator, one can write the partition function for the theory,

$$\mathcal{Z} = \mathrm{Tr}[e^{-\beta\hat{H}}] = \int DA_i(\mathbf{x}) D\Phi(\mathbf{x}) \, \langle\chi(\mathbf{x})|e^{-\beta\hat{H}}|\chi(\mathbf{x})\rangle \tag{2.2.8}$$

Here $|\chi(\mathbf{x})\rangle = |A(\mathbf{x}), \Phi(\mathbf{x})\rangle$. In the above 'Tr' is trace over all physical states of the system. The physical states satisfy the Gauss's law,

$$[D.E(\mathbf{x}) - \rho]|\chi\rangle = 0 \tag{2.2.9}$$

Here ρ is the charge density operator, is given by,

$$\rho = i \int d^3x \, [\Phi^\dagger \Pi_{\Phi^\dagger} - \Phi \Pi_\Phi] \tag{2.2.10}$$

As in the pure gauge case, the Gauss law constraint can be taken into account by considering that the physical states are invariant under the operator $\hat{P}$

$$\hat{P} = \int D\Lambda(\mathbf{x}) \exp\left(i \int d^3x \, \hat{\mathrm{Tr}} \Lambda[(D.E) - [\Phi^\dagger \Pi_{\Phi^\dagger} - \Phi \Pi_\Phi]] \right) \tag{2.2.11}$$

The physical states satisfy the condition $\hat{P}|\chi\rangle = |\chi\rangle$. The operator $\hat{P}$ commutes with the Hamiltonian. As in the previous section $\hat{P}$ operator effectively gives rise to an additional term in the Hamiltonian in the partition function as,

$$\hat{H}_p = \hat{H} + i \int \frac{d^3x}{\beta} \, \mathrm{Tr}[(E.D\Lambda) - \Lambda[\Phi^\dagger \Pi_{\Phi^\dagger} - \Phi \Pi_\Phi]] \tag{2.2.12}$$

The partition function with gauss law constraint is given by,

$$\mathcal{Z} = \int d\Lambda(\mathbf{x}) dA_i(\mathbf{x}) d\Phi(\mathbf{x}) \, \langle \chi(\mathbf{x}) | e^{-\beta \hat{H}_p} | \chi(\mathbf{x}) \rangle \tag{2.2.13}$$

Here $A_i(\mathbf{x}) = A_i(\mathbf{x}, 0) = A_i(\mathbf{x}, \beta)$ and $\Phi(\mathbf{x}) = \Phi(\mathbf{x}, 0) = \Phi(\mathbf{x}, \beta)$. As in pure gauge case $e^{-\beta \hat{H}_p}$ is written as $(e^{-\epsilon \hat{H}_p})^{\mathcal{N}}$ inserting $\mathcal{N} - 1$ complete set of states $|\chi(\mathbf{x}), j\epsilon\rangle$ and $|\Pi(\mathbf{x}), j\epsilon\rangle$, $j = 1, 2, 3...\mathcal{N} - 1$. Following similar steps as in the last section we arrive at the following form of the partition function in the limit $\mathcal{N} \to \infty$,

$$\mathcal{Z} = \lim_{\mathcal{N} \to \infty} \mathrm{Tr}(e^{-\epsilon \hat{H}_p})^{\mathcal{N}} = \int [DA][D\Phi] e^{-S_E[A,\Phi]} \tag{2.2.14}$$

The path integral in (2.2.14) is over periodic gauge and Higgs field, i.e $A_\mu(\mathbf{x},0) = A_\mu(\mathbf{x},\beta)$ and $\Phi(\mathbf{x},0) = \Phi(\mathbf{x},\beta)$. The Euclidean gauge action in (2.2.14) is given by,

$$S_E[A,\Phi] = \int_V d^3x \int_0^\beta d\tau \left\{ \frac{1}{2}\mathrm{Tr}\left(F^{\mu\nu}F_{\mu\nu}\right) + \frac{1}{2}(D_\mu\Phi)^\dagger(D_\mu\Phi) + \frac{\bar{m}^2}{2}\Phi^\dagger\Phi + \frac{\bar{\lambda}}{4}(\Phi^\dagger\Phi)^2 \right\} \tag{2.2.15}$$

In the following, we discuss the Z_N symmetry in pure SU(N) gauge theory followed by the SU(N)+Higgs theory.

2.3 Z_N symmetry in pure SU(N) gauge theory

As mentioned above the Euclidean action is invariant under the following gauge transformation of the gauge fields:

$$A_\mu(\mathbf{x},\tau) \longrightarrow V(\mathbf{x},\tau)A_\mu(\mathbf{x},\tau)V^{-1}(\mathbf{x},\tau) - \frac{i}{g}\left(\partial_\mu V^{-1}(\mathbf{x},\tau)\right)V(\mathbf{x},\tau) \tag{2.3.1}$$

All gauge transformations are allowed as long as they preserve the periodicity of the gauge fields in the temporal direction, i.e $A_\mu(\mathbf{x},0) = A_\mu(\mathbf{x},\beta)$. It turns out that the gauge transformations $V(\mathbf{x},\tau)$ which preserve the periodicity of the gauge field along the temporal direction so keep the action (2.1.29) invariant are of the form

$$V(\mathbf{x},\tau=0) = zV(\mathbf{x},\tau=\beta) \tag{2.3.2}$$

Where $z = \mathbb{1}\exp(\frac{2\pi i n}{N})$, $\mathbb{1}$ is the $N\times N$ identity matrix, $(n = 0,1,2...N-1)$. Here $z \in Z_N$, where Z_N is the center of the gauge group SU(N). Since the elements of Z_N commute with A_μ, under the gauge transformations (2.3.1), it is easy to see that the gauge fields remain periodic. The gauge transformations at finite temperatures are not necessarily periodic and can be characterized by z or the Z_N group according to equation (2.3.2). The Wilson

line,

$$P(\mathbf{x}) = \frac{1}{N}\mathrm{Tr}\left[\mathrm{P}\left\{\exp\left(ig\int_0^\beta A_0(\mathbf{x},\tau)d\tau\right)\right\}\right], \tag{2.3.3}$$

Under the gauge transformations (2.3.2), $P(\mathbf{x})$ transforms as $P(\mathbf{x}) \to zP(\mathbf{x})$ [1, 47]. All gauge transformations (2.3.2) which correspond to z, lead to same transformations of the Polyakov loop. Therefore, it is useful to classify the all gauge transformations by Z_N group. The pure SU(N) action is invariant under these gauge transformations. So pure gauge partition function has Z_N symmetry. It can be shown that the Polyakov loop thermal average (L)is related to the free energy F_q of a isolated static fermion or boson [48, 49],

$$L \sim e^{-(F_q)} \tag{2.3.4}$$

Confinement requires that F_q is infinite, so $L = 0$. On the other hand the possibility of isolated charges in the deconfinement phase requires the free energy F_q to be finite. In this case $L \neq 0$ which leads to the spontaneous breaking of the Z_N symmetry. Non-perturbative lattice studies show that the pure SU(N) gauge theory undergoes the confinement-deconfinement (CD) transition at high temperature $T = T_c$. These studies show that the thermal average of the Polyakov loop vanishes at low temperatures and acquires non-zero values for temperature above a critical temperature $T_c(N)$, i.e

$$\begin{aligned} L \neq 0 \quad &\text{(Deconfinement)} \quad (\mathrm{F_q\ finite}) \\ L = 0 \quad &\text{(Confinement)} \quad (\mathrm{F_q\ infinite}) \end{aligned} \tag{2.3.5}$$

Thus, the Polyakov loop serves as an order parameter for the CD transition [2]. Since L is the trace of an SU(N) matrix, for $N = 2$ the range of values L can take is $[-1, 1]$. For $N > 2$, it can take any value in a $n-$polygon in the complex plane whose vertices are given by $e^{i\frac{2\pi n}{N}}$, $(n = 0, 1, ...N-1)$. It is important to note that the Z_N symmetry is the symmetry of the pure SU(N) gauge theory partition function [50–52]. This means the Z_N symmetry and Polyakov loop are useful only when the system described by SU(N) gauge theory is in equilibrium. It is interesting to note that the behavior of L under Z_N transformations

is exactly like the magnetization in $N-$state Pott model. Non-perturbative studies have shown that thermodynamic behavior of L is also similar to the magnetization in $N-$state Potts model. The finite temperature SU(N) gauge theory and $N-$state Pott's model. The order of the SU(N) CD transition is found to be same as the magnetization transition in $N-$state Pott's model.

2.4 Z_N symmetry in the presence of fundamental matter fields

Partition function for SU(N) gauge theory with matter fields is given by (2.2.1),

$$Z = \int [DA]\ [D\Phi]\ e^{-S_E[A,\Phi]}. \tag{2.4.1}$$

where the Euclidean action $S_E[A,\Phi]$ is

$$S_E[A,\Phi] = \int_V d^3x \int_0^\beta d\tau \left[\frac{1}{2}\mathrm{Tr}\left(F^{\mu\nu}F_{\mu\nu}\right) + (D_\mu\Phi)^\dagger(D_\mu\Phi) + V_1(\Phi^\dagger\Phi)\right]. \tag{2.4.2}$$

Since the gauge field A_μ and Higgs field Φ are bosonic, they satisfy the following boundary conditions in Euclidean space,

$$\begin{aligned} A(\mathbf{x},0) &= A(\mathbf{x},\beta) \\ \Phi(\mathbf{x},0) &= \Phi(\mathbf{x},\beta). \end{aligned} \tag{2.4.3}$$

As mentioned before the Euclidean action is invariant under the gauge transformation of the gauge and matter fields. The gauge fields transform as,

$$A_\mu(\mathbf{x},\tau) \longrightarrow V(\mathbf{x},\tau)A_\mu(\mathbf{x},\tau)V^{-1}(\mathbf{x},\tau) - \frac{i}{g}\left(\partial_\mu V^{-1}(\mathbf{x},\tau)\right)V(\mathbf{x},\tau).$$

The matter fields, being in the fundamental representation, transform as,

$$\Phi(\mathbf{x},\tau) \longrightarrow V(\mathbf{x},\tau)\Phi(\mathbf{x},\tau). \tag{2.4.4}$$

Under a Z_N gauge transformation (2.3.2) such that $V(\mathbf{x},\beta) = zV(\mathbf{x},0)$ with $z \in Z_N$, the transformed gauge field is periodic in the temporal direction (2.4.3). The gauge transformed matter fields Φ_g on the other hand satisfy the following boundary condition.

$$\Phi_g(\mathbf{x},\beta) = z\Phi_g(\mathbf{x},0). \tag{2.4.5}$$

It is obvious that the gauge transformed bosonic fields are periodic only when the gauge transformations are periodic i.e $z = \mathbb{1}$. Φ_g are not allowed field configurations and can not contribute to the partition function. One can still consider the Z_N gauge transformations with $z \neq \mathbb{1}$ but acting only on the gauge fields. However any gauge transformations acting only on the gauge fields will likely result in change in the action. The action for two configurations (A_μ, Φ) and (A^g_μ, Φ), where A^g_μ is Z_N gauge transformed with $z \neq \mathbb{1}$, will be different. Therefore the action is not invariant under all Z_N gauge transformations. Though the total action is not invariant, the pure gauge part of the action is invariant under these transformations. The situation is similar to Z_N spin systems in the presence of external field. Some terms in the Hamiltonian for the Z_N spins are invariant under the Z_N transformations and others are not. Hence the Z_N symmetry is explicitly broken in the presence of dynamical matter fields. The explicit breaking of the Z_N will affect the CD transition, as external field affects the magnetization transition in spin systems. The extent to which the CD transition is affected depends on the strength of the explicit symmetry breaking. For large explicit symmetry breaking the CD transition may become a crossover transition from a first order pure gauge CD transition. In Z_N spin systems the strength of the explicit symmetry breaking is the magnitude of the external field. Though it is easy to argue that Z_N symmetry of pure SU(N) gauge theory is explicitly broken in the presence of matter fields, the strength of the explicit symmetry breaking is very difficult

to calculate. In field theories as in the present case explicit symmetry breaking of Z_N symmetry in the action will not necessarily imply that all fluctuations of the fields break this symmetry explicitly.

3 Polyakov loop effective potential calculations

In this chapter we derive the effective potential for the Polyakov loop following works of Nathan Weiss and others [6, 37, 46]. In these analytic calculation it is possible to see the explicit breaking of Z_N symmetry in the presence of matter fields. In these studies the Euclidean action is expanded around the minimum upto quadratic order in the fluctuations of the fields [37, 53]. This allows the analytic calculation of the partition function. In the following we derive the effective potential calculations [6, 37, 46]. These calculations are reliable at high temperatures ($T >> T_c$) where higher order fluctuations of the fields are small, so can be ignored.

3.1 Effective potential for pure SU(N) gauge theory

The Euclidean partition function for SU(N) pure gauge theory is given by (2.1.27),

$$Z = N \int [\mathcal{D}(g\beta A_0)][DA_i(\mathbf{x}, t)]\, e^{-S_E},$$

with the Euclidean action,

$$S_E = \frac{1}{2} \int_0^\beta dt \int d^3x [(\partial_0 A_i - \partial_i A_0 + g A_0 \times A_i)^2 + B_i^2]. \tag{3.1.1}$$

The functional integration over A_0 is carried on compact SU(2) space. It is preferable to work in the gauge in which the A_0 field depends only on $\mathbf{x}$ and not on the temporal variable t [46]. Unlike the zero temperature case, at finite temperature we can not set $A_0 = 0$ by a gauge transformations. Such a gauge transformation well be dependent on time, so will spoil the periodic boundary condition of the $A_i(\mathbf{x}, \tau)$ gauge fields. Still it is possible to pick a gauge in which,

$$A_0{}^a(\mathbf{x}) = \delta_{a3}\phi(\mathbf{x}). \tag{3.1.2}$$

With this choice of A_0 the partition function can be written as,

$$\begin{aligned} Z = N \int \prod_{\mathbf{x}} [1 - \cos[g\beta\phi(\mathbf{x})]][D\phi(\mathbf{x})][DA_i(\mathbf{x}, t)] \\ \exp\left(-\frac{1}{2}\int_0^\beta dt \int d^3x \, [(\nabla\phi)^2 + (\partial_0 A_i + g\phi^{\hat{3}} \times A_i)^2 + B^2]\right). \end{aligned} \tag{3.1.3}$$

where $\hat{3}_a = \delta_{a3}$. The factor $(1 - \cos[g\beta\phi])$ comes from the Haar measure of SU(2) [54]. Using eqn.(3.1.2), the Polyakov loop is determined in terms of ϕ as,

$$L(\mathbf{x}) = \cos\left(\frac{\beta g\phi(\mathbf{x})}{2}\right), \tag{3.1.4}$$

It is convenient to calculate the effective potential in terms of ϕ instead of L. Later one can always make the change of variables $\phi \rightarrow L$. The action in (3.1.1) is minimized when $\phi(\mathbf{x}) = C/g$, is independent of $\mathbf{x}$ and $A_i^a = 0$. In this case $S_E = 0$ for all values of $g\phi(\mathbf{x}) = C$. So the Polyakov loop at the zeroth order of the fluctuations can take any value between -1 to 1, i.e the effective potential is independent of L. We will see that the fluctuations upto second order will modify the zeroth order effective potential.

The 1-loop effective potential which includes fluctuations upto second order is evaluated by writing $\phi(\mathbf{x}) = \frac{C}{g} + \delta\phi(\mathbf{x})$ and $A_i^a(\mathbf{x}, t) = \delta A_i^a(\mathbf{x}, t)$ in the action and keeping terms upto second order in $\delta\phi(\mathbf{x})$ and $A_i^a(\mathbf{x}, t)$. The measure term $\prod_x[1 - \cos[g\beta\phi(\mathbf{x})]]$ can

be written as

$$\exp\left(\ln\{\prod_x[1-\cos[g\beta\phi(\mathbf{x})]]\}\right) = \exp\left(\int d^3x\,\ln\{1-\cos[g\beta\phi(\mathbf{x})]\}\int d^3k/(2\pi)^3\right). \tag{3.1.5}$$

The summation over x can be written as an integration multiplied by the momentum space volume factor. Conventionally the summation over momentum k is written as an integral in k times physical volume. The action with the measure term is given by,

$$\begin{aligned} S = \frac{1}{2}\int_0^\beta dt\int d^3x\,[(\nabla\delta\phi)^2 + (\partial_0 A_i + C\hat{3}\times\delta A_i)^2 + \frac{1}{2}(\partial_i\delta A_j - \partial_j\delta A_i)^2] \\ - \int\frac{d^3k}{(2\pi)^3}d^3x\ln(1-\cos\beta C) + O(g^2). \end{aligned} \tag{3.1.6}$$

There will be a term from the measure, quadratic term of the fluctuation. But it is ignored because it is higher order in g. Since Z is in the form of a Gaussian integral, the integration over $\delta\phi(\mathbf{x})$ and $A_i^a(\mathbf{x},t)$ can be carried out. It is convenient to expand the fields in Fourier modes as in the following,

$$\delta\phi(x) = \sqrt{\frac{1}{V}}\sum_k e^{i(\mathbf{k}.\mathbf{x})}\phi(k) \tag{3.1.7}$$

$$\delta A_i^a(x,\tau) = \sqrt{\frac{\beta}{V}}\sum_{\omega,k} e^{i(\mathbf{k}.\mathbf{x}.+\omega\tau)}\chi_i^a(k) \tag{3.1.8}$$

Note that since the gauge field fluctuations are periodic in $\tau=\beta$, $\omega=\frac{2\pi n}{\beta}$ where n is any integer. Substituting the Fourier modes in the above action leads to five separate terms as,

$$S_\phi(k) = \sum_k k^2\phi(k)\phi(k) \tag{3.1.9}$$

$$S^T_{\chi_3} = \sum_{k,\omega}(\omega^2+k^2)\chi^3_T(k,\omega)\chi^3_T(k,\omega) \tag{3.1.10}$$

$$S^L_{\chi_3} = \sum_\omega \omega^2\chi^3_L(k,\omega) * \chi^3_L(k,\omega) \tag{3.1.11}$$

$$S^T_{\chi_{1,2}} = \sum_{n,k}\begin{pmatrix}A^1_T(\omega,k) & A^2_T(\omega,k)\end{pmatrix} M^T \begin{pmatrix}A^1_T(\omega,k)\\ A^2_T(\omega,k)\end{pmatrix} \tag{3.1.12}$$

$$S^{L}_{\chi_{1,2}} = \sum_{n,k} \begin{pmatrix} A^1_T(\omega,k) & A^2_T(\omega,k) \end{pmatrix} M^L \begin{pmatrix} A^1_T(\omega,k) \\ A^2_T(\omega,k) \end{pmatrix} \tag{3.1.13}$$

The 2×2 matrices M^T and M^L are given by

$$M^T = \begin{pmatrix} \omega^2 + C^2 + k^2 & i2\omega C \\ -i2\omega C & \omega^2 + C^2 + k^2 \end{pmatrix}. \tag{3.1.14}$$

$$M^L = \begin{pmatrix} \omega^2 + C^2 & i2\omega C \\ -i2\omega C & \omega^2 + C^2 \end{pmatrix}. \tag{3.1.15}$$

As we see that the action is diagonal in the Fourier modes $\phi(k)$'s and in both transverse and longitudinal modes $A^3_i(\omega,k)$. The action has both diagonal and off diagonal terms the modes $A^1_i(\omega,k)$ and $A^2_i(\omega,k)$ eqn.(3.1.14, 3.1.15). It is easy to diagonalize the matrices involving M^T and M^L. So in all we have the eigen values k^2 for $\phi(k)$, $\omega^2 + k^2$ for transverse component of $A^3_i(\omega,k)$, ω^2 for longitudinal component of $A^3_i(\omega,k)$, $(\omega^2 \pm C)^2 + k^2$ for transverse component of $A^1_i(\omega,k)$ and $A^2_i(\omega,k)$, $\omega^2 \pm C^2$ for longitudinal component of $A^1_i(\omega,k)$ and $A^2_i(\omega,k)$. The integration of the Fourier modes give the partition function in terms of the eigen values,

$$\mathcal{Z} \propto \left(\prod_{\omega,k} k^2(\omega^2+k^2)^2\omega^2((\omega^2-C)^2+k^2)^2((\omega^2+C)^2+k^2)^2(\omega+C)^2(\omega-C)^2 \right)^{-\frac{1}{2}} \exp\left[-\int \frac{d^3k}{(2\pi)^3} d^3x \ln(1-\cos\beta C) \right]. \tag{3.1.16}$$

The free energy is obtained using the formula $F = -\frac{ln(Z(\beta))}{\beta}$. As the momenta are integrated

out, the free energy F depends only on $\beta = \frac{1}{T}$ and C,

$$F(\beta) = \frac{1}{\beta}\frac{V}{2}\sum_{-\infty}^{\infty}\int\frac{d^3k}{(2\pi)^3}\{\ln k^2 + 2\ln[(\omega+C)^2+k^2] + 2\ln[(\omega-C)^2+k^2] + 2\ln[\omega^2+k^2] \\ +\ln[\omega^2+C^2] + \ln[\omega^2-C^2] + \ln\omega^2\} - \frac{1}{\beta}V\int\frac{d^3k}{(2\pi)^3}\ln(1-\cos\beta C). \tag{3.1.17}$$

The summation of ω can be handled in the following way. Let us consider the second and fourth term in the above,

$$F_1 = \sum_{-\infty}^{\infty}\int d^3k\left\{\ln[(\omega+C)^2+k^2] - \ln[\omega^2+k^2]\right\}. \tag{3.1.18}$$

The summation over ω of the integrand can be written in the following form,

$$\sum_{-\infty}^{\infty}\left\{\ln[(\omega+C)^2+k^2] - \ln[\omega^2+k^2]\right\} = \sum_{-\infty}^{\infty}\int dk^2\left(\frac{1}{(\omega+C)^2+k^2} - \frac{1}{\omega^2+k^2}\right). \tag{3.1.19}$$

The summation of the integrands on the r.h.s are computed using the following formulas,

$$\sum_{-\infty}^{\infty}\left(\frac{1}{n^2+a^2}\right) = \frac{\pi coth[a\pi]}{a} \tag{3.1.20}$$

$$\sum_{-\infty}^{\infty}\left(\frac{1}{(n+b)^2+a^2}\right) = \frac{\pi sinh[2a\pi]}{a(cosh[2a\pi] - cos[2b\pi])} \tag{3.1.21}$$

Using these formula, the summation over ω in (3.1.19) is given by

$$\sum_{-\infty}^{\infty}\int dk^2\left(\frac{1}{(\omega+C)^2+k^2} - \frac{1}{\omega^2+k^2}\right) \\ = \int dk^2\frac{\beta}{2k}\left(\frac{sinh\beta k}{cosh\beta k - cos\beta C} - \frac{sinh\beta k}{cosh\beta k - 1}\right) = \ln(cosh\beta k - cos\beta C) - \ln(cos\beta k - 1). \tag{3.1.22}$$

The integration constant is fixed by requiring that the above integral vanishes for $C = 0$.

Using eqn. (3.1.22), F_1 can be written as,

$$F_1 = \int d^3k \ln(1 - 2cos\beta C e^{-\beta k} + e^{-2\beta k}) + \int d^3k \ln(1 - 2e^{-\beta k} + e^{-2\beta k}). \tag{3.1.23}$$

The second term is singular but independent of C. Following the above steps to carry out summation over ω for the 5th and 7th term in (3.1.17) we get the result,

$$\sum_{-\infty}^{\infty} \int d^3k \left(\ln(\omega + C)^2 - \ln\omega^2\right) = \int d^3k \ln(1 - cos\beta C) + \bar{f}(\beta). \tag{3.1.24}$$

$\bar{f}(\beta)$ is independent of C. From (3.1.17), (3.1.23) and (3.1.24), we arrive at the following expression for the effective potential

$$V_{eff}(C) = -\frac{F(\beta, C)}{V} = \frac{1}{2\beta(2\pi)^3} \int d^3k \{4\ln(1 - 2cos\beta C e^{-\beta k} + e^{-2\beta k}) + 2\ln(1 - cos\beta C)\} \\ -\frac{1}{\beta} \int \frac{d^3k}{(2\pi)^3} \ln(1 - \cos\beta C) + f'(\beta). \tag{3.1.25}$$

The last term $f'(\beta)$ independent of C, hence can be dropped from the effective potential. The measure/ghost term cancels the longitudinal gluon contribution, so we have,

$$\begin{aligned} V_{eff}(C) &= \frac{1}{2\beta} \int \frac{d^3k}{(2\pi)^3} 4\ln(1 - 2\cos\beta C e^{-\beta k} + e^{-2\beta k}) \\ &= \frac{2}{(2\pi)^3\beta^4} \int dx\, x^2 \ln(1 - 2cos\beta C e^{-x} + e^{-2x}). \end{aligned} \tag{3.1.26}$$

The $x-$integration is carried out by writing the factor,

$$\begin{aligned} \ln(1 - 2cos\beta C e^{-x} + e^{-2x}) &= \ln(1 - e^{-x}e^{i\beta C}) + \ln(1 - e^{-x}e^{-i\beta C}) \\ &= 2\mathrm{Re}[\ln(1 - e^{-x}e^{i\beta C})] \\ &= -2\sum_{n=1}^{n=\infty} \frac{e^{nx} cos(n\beta C)}{n}. \end{aligned} \tag{3.1.27}$$

Using the above series form for $\ln(1 - 2cos\beta C e^{-x} + e^{-2x})$ in (3.1.26) we get,

$$\begin{aligned} V_{eff}(C) &= -\frac{1}{2(2\pi)^3\beta^4}\sum_{1}^{\infty}\frac{cos(n\beta C)}{n^4} \\ &= -\frac{2\pi^2}{\beta^4}\left(\frac{1}{45} - \frac{1}{24}\left[1 - \left[\left(\frac{\beta C}{\pi}\right)_{mod2} - 1\right]^2\right]^2\right). \end{aligned} \tag{3.1.28}$$

Equation (3.1.28) is the effective potential for the Polyakov loop considering fluctuations upto one loop. The potential is periodic in βC with period 2π. In the following Fig. 3.1, we plot the effective potential as a function of βC [37]. There are two degenerate minima at $\beta C = 0$ and $\beta C = 2\pi$. These two values of βC correspond to $L = 1$ and $L = -1$, so there is spontaneous breaking of Z_2 symmetry. The value of effective potential at the degenerate minima corresponds to the free energy of an ideal gas of gluons. Note that the results do not depend on the gauge coupling constant g.

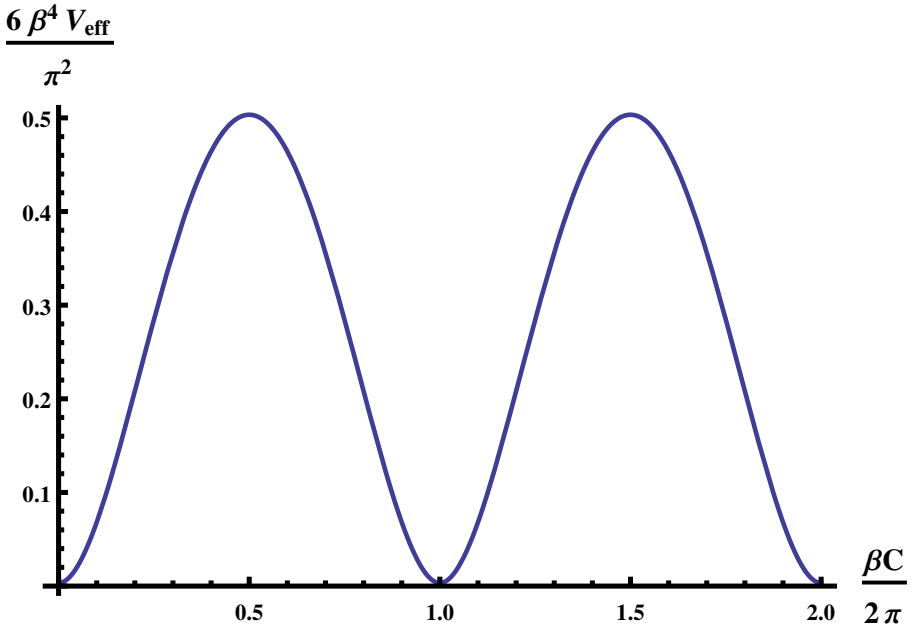

Figure 3.1. $\frac{6\beta^4 V_{eff}}{\pi^2}$ vs $\frac{\beta C}{2\pi}$ is plotted for SU(2).

The barrier between the minima decreases with temperature. For small enough height of the barrier there will be fluctuations connecting the minima. So it is possible that this will result in a distribution of the Polyakov loop in physical space, such that equal spatial volume fraction in $L = 1$ and $L = -1$. Such a state will have properties of confinement

as the thermal average of the Polyakov loop will vanish. The perturbative calculations of effective potential for SU(3) slightly involved but show spontaneous breaking of the Z_3 symmetry. In the following, we briefly review the effective potential calculations for the Polyakov loop in the presence Higgs field. We will restrict our discussions to ideal gas of Higgs bosons coupled to the SU(2) gauge fields.

3.2 Effective potential for SU(2)+Higgs theory

In this section, we describe the derivation of the effective potential for the Polyakov loop for SU(2) gauge theory in the presence of Higgs fields in the fundamental representation. The calculations are only upto one loop [6, 46]. The effective potential calculations in the presence of Higgs field proceeds similar to the last section. The partition function for SU(2)+Higgs theory with vanishing quartic coupling is given by,

$$Z = N \int [D\Phi^{\dagger}][D\Phi][\mathcal{D}(g\beta A_0)][DA_i] \exp(-S_E), \tag{3.2.1}$$

with the Euclidean action,

$$\begin{aligned} S_E = \frac{1}{2} \int_0^{\beta} dt \int d^3x \, \{ & [(\partial_0 A_i - \partial_i A_0 + g A_0 \times A_i)^2 + B^2] \\ & + \frac{1}{2} (D_\mu \Phi)^{\dagger} (D_\mu \Phi) + \frac{m_H^2}{2} \Phi^{\dagger} \Phi \}. \end{aligned} \tag{3.2.2}$$

The covariant derivative $D_\mu \Phi = \partial_\mu \Phi + i g A_\mu \Phi$. As in the previous section, the gauge field A_0 is considered to be $A_0^a = \delta_{a3} \phi(\mathbf{x})$. With this choice of A_0 the action is minimized by

$$\phi(\mathbf{x}) = \frac{C}{g}, A_i^a = 0, \Phi = 0. \tag{3.2.3}$$

Here C is independent of $\mathbf{x}$. The Euclidean action vanishes at the minimum. The full fields expanded around the minima as,

$$\phi(\mathbf{x}) = \frac{C}{g} + \delta\phi(\mathbf{x}), A_i^a = \delta A_i^a(x), \Phi(x) = \delta\Phi(x). \tag{3.2.4}$$

Assuming the fluctuations $\delta\phi(\mathbf{x})$, $\delta A_i^a(x)$ and $\delta\Phi(x)$ are small, the action (3.2.2) is expanded around the minimum configuration (3.2.4). When the fluctuations are considered upto one loop, i.e terms which are upto 2nd order in the fluctuations, the gauge part and matter part separate. However the temporal covariant derivative of the Higgs field still depends on the zero mode of $\phi(\mathbf{x})$, i.e $\frac{C}{g}$. Hence we need here only to consider the effective potential for the Polyakov loop coming only from the Higgs field. The part for the gauge fields can be taken over from the previous section. The relevant partition function is now given by,

$$Z \propto \int [D\Phi^\dagger][D\Phi]\exp[-\frac{1}{2}\left(\frac{\partial\delta\Phi^\dagger}{\partial\tau} + \frac{iC}{2}\delta\Phi^\dagger\right)\left(\frac{\partial\delta\Phi}{\partial\tau} - \frac{iC}{2}\delta\Phi\right) - \frac{1}{2}\nabla\Phi^\dagger\nabla\Phi - \frac{m_H^2}{2}\Phi^\dagger\Phi]. \tag{3.2.5}$$

This partition function is that of an ideal bosonic gas with an imaginary chemical potential iC. Note that $\Phi(x)$ is a doublet field. So the partition function (3.2.1), for the choice of A_0 field, will be square of the partition function of a complex scalar field. We follow the computation [55], of the partition function of a complex scalar field $\Phi(x) = \phi_1(x) + i\phi_2(x)$. As in the previous section the fields, now $\delta\phi_1(x)$ and $\delta\phi_2(x)$, are expressed in Fourier modes,

$$\delta\phi_1(x,\tau) = \sqrt{\frac{\beta}{V}}\sum_{\omega,k} e^{i(\mathbf{k}.\mathbf{x}+\omega\tau)}\phi_1(\omega,k) \tag{3.2.6}$$

$$\delta\phi_2(x,\tau) = \sqrt{\frac{\beta}{V}}\sum_{\omega,k} e^{i(\mathbf{k}.\mathbf{x}+\omega\tau)}\phi_2(\omega,k), \tag{3.2.7}$$

Since the Higgs field must be periodic in the temporal direction, $\omega = \frac{2\pi n}{\beta}$ with integer n. The partition function in terms of the Fourier modes is given by,

$$Z = N \prod_{\omega} \prod_{k} \int d\phi_1(\omega, k) d\phi_2(\omega, k) e^{-S}, \tag{3.2.8}$$

where

$$S = \frac{1}{2} \sum_{\omega} \sum_{k} \begin{pmatrix} \phi_1(-\omega, -k) & \phi_2(-\omega, -k) \end{pmatrix} M \begin{pmatrix} \phi_1(\omega, k) \\ \phi_2(\omega, k) \end{pmatrix} \tag{3.2.9}$$

where

$$M = \begin{pmatrix} \beta^2(\omega^2 + \omega_k - \mu^2) & -2\mu\omega \\ 2\mu\omega & \beta^2(\omega^2 + \omega_k - \mu^2) \end{pmatrix}. \tag{3.2.10}$$

Here $\omega_k = \sqrt{(k^2 + m_H^2)}$ and $\mu = \frac{iC}{2}$. The matrix M can be diagonalized. The integrations of the Fourier modes gives the partition function in terms of the eigen values is given by,

$$\begin{aligned} \ln\mathcal{Z} &= -\frac{1}{2} \ln \left\{ \prod_{\omega} \prod_{k} \beta^2 \left(\omega^2 + (\omega_k - \mu)^2 \right) \right\} + -\frac{1}{2} \ln \left\{ \prod_{\omega} \prod_{k} \beta^2 \left(\omega^2 + (\omega_k + \mu)^2 \right) \right\} \\ &= -\frac{1}{2} \sum_{\omega} \sum_{k} \ln \left\{ \beta^2 \left(\omega^2 + (\omega_k - \mu)^2 \right) \right\} + -\frac{1}{2} \sum_{\omega} \sum_{k} \ln \left\{ \beta^2 \left(\omega^2 + (\omega_k + \mu)^2 \right) \right\}. \end{aligned} \tag{3.2.11}$$

The summation over ω can be carried out as in the previous section using the formula (3.1.22). Replacing μ by $\frac{iC}{2}$ the resulting expression for the logarithm of the partition function given by,

$$\ln\mathcal{Z} = -\sum_{k} \left\{ \beta\omega_k + \ln\left(1 - e^{-\beta(\omega_k - \frac{iC}{2})}\right) + \ln\left(1 - e^{-\beta(\omega_k + \frac{iC}{2})}\right) \right\} \tag{3.2.12}$$

The first term is independent of C, so can be dropped from the effective potential $V_h(\beta, C) = \frac{\ln\mathcal{Z}}{\beta V}$, where V is the spatial volume.

$$V_h(\beta, C) = \frac{2}{\beta} \int \frac{d^3k}{(2\pi)^3} \left\{ \ln\left(1 - e^{-\beta(\omega_k - \frac{iC}{2})}\right) + \ln\left(1 - e^{-\beta(\omega_k + \frac{iC}{2})}\right) \right\} \tag{3.2.13}$$

The factor 2 above is to account for the Higgs doublet. The integration over k can be carried out for massless case ($m_H = 0$) as in the last section. The effective potential contribution from the Higgs $V_h(\beta, C)$ in this case is given by,

$$V_h(C) = -\frac{2\pi^2}{\beta^4}\left(\frac{1}{45} - \frac{1}{24}\left[1 - \left[\left(\frac{\beta C}{2\pi}\right)_{mod2} - 1\right]^2\right]^2\right). \tag{3.2.14}$$

So for massless Higgs V_h is periodic over $\beta C = 4\pi$. As a result $\beta C = 0$ and $\beta C = 2\pi$ do not have same value of V_h. As a result $L = -1$ and $L = -1$ are non-degenerate. Clearly the Z_2 symmetry is explicitly broken for $m_H = 0$ as shown in Fig. 3.2 , with $L = 1$ is the only ground state. $L = -1$ corresponds to the peak of the Fig. 3.2. The strength of the

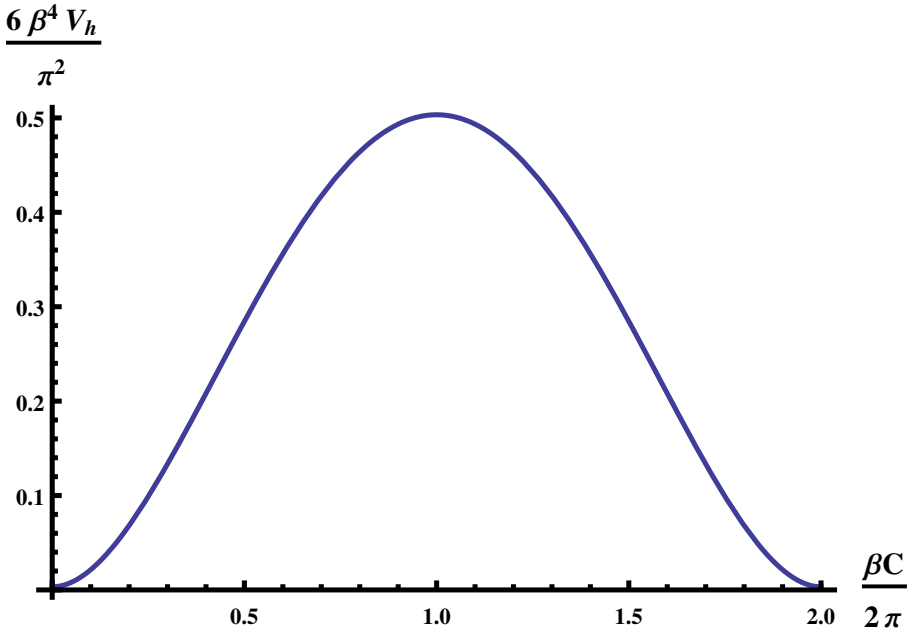

Figure 3.2. $\frac{6\beta^4 V_h}{\pi^2}$ vs $\frac{\beta C}{2\pi}$ is plotted for SU(2)+Higgs when $m_H = 0$.

explicit symmetry breaking will decrease with m_H. It is clear that in the limit $m_H = \infty$, V_h will not have any C dependence, restoring the Z_2 symmetry. For number of Higgs doublets. The full effective potential $V_g + V_h$ has a local minimum at $L = -1$, a meta-stable state. The explicit symmetry breaking increases with number of Higgs doublets. For four Higgs doublets the meta-stable state at $L = -1$ disappear. For number of Higgs doublets $N_b > 4$, there will be a critical $m_H(N_b)$ below which there will be no meta-stable

states. The one loop calculations show that the Z_2 (Z_N) symmetry is explicitly broken by the presence of the Higgs fields. However these fields couple only to the zero mode of the A_0, A_i fields at 1−loop. In the pure gauge case these modes give rise to the Z_2 symmetry of the effective potential. Therefore one should couple these modes also with the Higgs field to see explicit breaking of the Z_2 (Z_N) symmetry. Though the perturbative calculations have been successful in demonstrating the Z_N symmetry and its explicit breaking in the effective potential of the Polyakov loop, these calculations are not reliable near the CD transition. The gauge coupling is expected to grow as the temperature is lowered towards T_c and so also the fluctuations.

4 Strong coupling methods

Perturbative studies on Z_N symmetry in gauge theories are limited to high temperatures away from the transition region. These studies are not reliable as both the gauge coupling, fluctuations are large near the CD transition. In this strong coupling limit mean field approximation offer understanding of the Z_N symmetry and the CD transition. For SU(N) with dynamical quarks [15], these studies show that the inverse of the quark mass play the role of an external field for the Polyakov loop. For SU(3) as the quark masses decreases the first order CD transition becomes weaker. For a critical value of the quark masses the transition becomes second order. Further decrease in the masses lead to a crossover CD transition. These results are in qualitative agreement with non-perturbative studies [9]. In the strong coupling limit, mean field study of the SU(2)+Higgs theory have shown that the CD transition is a crossover for finite Higgs mass [38].

In this chapter, we derive the lattice action for SU(N) Higgs theory. Following this we derive the mean field studies of Z_N symmetry and CD transition in the strong coupling limit focusing on $N = 2$.

4.1 Discretization of continuum SU(N)+Higgs action on the lattice

Partition function for SU(N)+Higgs theory is given by,

$$\mathcal{Z} = \int [DA][D\Phi]\, e^{-S_E[A,\Phi]} \tag{4.1.1}$$

Where $S_E[A, \Phi]$ is the Euclidean action which describes the interaction of the gauge field $A_\mu(x_E)$ and the Higgs field $\Phi(x_E)$ and is given by (2.2.15).

$$S_E[A, \Phi] = \int_V d^3x \int_0^\beta d\tau \left\{ \frac{1}{2}\mathrm{Tr}\left(F^{\mu\nu}F_{\mu\nu}\right) + \frac{1}{2}(D_\mu\Phi)^\dagger(D_\mu\Phi) + \frac{\bar{m}^2}{2}\Phi^\dagger\Phi + \frac{\bar{\lambda}}{4!}(\Phi^\dagger\Phi)^2 \right\} \tag{4.1.2}$$

Here x_E is the Euclidean four vector, gauge field(A) is $N \times N$ traceless matrix and Higgs field Φ is a $1 \times N$ complex scalar field. The Higgs field Φ is in the fundamental representation of SU(N).

We first consider discretization of the gauge fields. The corresponding gauge action is given by,

$$S_E[A] = \int_V d^3x \int_0^\beta d\tau\, \frac{1}{2}\left[\mathrm{Tr}(F_{\mu\nu}F_{\mu\nu})\right]. \tag{4.1.3}$$

This theory in (4.1.3) can be regularized by discretizing it on a four dimensional lattice. The four space-time vector $x_E(\mathbf{x}, \tau)$ is replaced by na, where n is the co-ordinate of the Euclidean lattice, i.e $n = (n_1, n_2, n_3, n_4)$. For a lattice $N_s^3 \times N_\tau$, there are N_τ points in temporal direction and N_s points in (x,y,z) directions. Given a lattice spacing "a", the temperature is given by $T = \frac{1}{aN_\tau}$ and the size of the given system is given by $L = N_s a$. The gauge fields are defined only on the lattice points i.e $A_\mu(n)$ and the action is written in-terms of these discretized fields. The requirement of any discrete lattice action is that it should lead to the continuum action in the limit $a \to 0$. If the continuum action has gauge symmetry than the discretized action must be gauge invariant under gauge transformations

defined on the lattice. Instead of the discretized gauge field $A_\mu(n)$ the lattice action is written in terms of gauge link $U_{n,\mu} = e^{iagA_\mu(n)}$. $U_{n,\mu}$ is the link connecting lattice site n and $n + \hat{\mu}$, where $\hat{\mu}$ is a unit vector in the μth direction, with ($\mu = 1, 2, 3, 4$). Since $A_\mu = A^a_\mu T^a$ the gauge links $U_{n,\mu}$ are SU(N) matrices. Under a gauge transformation V_n, the gauge links transform as,

$$U_{n,\mu} \rightarrow V_n U_{n,\mu} V^{-1}_{n+\hat{\mu}}. \tag{4.1.4}$$

It can be shown that this leads to eqn.(2.3.1) in the continuum limit. Due to the transformation property of the links, the gauge invariant objects can be formed purely from the trace of path ordered product of links along closed loops. The simplest path ordered product of links along an elementary square is called a plaquette as given by,

$$U_P = U_{n,\mu} U_{n+\hat{\mu},\nu} U^\dagger_{n+\hat{\nu},\mu} U^\dagger_{n,\nu} \tag{4.1.5}$$

The plaquette U_p with co-ordinate n lies in the $\mu - \nu$ plane. Here $U^{-1}_{n,\mu} = U^\dagger_{n,\mu}$ and $1 \leq \mu < \nu \leq 4$. A sketch of an gauge link elementary plaquette defined in the counterclockwise

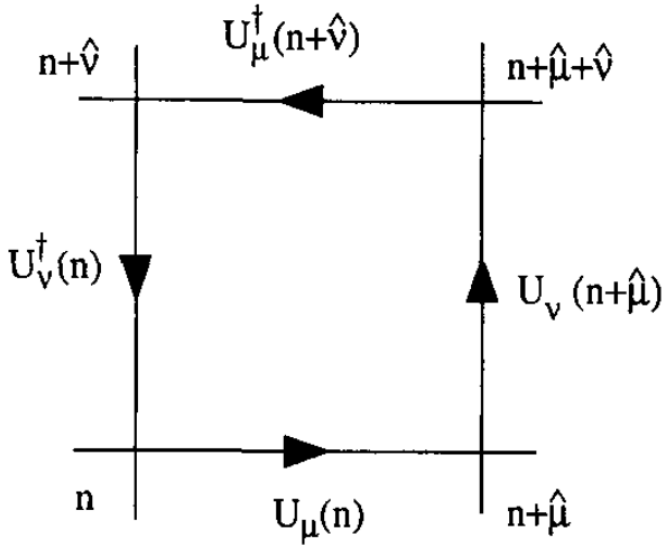

Figure 4.1. Sketch of an elementary plaquette U_P

direction is shown in Fig. 4.1 and the notation $U_\mu(n)$ in figure is same as $U_{n,\mu}$. Using

Baker-Campbell-Housdorff formula,

$$e^A e^B = e^{A+B+\frac{1}{2}[A,B]+\ldots} \tag{4.1.6}$$

one can relate the plaquette with the gauge field strength tensor,

$$U_P = e^{ia^2 g F_{\mu\nu}(n)} \tag{4.1.7}$$

The exponential term in U_P can be expanded as follows for small lattice spacing a,

$$\begin{aligned} U_P &= 1 + ia^2 g F_{\mu\nu}(n) - \frac{a^4 g^2}{2}[F_{\mu\nu}(n)]^2 - i\frac{a^6 g^3}{6}[F_{\mu\nu}(n)]^3 + \ldots \\ U_P^\dagger &= 1 - ia^2 g F_{\mu\nu}(n) - \frac{a^4 g^2}{2}[F_{\mu\nu}(n)]^2 - i\frac{a^6 g^3}{6}[F_{\mu\nu}(n)]^3 + \ldots \end{aligned} \tag{4.1.8}$$

Adding the above two equations, taking trace both sides and rearranging, we have,

$$\mathrm{Tr}[F_{\mu\nu}(n)]^2 + O(a^2) \simeq \frac{1}{a^4 g^2}\mathrm{Tr}\left[2 - U_P - U_P^\dagger\right] \tag{4.1.9}$$

The four-dimensional volume integral is discretized as,

$$\int d^4 x_E \to a^4 \sum_n \tag{4.1.10}$$

Making use of the above discretized form of space and eqn. (4.1.9), we have the discretized action,

$$S_G[U] = \beta_g \sum_P \left[1 - \frac{1}{2N}\mathrm{Tr}\left(U_P + U_P^\dagger\right)\right]. \tag{4.1.11}$$

Here $\beta_g = \frac{2N}{g^2}$ is the gauge coupling. The sum over plaquette takes care of the extra factors. As $a \to 0$ the discretized action in (4.1.11) approaches to the continuum action (4.1.3) upto an error of $O(a^2)$.

For the Higgs discretization the relevant action is

$$S_E[\Phi] = \int_V d^3x \int_0^\beta d\tau \left\{ \frac{1}{2}(D_\mu \Phi)^\dagger (D_\mu \Phi) + \frac{\bar{m}^2}{2}\Phi^\dagger \Phi + \frac{\bar{\lambda}}{4}(\Phi^\dagger \Phi)^2 \right\}. \tag{4.1.12}$$

The Higgs fields live on the lattice sites $\Phi(na)$. The lattice variables are obtained by making the following substitutions,

$$\begin{aligned} \Phi(x_E) &\to \Phi(n) \\ \int d^4x_E &\to a^4 \sum_n \\ \Box\Phi(x_E) &\to \frac{1}{a^2}\hat{\Box}\Phi(n) \\ D_\mu\Phi(x_E) &\to D_\mu\Phi(n). \end{aligned} \tag{4.1.13}$$

where

$$\begin{aligned} \hat{\Box}\Phi(n) &= \sum_\mu [\Phi(n+\hat{\mu}) + \Phi(n-\hat{\mu}) - 2\Phi(n)] \\ \partial_\mu\Phi(n) &= [\Phi(n+\hat{\mu}) - \Phi(n)] \\ D_\mu\Phi(n) &= \partial_\mu\Phi(n) + \frac{(1-U_\mu)}{a}\Phi(n). \end{aligned} \tag{4.1.14}$$

Following the above discretized form of field, derivative and double derivative, the total action in (4.1.2) can be expressed in terms of discretized variables like given below,

$$\begin{aligned} S[U,\Phi] = \sum_n \Bigg[\beta_g \sum_P [1 - \frac{1}{2N}\mathrm{Tr}(U_P + U_P^\dagger)] + \frac{8a^2}{2}\mathrm{Tr}(\Phi_n^\dagger \Phi_n) \\ -a^2 \sum_\mu \mathrm{ReTr}(\Phi_{n+\mu}^\dagger U_{n,\mu} \Phi_n) - \frac{\bar{m}^2 a^4}{2}\mathrm{Tr}(\Phi_n^\dagger \Phi_n) + \frac{\bar{\lambda} a^4}{2}\mathrm{Tr}(\Phi_n^\dagger \Phi_n)^2. \end{aligned} \tag{4.1.15}$$

In the following, we describe mean field approximation of the strong coupling limit of the above theory.

4.2 Strong coupling expansion in SU(2)+Higgs theory

The study of confinement-deconfinement transition in the presence of dynamical matter fields require non-perturbative lattice simulations. However the lattice partition function for analytic studies in the strong coupling limit, $\beta_g \rightarrow 0$. The confinement of static color charges can be analytically demonstrated in this regime. The mean field approximations coupled with strong coupling techniques provide qualitative understanding of the CD transition in the presence of dynamical matter fields. Previous study of SU(N) gauge theory with dynamical quarks show that the effect of dynamical quarks is equivalent to an external field on the Polyakov loop [15]. The effective external field is given by $2n_f\ (\kappa^{N_\tau})$, where n_f is number of flavors, κ is the hopping parameter. The hopping parameter vanishes in the limit of infinite heavy quarks. Similar studies have been done in SU(N) theory with dynamical bosons [38]. Here we describe these calculations with $\lambda = 0$ for SU(2)+Higgs theory. The lattice Euclidean partition function is given by,

$$Z = \int [DU][D\Phi]\ e^{\beta_g \sum_P \{1-\frac{1}{2N}[\mathrm{Tr}U_P+\mathrm{Tr}U_P^\dagger]\}-\sum_{n,m}\Phi_n^\dagger Q_{\mu,nm}\Phi_m} \tag{4.2.1}$$

In the pure gauge part of the action, the constant term can be ignored as it gives rise to a overall constant factor. $Q_{\mu,nm}$ is given by,

$$Q_{\mu,nm} = \frac{1}{2}[\delta_{n,m}\mathbb{1} - 2\kappa[\delta_{n,m-\mu}U_{n,\mu} + \delta_{n,m+\mu}U_{n,\mu}^\dagger]]. \tag{4.2.2}$$

where κ is the hopping parameter given by $\frac{1}{m_H{}^2a^2+8}$. The Higgs part in the partition function (4.2.1) is Gaussian, therefore the Higgs field integration can be carried out exactly. After integrating the Higgs fields, the partition function in terms of the remaining $U_{n,\mu}$'s is given by,

$$Z = \int [DU]\ e^{\beta_g \sum_P \{\frac{1}{2N}[(\mathrm{Tr}U_P+\mathrm{Tr}U_P^\dagger)]\}-\frac{1}{2}\mathrm{Trln}Q}. \tag{4.2.3}$$

We can ignore the factor $\frac{1}{2}$ in Q as it will only lead to a constant factor multiplying the partition function, therefore will not affect the behavior of the CD transition. We first consider the partition function without the Higgs part, $\kappa = 0$. In the strong coupling limit $\beta_g \to 0$, spatial plaquettes can be ignored [48, 49, 56] as they are not crucial for the CD transition. Therefore, the spatial links can be integrated out resulting in following partition function in terms of character expansion,

$$Z_{eff}(\kappa = 0) = \int \prod_n dW_n \prod_{n,e} \left[1 + \sum_r z_r(\beta)^{N_\tau} \chi_r(W_n) \chi_r(W^\dagger_{n+e}) \right] \tag{4.2.4}$$

Here $n = (n_1, n_2, n_3)$ and W_n is,

$$W_n = \left[\prod_{n_4=1}^{N_\tau} U_{(n,n_4),4} \right], \tag{4.2.5}$$

the Polyakov loop/Wilson line variable, χ_r represents character of the r fundamental representation of the group and z_r's are the character coefficients. z_r's can be expressed in terms of series expansion of β_g, and are increasingly higher order in β_g as r increases. In the strong coupling limit i.e small enough β_g, the term corresponding to the fundamental representation $r \equiv (1:0)$ will dominate in eqn. (4.2.4) [57]. The partition function with only the contribution of the fundamental representation is given by,

$$Z_{eff}(\kappa = 0) \cong \int \prod_n dW_n \, e^{\beta' \sum_{n,e} [\mathrm{Tr} W_n \mathrm{Tr} W^\dagger_{n+e} + c.c]} \tag{4.2.6}$$

For SU(2), $\beta' = \frac{1}{2} \left[\frac{I_2(\beta_g)}{I_1(\beta_g)} \right]^{N_\tau}$, where $I_n(\beta_g)$ is the modified Bessel function of order n. Eqn. (4.2.6) is the effective theory for the Polyakov loop in the strong coupling limit. Deriving the effective potential for the Polyakov loop from the above partition function is difficult due to the integration measure dW. But this theory can be used to study the CD transition in the mean field approximation. Note that the effective theory is manifestly Z_N invariant. The symmetry can be realized by looking at the transformation property of the Polyakov loop which under the global Z_N transformation transforms $W \to zW$, where $z \in Z_N$. In the

action z and $z^\dagger$ can cancel each other leaving it invariant. The partition function (4.2.6) looks similar to that of a ferromagnetic Z_N spin system.

In the limit of large but finite bare Higgs mass, the hopping parameter is small. In this limit, one can expand $\ln\det Q$ in powers of κ,

$$\ln\det Q = \mathrm{Tr}\ln Q = -\sum_l \mathrm{Tr}(\frac{\kappa^l}{l} M^l) \tag{4.2.7}$$

Where $M = \delta_{n,m-\mu} U_{n,\mu} + \delta_{n,m+\mu} U^\dagger_{n,\mu}$ and $\kappa \to 2\kappa$ .The sum in eqn. (4.2.7) is over all closed loops of length l in units of a. For $N_\tau < 4$ the leading term is given by,

$$\ln\det Q \simeq -h \sum_n [\mathrm{Tr}W_n + \mathrm{Tr}W_n^\dagger]. \tag{4.2.8}$$

Here $h = (2\kappa)^{N_\tau}$. This contribution comes from hopping in the temporal direction. The effective partition function for the gauge Higgs system in the strong coupling limit for $N_\tau < 4$ is given by

$$Z_{eff} = \int \prod_n dW_n \exp\left[\beta' \sum_{n,e} [\mathrm{Tr}W_n \mathrm{Tr}W^\dagger_{n+e} + c.c] + h \sum_n [\mathrm{Tr}W_n + \mathrm{Tr}W_n^\dagger]\right] \tag{4.2.9}$$

The partition function (4.2.9) is now not invariant under the Z_2 symmetry due to last two terms in the effective action. The free energy can be calculated from the partition function by

$$F = -\frac{1}{V} \ln Z_{eff} \tag{4.2.10}$$

To calculate the free energy in the mean field approximation, each Wilson loop on site n is considered to be under the influence of an average field J, trace of an SU(2) matrix. This is achieved by replacing the nearest neighbor Polyakov loop/Wilson line $\mathrm{Tr}(W_{n+\mu})$, $(\mu \to 1....2d)$, by $V = J/2d$. d is the number of spatial dof. Now the partition function for

the Polyakov loop/Wilson line TrW at site n is given by,

$$Z_{ss}(J, J^\dagger) = \int [dW] \exp\left[\beta'(\mathrm{Tr}W\ J^\dagger + J\ \mathrm{Tr}W^\dagger) + h[\mathrm{Tr}W + \mathrm{Tr}W^\dagger]\right] \tag{4.2.11}$$

Here $Z_{ss}(J, J^\dagger)$ is the single site partition function in the mean field approximation. The free energy is given by,

$$F_{ss} = -\ln(Z_{ss}) \tag{4.2.12}$$

A self consistent condition is imposed, in which the partition function average of the Polyakov loop/Wilson line at site i equals the mean field V_k of the neighboring sites,

$$\langle W \rangle = V = J/2d \tag{4.2.13}$$

From equations (4.2.12) and (4.2.13), we can write the following condition,

$$\frac{-1}{\beta'}\frac{\partial F_{ss}}{\partial J^\dagger} = \frac{1}{2d}J \tag{4.2.14}$$

A free energy F_{MF} is written in terms of the mean field J [58],

$$F_{MF} = \frac{\beta'}{2d}\mathrm{Tr}J^\dagger J + F_{ss}(J, J^\dagger) \tag{4.2.15}$$

So that at the extremum condition,

$$\frac{\partial F_{MF}}{\partial J^\dagger} = 0 \tag{4.2.16}$$

one recovers equation (4.2.14). The free energy (4.2.12) can be evaluated exactly for SU(2) [59]. For SU(2), Tr(W) and J are real. The self consistent condition, eqn. (4.2.13) can be written as,

$$\mathrm{Tr}(W) = \frac{2I_2(12\beta'\mathrm{Tr}(W) + 4h)}{I_1(12\beta'\mathrm{Tr}(W) + 4h)} \tag{4.2.17}$$

To solve the equation (4.2.17) numerically we consider $L = \frac{1}{2}\langle \mathrm{Tr}(W)\rangle$. When $h = 0$, the above equation has always a solution for $L = 0$. For $\beta_g > (\beta_{gc} = 1.8512)$, there appears three solutions $(0, L, -L)$. For $\beta_g > \beta_{gc}$, the mean field free energy calculation show that the solutions L and $-L$ only correspond to the minima of the free energy. For β_g near above β_{gc} has singular behavior implying a second order phase transition as in seen Fig. 4.2. In this case the theory has Z_2 symmetry, and is spontaneously broken above β_{gc}.

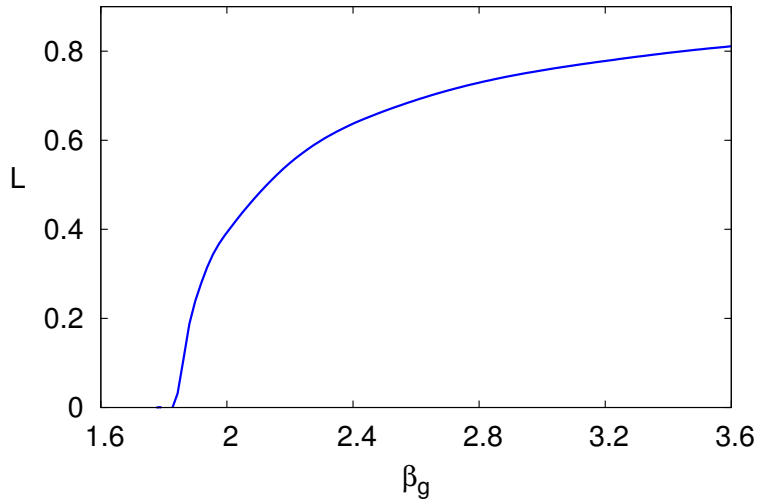

Figure 4.2. Polyakov loop plotted as a function of β_g for $N_\tau = 2$ and $h = 0$.

For $h \neq 0$, there are no pair solutions $(L,-L)$ of eqn. (4.2.17) as in $h = 0$. If L is the solution of eqn. (4.2.17) then $-L$ is not a solution. This shows that the Z_2 symmetry is explicitly broken. In figure we show $L(\beta_g, h)$ for $h = 0.0225, 0.1$ values of h.

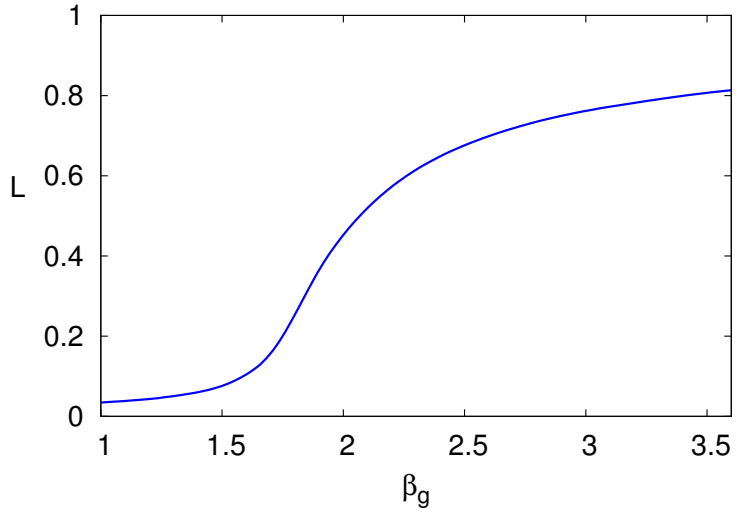

Figure 4.3. Polyakov loop plotted as a function of β_g for $N_\tau = 2$ and $h = 0.0225$.

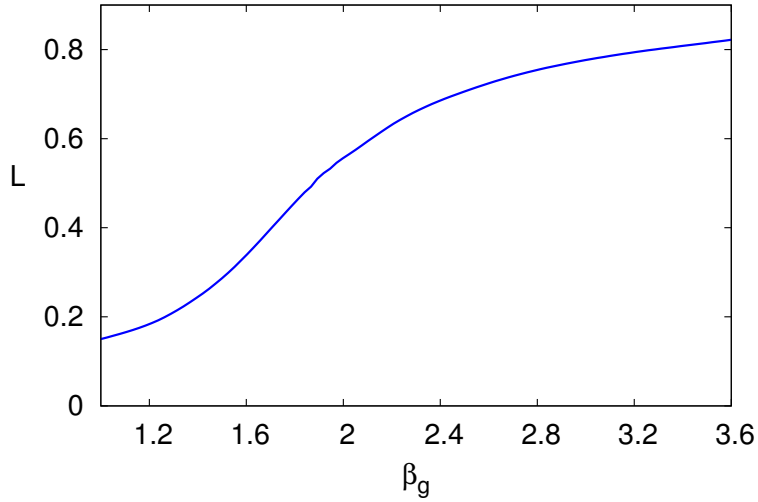

Figure 4.4. Polyakov loop plotted as a function of β_g for $N_\tau = 2$ and $h = 0.1$.

It is clearly seen form the Figs. 4.3 and 4.4 that with increase in h, decrease in Higgs mass, the dependence of L on β_g becomes increasingly smoother, suggesting that the transition is becoming weaker. These results do agree with the non-perturbative simulations for $N_\tau = 2$ [38]. It is however important to note that N_τ considered here is very small. For larger N_τ our simulation studies, presented in this thesis, show that the Z_2 symmetry is restored for all values of the bare Higgs mass.

5 Numerical Methods

In this chapter, we briefly discuss numerical methods which are used to perform Monte Carlo simulations of the lattice partition function of the SU(N)+Higgs theory. It is difficult to calculate the $SU(N)$+ Higgs partition function,

$$\mathcal{Z} = \int [DA][D\Phi] e^{(-S_E[A,\Phi])}, \tag{5.0.1}$$

analytically. This is because there are interaction terms such as, gauge field self coupling, Higgs quartic coupling interaction and gauge Higgs coupling. Perturbative treatment is possible when all the couplings are suitably small. Near the CD transition perturbative calculations are not reliable as couplings and fluctuations are not small. The problem becomes tractable on a finite lattice, where the degrees of freedom are finite. The partition function on lattice is given by ,

$$\mathcal{Z} = \int [DU_{n,\mu}][D\Phi_n] e^{(-S[U_{n,\mu},\Phi_n])} \tag{5.0.2}$$

The discretized lattice action is given by (4.1.15),

$$\begin{aligned} S[U_{n,\mu},\Phi_n] = \beta_g \sum_p \left(1 - \frac{1}{2N}\mathrm{Tr}(U_p + U_p^\dagger)\right) - \kappa \sum_{\mu,n} \mathrm{ReTr}\left[(\Phi^\dagger_{n+\mu} U_{n,\mu} \Phi_n)\right] \\ + \sum_n \left[\frac{1}{2}\mathrm{Tr}\left(\Phi_n^\dagger \Phi_n\right) + \lambda\left(\frac{1}{2}\mathrm{Tr}\left(\Phi_n^\dagger \Phi_n\right) - 1\right)^2\right] \end{aligned} \tag{5.0.3}$$

The above action is obtained from Eqn. (4.1.15) by scaling the Φ field parameters $\bar{\lambda}$ and the Higgs mass $\bar{m}$ [60] in the following way,

$$\Phi(x_E) \rightarrow \frac{\sqrt{\kappa}\Phi_n}{a},\ \bar{\lambda} \rightarrow \frac{\lambda}{\kappa^2},\ \bar{m}^2 \rightarrow \frac{(1-2\lambda-8\kappa)}{a^2\kappa} \tag{5.0.4}$$

All the field variables and parameters in the above action are now dimensionless. Numerically computing the above partition function, with number of integrations of the order of number of lattice points, is almost impossible. In numerical simulations, partition functions therefore are never computed. The problem becomes numerically tractable by realizing that given a set of parameters of the theory, not all configurations of $U_{n,\mu}$ and Φ_n contribute equally to the partition function. Only a fraction of the space in functional space contribute substantially to the partition function. In the Monte Carlo simulations, a sequence of statistically independent configurations of $(\Phi_n, U_{n,\mu})$ are generated. This is achieved by repeatedly updating an arbitrary initial configuration using numerical methods which maintain the Boltzmann probability factor e^{-S} and the principle of detailed balance among the configurations in the sequence. To update the gauge fields, we use the standard heat bath algorithm [11,61], and then update the Higgs fields using the pseudo-heat bath algorithm [13]. The gauge link updates and Higgs field updates are followed by over-relaxation steps which tend to reduce the correlation among the generated configurations [14]. To further reduce auto-correlation between successive configurations along the sequence (Monte Carlo history), we carry out ten cycles of this updating procedure between subsequent measurements.

5.1 Monte carlo techniques

Monte Carlo simulations sample configurations in the functional space according to their contribution to the partition function. The physical observables, their fluctuations and higher order cumulants on the lattice are calculated by averaging over the configurations

generated by Monte Carlo history. The sampling of the configurations in functional space by the Monte Carlo simulations must obey the following Markov chain rules,

- From any configuration of the system $A \equiv (U, \Phi)$, it must be possible to evolve the system to any other configurations $A' \equiv (U', \Phi')$by applying the evolution (Monte Carlo updates) a sufficiently large number of times, known as the ergodicity condition.

- The transition probabilities between two configurations must satisfy the detailed balance condition:

$$P(A)P(A|A') = P(A')P(A'|A) \tag{5.1.1}$$

  Where $P(A)$ and $P(A')$ are the Gibb's probabilities of states A and A' respectively. $P(A|A')$ is the transition probability of state from A to A' and $P(A'|A)$ is the transition probability of from A' to A.

The most important and simple algorithm based on the above Markov chain rules is the Metropolis-Hastings algorithm. The Metropolis-Hastings algorithm [62] consists of the following steps:

- Pick an initial configuration A_0;

- Set $t = 0$;

- Iterate

  Generate: randomly generate a new state A' from A_t according to $g(A'|A_t)$

- Calculate: calculate the acceptance probability

  $P_{acc}(A'|A_t) = \min\left(1, \frac{P(A')}{P(A_t)}\frac{g(A_t|A')}{g(A'|A_t)}\right)$;

  Here distribution $g(A_t|A')$ is the conditional probability of proposing a state A_t given A'.

- Accept/Reject: generate a uniform random number $r \in [0, 1]$;

  if $r \leq P_{acc}(A'|A_t)$, accept the new state and set $A_{t+1} = A'$;

  if $r > P_{acc}(A'|A_t)$, reject the new state, and copy the old state forward $A_{t+1} = A_t$;

- Increment: set $t = t + 1$;

5.2 Heat bath algorithm

The Metropolis algorithm is not efficient for simulations of SU(N) gauge theory. It is difficult to use Metropolis-Hastings algorithm for continuous variables. The heat bath algorithm improves on many shortcomings of the Metropolis algorithm. In the following, we will discuss the heat bath algorithm for SU(2). This same method is used to update SU(2) sub spaces of SU(N) matrices. Consider the following Wilson action for SU(2) gauge theory (4.1.11).

$$S[U] = \beta_g \sum_P [1 - \frac{1}{4}\text{ReTr}\,(U_P + U_P^\dagger)] = \beta_g \sum_P [1 - \frac{1}{2}\text{ReTr}\,U_P] \tag{5.2.1}$$

Since the trace of SU(2) matrices are real, there is only $\text{Tr}(U_P)$ in the action. To update any link U, we write an action S[U] by considering only terms in Eqn. (5.2.1) which depend on the link U. The link U appears in six plaquettes, so there are six terms in Eqn. (5.2.1). Let us denote the plaquettes by U_P, $P = 1, ...6$. Also let us denote the staple matrices connecting to the gauge link U by V_P, $P = 1, 2, ..6$. The action $S[U]$ is given by,

$$S[U] \sim \left(6 - \frac{\beta_g}{2}\text{ReTr}\sum_{P=1,2,..6}(UV_P)\right) \tag{5.2.2}$$

Since U and V_P's are SU(2) matrices, we can write $\sum_P \text{Tr}(UV_P) = \text{Tr}(U\sum_P V_P) = \bar{c}\text{Tr}(UV)$, where $\bar{c}V = \sum_P V_P$. Note that sum of two SU(2) matrices is an SU(2) matrix upto an overall factor. Therefore, V is a SU(2) matrix and the action $S[U]$ is given

by,

$$S[U] \sim (6 - c\mathrm{ReTr}(UV)), \quad c = \frac{\bar{c}\beta_g}{2} \tag{5.2.3}$$

Given the above action the probability distribution of the link U is given by,

$$P[U]dU \propto \exp(c\mathrm{ReTr}(UV))\, dU \tag{5.2.4}$$

Further we replaces $U \rightarrow UV^{-1} = W$ in the above equation, which gives

$$P[W]dW \propto \exp(-(c/2)\mathrm{Tr}(U))\, dW \tag{5.2.5}$$

Since the group measure is invariant under $U \rightarrow W$, one can generate U matrix according to the probability

$$P[U]dU \propto \exp(-(c/2)\mathrm{Tr}(U))\, dU \tag{5.2.6}$$

and then replace it with UV^{-1}. To generate U according to the above probability, U is written in the following form,

$$U = a_0 \mathbb{1} + i\vec{a}.\vec{\sigma} \tag{5.2.7}$$

$\vec{\sigma} = (\sigma_1, \sigma_2, \sigma_3)$ are the Pauli matrices. Now $\mathrm{Tr}(U) = 2a_0$. So the probability $P[U]$ depends only on a_0. The vector $\vec{a}$ can take any value on the surface of a sphere whose radius is $\sqrt{(1 - a_0^2)}$. The Haar measure dU can be written as,

$$dU = da_0 da_i\, \delta(1 - a_0^2 - \vec{a}.\vec{a}). \tag{5.2.8}$$

In terms of the polar coordinates $(a_x, a_y, a_z) = (r, \theta, \phi)$

$$dU = \frac{1}{2}(1 - a_0^2)^{\frac{1}{2}} da_0 dr d\theta d\phi sin\theta\, \delta(r - (1 - a_0^2)^{\frac{1}{2}}). \tag{5.2.9}$$

This implies that

$$P(a_0)da_0 \propto (1 - a_0^2)^{\frac{1}{2}} \exp(ca_0)da_0 \tag{5.2.10}$$

Conventionally two methods, Creutz method [11] and Kennedy-Peddleton method [61], are used to generate a_0 with the above probability distribution. In the Creutz method a_0 is generated using the exponential part of the above distribution. Then accept/reject the generated a_0 using the rest of the probability distribution. This doesn't work when c is large as the generated values are close to c. For such values of 1, the rejection rate due to $(1 - a_0^2)^{\frac{1}{2}}$ factor is large. To improve on this, in ref. [61], it was suggested that eqn. (5.2.10) can be written in the following form,

$$P'(\delta)d\delta = N'^{-1}(1 - \frac{1}{2}\delta^2)^{\frac{1}{2}}\delta^2\exp(-c\delta^2)\, d\delta \tag{5.2.11}$$

With $\delta = (1 - a_0^2)^{\frac{1}{2}}$ and $(0 \leq \delta \sqrt{2})$,

For large c, the probability distribution has a peak near 0. δ is generated using the distribution

$$g(\delta)d\delta = \bar{N}^{-1}\delta^2\exp(-c\delta^2)\, d\delta \tag{5.2.12}$$

The above distribution is Gaussian-like distributions and can be generated easily by manipulating a Gaussian distribution [61]. The generated δ then can be accepted/rejected using the factor $(1 - \frac{1}{2}\delta^2)^{\frac{1}{2}}$. The following steps are used in the code.

- Generate two uniformly distributed pseudo-random numbers r and r' in the interval [0,1];
- Let $x \leftarrow -(lnr)/c$ and $x' \leftarrow -(Inr')/c$;
- Set $C \leftarrow cos^2(2\pi r_1)$, with r_1 is another uniform random number in [0,1] ;
- Let $A \leftarrow xC$;
- Let $\bar{\delta} \leftarrow x' + A$;

- If $r_2 > 1 - \frac{1}{2}\bar{\delta}$, for r_2 uniform pseudo-random in (0,1], go back to first step;
- Set $a_0 \leftarrow 1 - \bar{\delta}$.

The above updating method is repeated for each and every link of the lattice. The heat bath updates for the gauge links is further augmented by over-relaxation routine to reduce the auto-correlation of the gauge field correlations. In the over-relaxation procedure, each link is rotated so that the gauge action is invariant. This is achieved by rotating the link U in (5.2.3) by $U \rightarrow VUV^{-1}$. This over-relaxation step is repeated again for each and every link on the lattice.

5.3 Pseudo-heat bath algorithm

Let us consider the lattice action for the SU(2)+Higgs theory (4.1.15),

$$S[U,\Phi] = \beta_g \sum_p \left(1 - \frac{1}{4}\mathrm{Tr}(U_p + U_p^\dagger)\right) - \kappa \sum_{\mu,n} \mathrm{Re}\left[\mathrm{Tr}(\Phi_{n+\mu}^\dagger U_{n,\mu} \Phi_n)\right] + \sum_n \left[\frac{1}{2}\mathrm{Tr}\left(\Phi_n^\dagger \Phi_n\right) + \lambda\left(\frac{1}{2}\mathrm{Tr}\left(\Phi_n^\dagger \Phi_n\right) - 1\right)^2\right]. \tag{5.3.1}$$

For convenience the Higgs doublet above has been replaced by its magnitude times a SU(2) matrix. The presence of the gauge Higgs interaction, the 2nd term, does not modify the updating algorithm for the gauge link described in the previous section. This term adds to the staples, so only modifies the constant c in eqn. (5.2.3). Following the previous section, to update the Higgs field Φ_n at the site n [13], we collect the terms in the action which depend on Φ_n. The action which depends only on Φ_n at a particular site n is given by,

$$S[\Phi] = -\kappa \sum_\mu \left[\mathrm{Re}\left[\mathrm{Tr}(\Phi_{n+\mu}^\dagger U_{n,\mu} \Phi_n)\right] + \mathrm{Re}\left[\mathrm{Tr}(\Phi_n^\dagger U_{n-\mu,\mu} \Phi_{n-\mu})\right]\right] + \left[\frac{1}{2}\mathrm{Tr}\left(\Phi_n^\dagger \Phi_n\right) + \lambda\left(\frac{1}{2}\mathrm{Tr}\left(\Phi_n^\dagger \Phi_n\right) - 1\right)^2\right]. \tag{5.3.2}$$

The gauge Higgs interaction term can be written as

$$S_{U-\Phi} = \sum_{n,\mu} \mathrm{Tr}(\Phi_n \Phi^{\dagger}_{n+\mu} U_{n,\mu} + \Phi^{\dagger}_n U_{n,n-\mu} \Phi_{n-\mu}) = \xi \mathrm{Tr}(\Phi B + c.c) \tag{5.3.3}$$

The matrix B is an overall factor times an SU(2) matrix, because only SU(2) matrices are involved. We make a further transition from the 2×2 matrix field to a four component scalar ϕ,

$$\phi(4) = \mathrm{Tr}(\Phi), \ \phi(i) = \mathrm{Tr}(\Phi \sigma_i). \tag{5.3.4}$$

In terms of the field ϕ the site action is given by, $S(\phi) = (\phi - b)^2 + (\phi^2 - 1)^2$. Here the four vector b is given by $b(4) = \mathrm{Tr}(B)$, $b(i) = \mathrm{Tr}(\sigma_i)$ The probability distribution for ϕ is,

$$P(\phi) \propto e^{-S(\phi)} \tag{5.3.5}$$

To generate a ϕ with the above distribution the following strategy is adopted. The site action $S[\phi]$ is split into two parts, one quadratic and quartic as follows,

$$S(\phi) = \alpha(\phi - \alpha^{-1} b)^2 + \lambda(\phi^2 - v_\alpha^2)^2 - c_\alpha \tag{5.3.6}$$

Where

$$v_\alpha^2 = 1 + \frac{\alpha - 1}{2\lambda} \tag{5.3.7}$$

Here α is a variable and c_α is a constant independent of ϕ. Unlike the Haar Measure dU in the last section, $d^4\phi$ does not influence distribution of ϕ. A new value of ϕ is drawn from the Gaussian distribution

$$P(\phi) \propto \exp[-\alpha(\phi - \alpha^{-1} b)^2] \tag{5.3.8}$$

The generated ϕ is then accepted/rejected using the second term of (5.3.6) with probability,

$$P_{accp} = \mathrm{Min}\,[1, e^{V(\phi_{old}) - V(\phi)}]. \tag{5.3.9}$$

Here $V(\phi)$ and $V(\phi_{old})$ are values of V evaluated at ϕ and ϕ_{old} respectively. Since α is a parameter, it can be tuned so as to maximize the acceptance rate of ϕ. The value of α for which the acceptance is found to be maximum is the positive root of the cubic equation [13],

$$\alpha^3 - (1 - 2\lambda)\alpha^2 - 4\lambda\alpha = 2\lambda b^2 \tag{5.3.10}$$

We numerically solve this equation in our code [13]. One can also use the following approximate solution [13],

$$\alpha = h_0 + [h_1 + h_2 b^2]^{\frac{1}{2}} \tag{5.3.11}$$

Here h_0, h_1 and h_2 are given below:

$h_0 = \alpha_0 - \frac{{\alpha_0}^2+4\lambda}{6\alpha_0+4\lambda-2}$

$h_1 = \left[\frac{{\alpha_0}^2+4\lambda}{6\alpha_0+4\lambda-2}\right]^2$

$h_2 = \frac{4\lambda}{6\alpha_0+4\lambda-2}$

$\alpha_0 = \frac{1}{2} - \lambda + \left[(\frac{1}{2} - \lambda)^2 + 4\lambda\right]^{\frac{1}{2}}$

The above algorithm can be used for $\lambda = 0$. For this case large values of κ lead to instabilities. This is due to negative Higgs mass, which drives the field to infinity. However, the above algorithm works fine for the case when $\lambda = 0$ and $m_H = 0$.

In the following we show Monte Carlo history of various observables in SU(2)+Higgs theory for $\lambda = 0.005$, $\kappa = 0.058865$ and $\beta_g = 2.35$. We plot in Fig. 5.1 the Monte carlo history of the Polyakov loop.

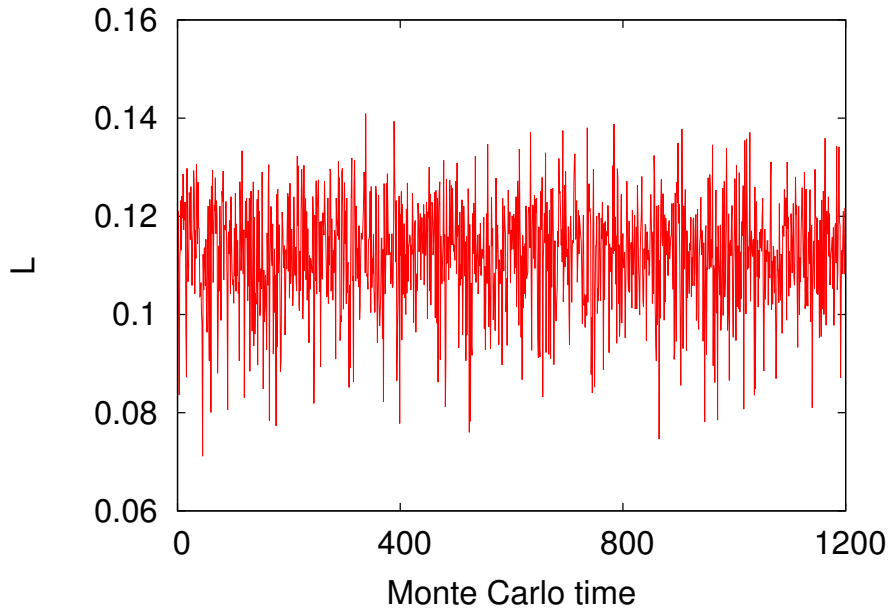

Figure 5.1. Monte Carlo history of the Polyakov loop for $16^3 \times 4$ lattice with $\lambda = 0.005$, $\kappa = 0.058865$ and $\beta_g = 2.35$ in SU(2)+Higgs theory.

In Fig. 5.2, we shows Monte carlo history of the observable $H2 = \sum_n \Phi_n^\dagger \Phi_n$.

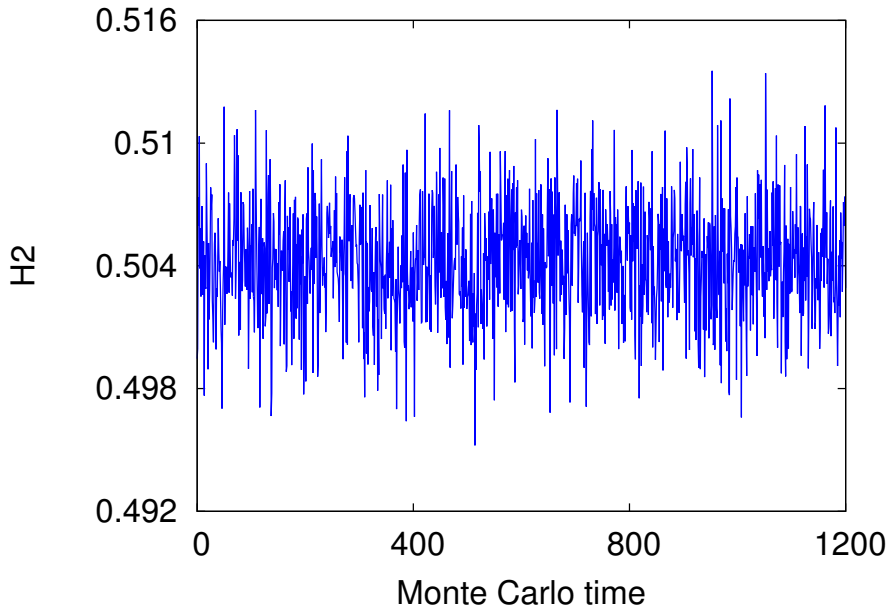

Figure 5.2. Monte Carlo history of $\sum_n \Phi_n^\dagger \Phi_n$ for $16^3 \times 4$ lattice with $\lambda = 0.005$, $\kappa = 0.058865$ and $\beta_g = 2.35$ in SU(2)+Higgs theory.

The Fig. 5.3 shows the Monte carlo history of the interaction term $KE = \sum_n \Phi^\dagger_{n+\mu} U_{n,\mu} \Phi_n$. In our simulations an initial configuration is specified to generate the Monte Carlo se-

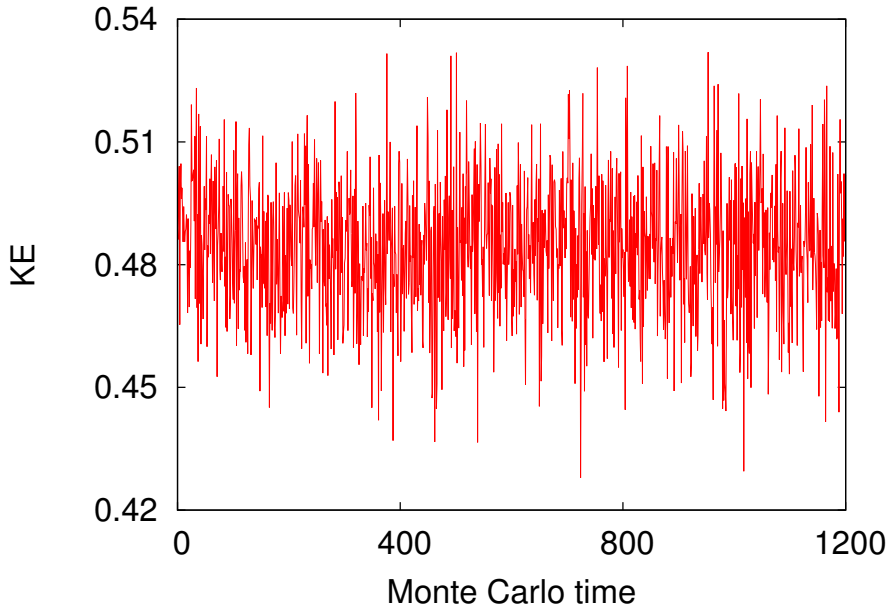

Figure 5.3. Monte Carlo history of $\sum_n \Phi^\dagger_{n+\mu} U_{n,\mu} \Phi_n$ for $16^3 \times 4$ lattice with $\lambda = 0.005$, $\kappa = 0.058865$ and $\beta_g = 2.35$ in SU(2)+Higgs theory.

quence. For various choice of the initial condition these observables thermalized to same equillibrium state, i.e same averages and higher order fluctuations. We have also checked that our code reproduces result for previous studies by others.

6 Dynamical symmetry restoration in SU(N)+Higgs theory: Simulations - I

For the simulations, we use the publicly available MILC code [63] and modify it to accommodate the Higgs fields. In the following, we explain the gauge link and Higgs field updating methods.

6.1 Lattice action and parameters

The issue of Z_N symmetry and the CD transition in the presence of Higgs field has been studied before. These studies showed that for SU(2) Higgs theory, the CD transition becomes a crossover [38] for $N_\tau = 2$. One observable, the β_g dependence of the Polyakov loop suggested a critical behavior in $12^3 \times 4$ lattices. This was thought to be due to the influence of the second order phase transition at infinitely heavy Higgs. These studies were not much focussed on the critical behavior of the Polyakov loop, as it was thought that since the action is not invariant under the Z_N transition the CD transition will always be a crossover.

The main motivation behind our study is to understand how the strength of the explicit symmetry breaking depends on the parameters of the theory and if the nature

of the explicit symmetry breaking and CD transition dependent on the cut-off. So we planned to study the Z_N symmetry by computing the distribution of the Polyakov loop for different values of the gauge Higgs coupling and the Higgs quartic coupling. When it seemed the distribution of the Polyakov loop is Z_N symmetric, we did finite volume studies to confirm the nature of the CD transition. We measure the following observables, Polyakov loop, $\Phi_n^\dagger \Phi_n$, $\Phi_{n+\mu}^\dagger U_{n,\mu} \Phi_n$ to study the interaction between the gauge and Higgs field, the Z_N symmetry and the CD transition [10].

6.2 Sketch of Higgs phase diagram

Let us consider the SU(N)+Higgs action

$$S[U,\Phi] = \beta_g \sum_p \left(1 - \frac{1}{4}\mathrm{Tr}(U_p + U_p^\dagger)\right) - \kappa \sum_{\mu,n} \mathrm{Re}\left[\mathrm{Tr}(\Phi_{n+\mu}^\dagger U_{n,\mu} \Phi_{n+\mu})\right] + \sum_n \left[\frac{1}{2}\mathrm{Tr}\left(\Phi_n^\dagger \Phi_n\right) + \lambda\left(\frac{1}{2}\mathrm{Tr}\left(\Phi_n^\dagger \Phi_n\right) - 1\right)^2\right].$$

The Polyakov loop $L(n_i)$ at a spatial site n_i is trace of the path ordered product of all temporal link variables on the temporal loop going through n_i. A Z_N rotation can be carried out by multiplying all temporal links on a fixed temporal slice of the lattice by an element of the Z_N group. This operation leaves all terms of the above action invariant except the κ dependent term. This term is solely responsible for the explicit breaking of the Z_N symmetry.

It is well known that for $N = 2$ [64–67] for the action (5.0.3) for a given β_g, there is a Higgs transition line on the $\lambda - \kappa$ plane. The transition is first order (crossover) for small (large) values of λ. For a fixed (λ, β_g) the parameter, κ plays the role of the transition parameter for the Higgs transition. For high κ ($\kappa > \kappa_c$) the system is found to be in the Higgs phase with a non-zero Higgs condensate. With decrease in κ, the condensate starts to melt and at the critical point $\kappa = \kappa_c$ the system undergoes transition

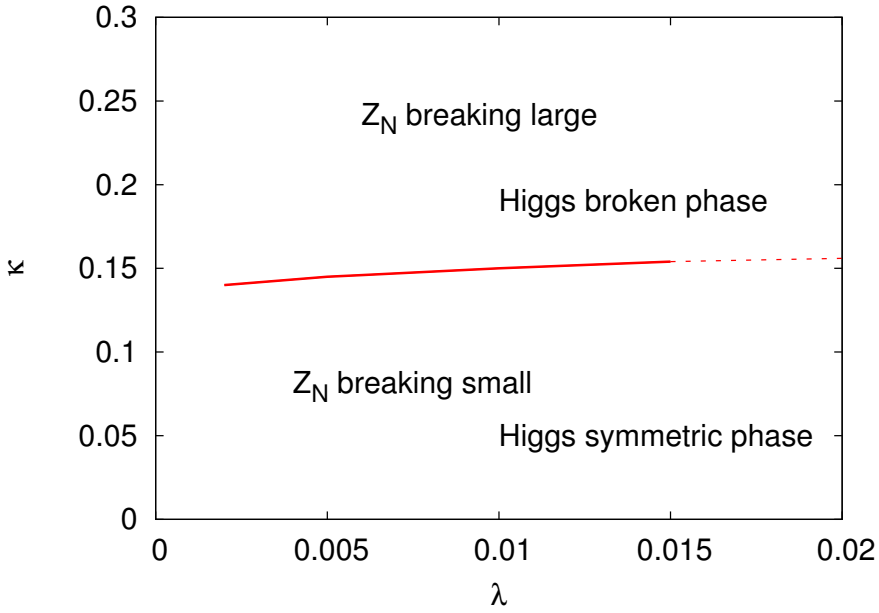

Figure 6.1. Theoretical expectations of explicit symmetry breaking on $(\lambda - \kappa)$ plane for SU(2) Higgs theory.

to the Higgs symmetric phase solid line in Fig. 6.1. For $\kappa < \kappa_c$ the Higgs condensate vanishes. Intuitively, when the system is in the Higgs phase, we can expect the matrix $\Phi_n \Phi^\dagger_{n+\mu}$ has large overlap with 2×2 identity matrix. This is because the Higgs field is supposed to be uniform (zero momentum mode) modulo the gauge transformations. This effectively results in the gauge Higgs term being proportional to $\mathrm{Tr}(U_{n,\mu})$. Such a term try to align the temporal links with the identity matrix. This will lead to a non-zero +ve real Polyakov loop, resulting in the symmetry breaking. In the Higgs symmetric phase however, the matrix $\Phi_n \Phi^\dagger_{n+\mu}$ can have any "orientation", so at least one expects the explicit symmetry breaking will be smaller than the Higgs phase as the temporal links are not forced to align with the identity matrix. So we expect that in the $\lambda - \kappa$ plane, in the Higgs phase the explicit symmetry breaking will be large and decrease as we move towards the Higgs symmetric phase. In Fig. 6.1, we sketch the expected relative strength of the explicit symmetry breaking on the $\lambda - \kappa$ plane.

6.3 Numerical simulations: Explicit breaking of Z_N symmetry

We carried out simulations for different values of β_g, κ and λ. For given values of κ and λ, we study variables which are sensitive to the Z_N symmetry in particular the Polyakov loop, by varying β_g. For our purpose it suffices to fix the coupling λ and study the Z_N symmetry at various values of κ. Given a (λ, κ), small (large) β_g corresponds to the confinement (deconfinement) phase. The CD transition takes place at the critical point $\beta_g = \beta_{gc}$. To study the Z_N symmetry at different κ, we compute the Polyakov loop distribution. In

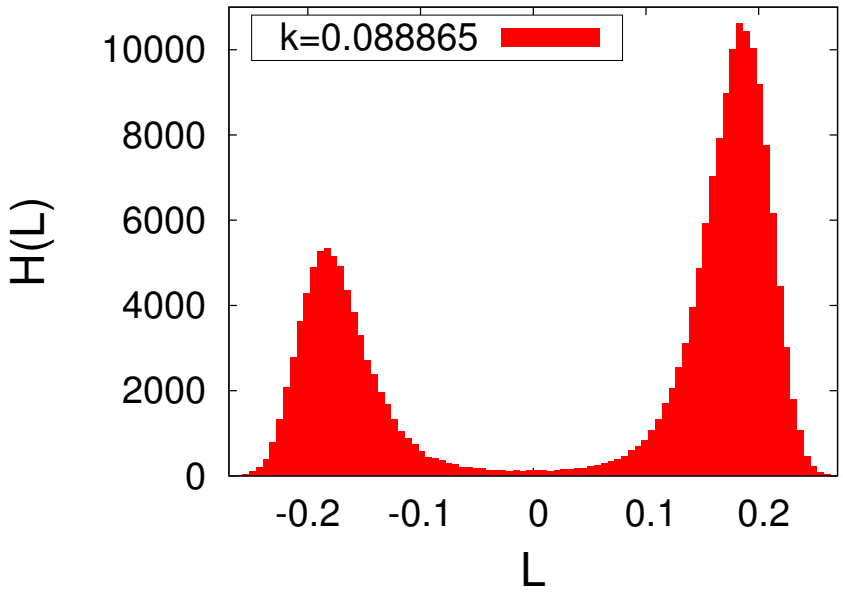

Figure 6.2. Distribution of Polyakov loop for SU(2), $16^3 \times 4$ lattice with $\kappa = 0.088865$, $\lambda = 0.005$ and $\beta_g = 2.31$

Fig. 6.2, we show the Polyakov loop distribution $H(L)$ is in the deconfined phase for $N = 2$ for $\lambda = 0.005$ and $\kappa = 0.088865$. The height of the peak on the right is higher, the ratio of the heights does not change when we add more statistics. This is a clear signature of the explicit breaking of Z_2 symmetry. The local maximum here corresponds to the meta-stable state of the system. The peak on the positive L axis corresponds to the ground state of the system. For $N \geq 3$ the Polyakov loop is complex. For better illustration, we

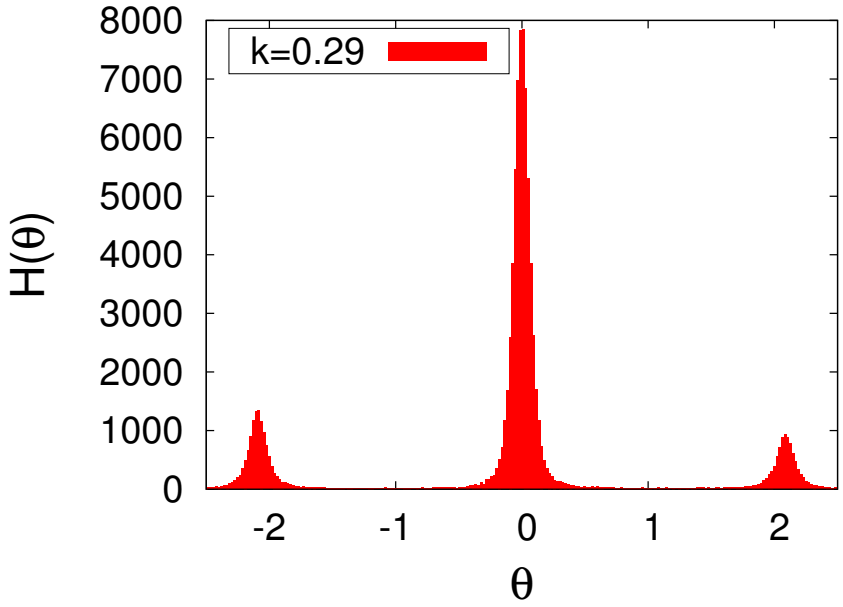

Figure 6.3. Distribution of Polyakov loop for SU(3), $8^3 \times 4$ lattice with $\kappa = 0.29$, $\lambda = 0.1$ and $\beta_g = 2.50$.

show the distribution of phase of the Polyakov loop $H(\theta)$ instead of $H(L)$ on the complex plain. This however will not work if the $\langle L \rangle = 0$. In Fig. 6.3, we show $H(\theta)$ for $\beta_g = 2.50$, $\lambda = 0.1$ and $\kappa = 0.29$ for $N = 3$. The peak at $\theta = 0$ clearly dominates the other two local maxima are a result of the Z_3 explicit symmetry breaking. For both $N = 2$ and $N = 3$, it has been observed that the asymmetry in the above distributions increases when κ is increased further. Beyond some value of κ (which depends on λ and N) the local maxima (the meta-stable states) disappear. The κ values considered above are below κ_c, in the Higgs symmetric phase.

6.4 Numerical simulations: Realization of Z_N symmetry

The Z_N symmetry is supposed to be there only when $\kappa = 0$ as the matter and gauge fields decouple. We find that for small enough κ values, in the Higgs symmetric phase, the Polyakov loop distribution exhibit the Z_N symmetry. For $N = 2$, $\kappa = 0.058865$, $\lambda = 0.005$

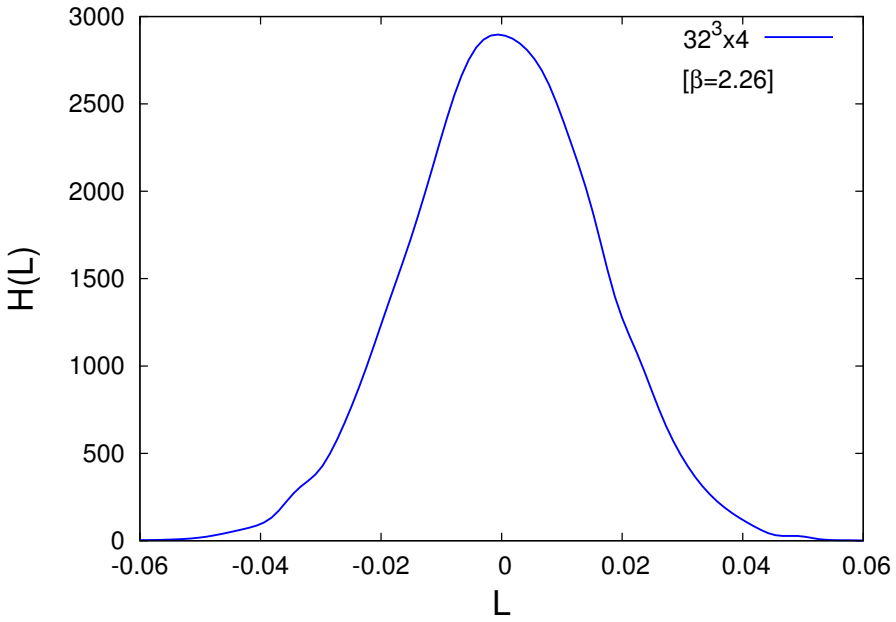

Figure 6.4. Histogram of Polyakov loop in the confinement phase for SU(2), $32^3 \times 4$ lattice with $\kappa = 0.058865$, $\lambda = 0.005$ and $\beta_g = 2.26$.

and $\beta_g = 2.26$ we observe the confinement phase. The distribution of the Polyakov loop in Fig. 6.4, for this value of β_g is symmetric around zero.

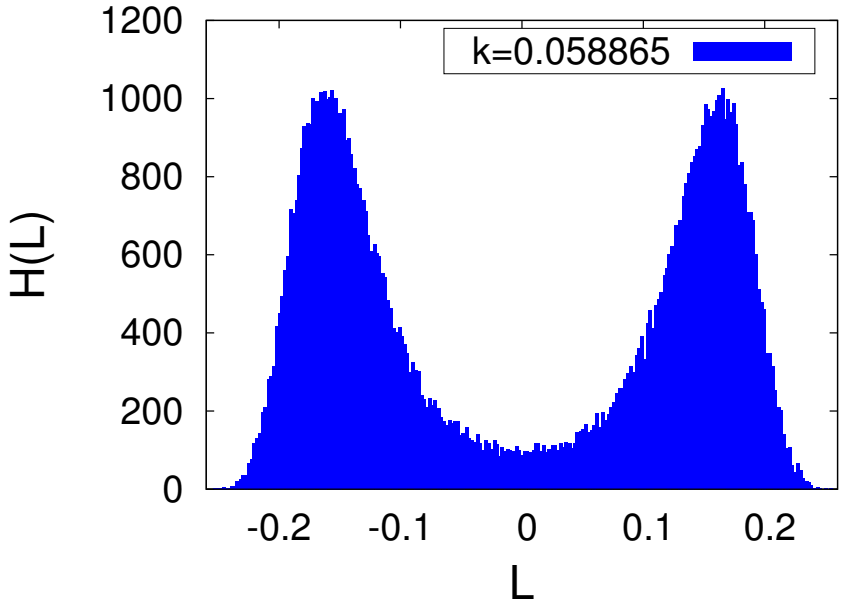

Figure 6.5. Distribution of Polyakov loop for SU(2), $16^3 \times 4$ lattice with with $\kappa = 0.058865$, $\lambda = 0.005$ and $\beta_g = 2.31$

The behavior of the Polyakov loop and fluctuations are found to be similar to the case of pure gauge theory. This is a signature of Z_2 symmetry in the confinement phase. When we considered β_g values larger than β_{gc}, Polyakov distribution clearly showed 2 degenerate peaks, which is the signature of spontaneous symmetry breaking of the Z_2 symmetry. This is evident in the distribution $H(L)$ of the Polyakov loop for $N = 2$ shown in Fig. 6.5. Similarly the distribution $H(\theta)$ for $N = 3$ shows the Z_3 symmetry shown in Fig. 6.6.

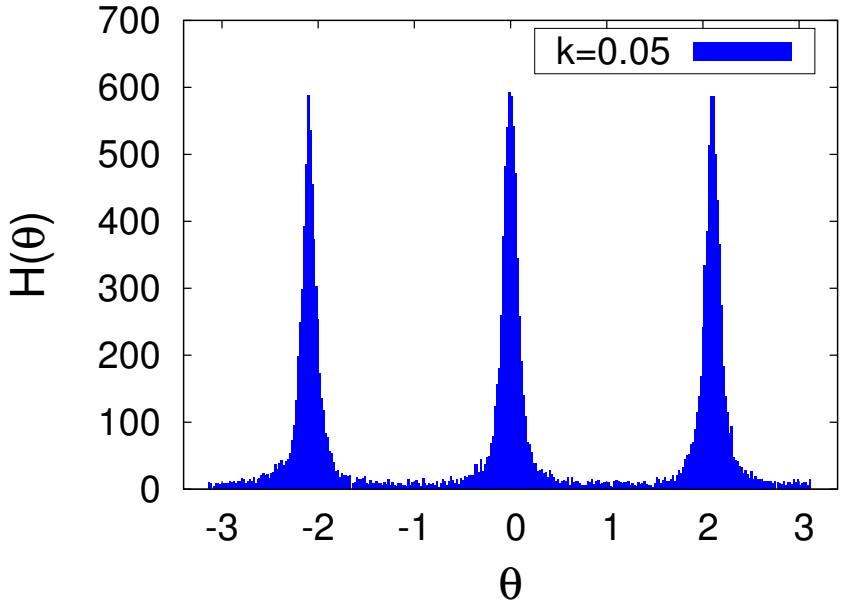

Figure 6.6. Distribution of Polyakov loop for SU(3), $8^3 \times 4$ lattice with with $\kappa = 0.05$, $\lambda = 0.1$ and $\beta_g = 1.90$

It is important to exclude that statistical or systematic errors are not causing the Z_N symmetry restoration. For small κ, the Higgs correlation length can become shorter than the lattice spacing, i.e Φ_n and $\Phi_{n+\mu}$ are not correlated. The product $\Phi_n \Phi^\dagger_{n+\mu}$ having no preferential orientation with respect to $U_{n,\mu}$ the κ term in (5.0.3) can not affect the Z_N symmetry. Though this is plausible but our simulations suggest that this is not the reason for the Z_N realization/restoration. The κ term was found to be non-zero finite. The product $\Phi_n \Phi^\dagger_{n+\mu}$ tends to align with $U_{n,\mu}$. When a Z_N rotation $((\Phi, U) \rightarrow (\Phi, U_g))$ is carried out on any configuration from the thermal ensemble, the resulting configuration is found to be out of equilibrium. This is because the new configuration has far higher action (5.0.3) than any configuration in the thermal ensemble. Interestingly this cost in the action can be compensated by varying the Φ field, i.e $\Phi \rightarrow \Phi'$, when the gauge link is Z_N rotated the links. Φ' can be obtained by Monte Carlo updates of Φ, though it is not clear how Φ and Φ' are related. We observed that the symmetry $((\Phi, U) \rightarrow (\Phi', U_g))$ is there only in the Higgs symmetric phase ($\kappa < \kappa_c$) and when the number of lattice points in the temporal direction is greater or equal to 4 ($N_\tau \geq 4$). Note that for Z_N realization for every (Φ, U) in the ensemble, there must (Φ', U_g) with same action. For smaller N_τ, this happens for only

a fraction of the configuration in the ensemble.

To see the Z_N symmetry in the Polyakov loop distribution for higher β_g in the deconfine-

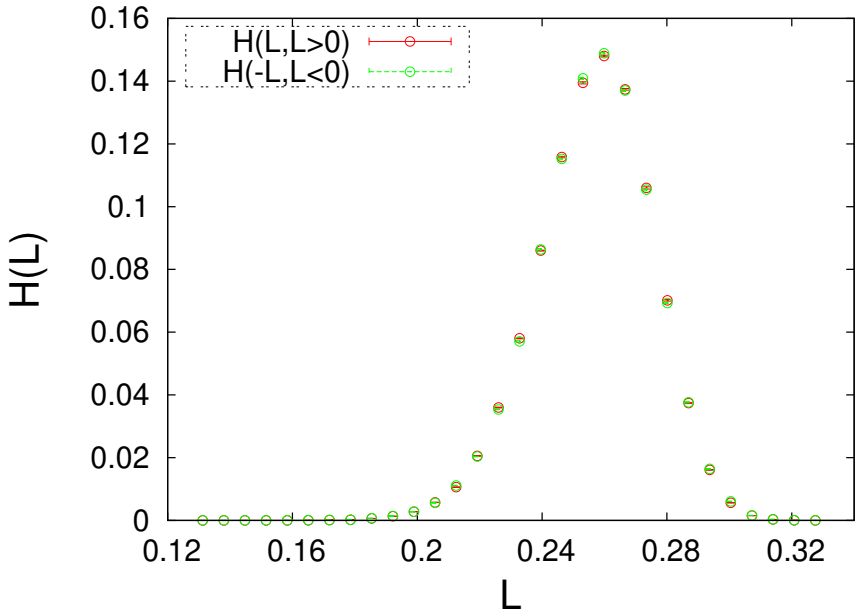

Figure 6.7. Histogram of the +ve and rotated −ve Polyakov loop with $\kappa = 0.058865$, $\lambda = 0.005$ for SU(2)+Higgs.

ment phase, the tunneling between the different Z_N sectors has to be high. The tunneling rate decreases away from the transition point and also for larger lattice sizes. For example, for $\beta_g = 2.38$ and $16^3 \times 4$ lattice, we do not see any tunneling between the different Z_2 sectors up to 2×10^6 statistics. However the histogram of the Polyakov loop in the two sectors are in perfect agreement when one distribution is Z_2 rotated, as is seen clearly in Fig. 6.7. Note here that the Histogram values are very much within the statistical error of 10^{-6}.

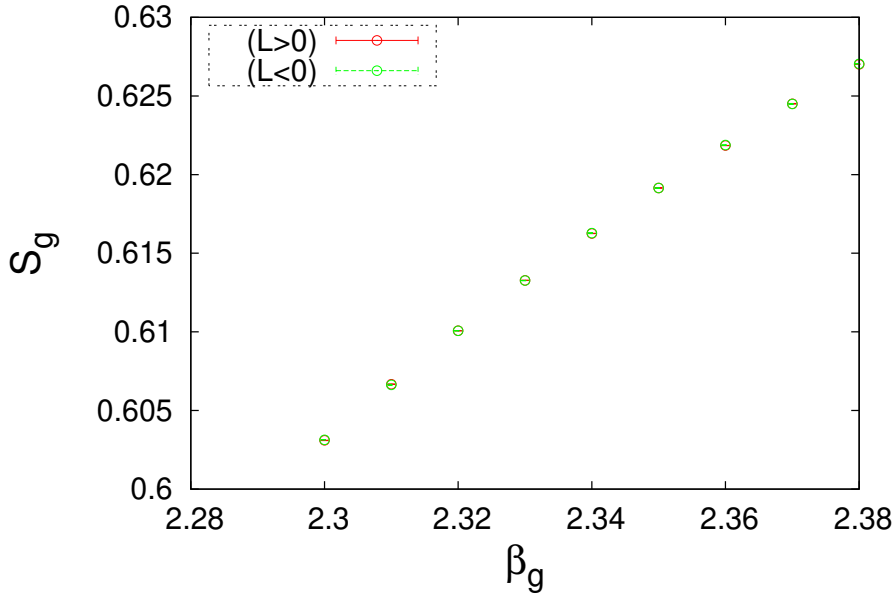

Figure 6.8. Average of gauge action for the +ve and −ve Polyakov loop with $\kappa = 0.058865$, $\lambda = 0.005$ for SU(2)+Higgs

Table-1: Average Gauge action

β_g	$S_g(L > 0)$	$S_g(L < 0)$
2.30	0.6030(11)	0.6031(12)
2.31	0.6066(12)	0.6066(40)
2.32	0.6100(11)	0.6100(11)
2.33	0.6132(10)	0.6132(12)
2.34	0.6162(11)	0.6162(11)
2.35	0.6191(11)	0.6191(11)
2.36	0.6218(10)	0.6218(12)
2.37	0.6245(20)	0.6244(19)
2.38	0.6270(09)	0.6270(11)

If the Z_N symmetry is indeed restored than the free energy of the different Polyakov loop states would have to be same. In Fig. 6.8, we show the average value of the gauge action vs β_g for the two Z_2 states (called +ve and −ve). The gauge action for the +ve (−ve) sector is calculated by taking the average over configurations for which the Polyakov loop is +ve (−ve). The gauge actions for the two Z_2 states are identical for all β_g. The free energy of each of these states can now be computed by integrating the gauge

action $S_g(\beta_g)$ in β_g [68, 69].

$$\left[\frac{f}{T^4}\right]_{\beta_{g0}}^{\beta_g} = N_\tau{}^4 \int_{\beta_{g0}}^{\beta_g} d\beta'(S_T - S_0) \tag{6.4.1}$$

Where S_T is the gauge action calculated at finite temperature and S_0 corresponds to the zero temperature gauge action. $\beta_{g0} = \beta_g$ is some gauge coupling for which $S_T = S_0$. Since the gauge action are identical, the free energy will be same for the two Polyakov loop sectors. The CD transition for $N = 2$ for small κ has been investigated previously

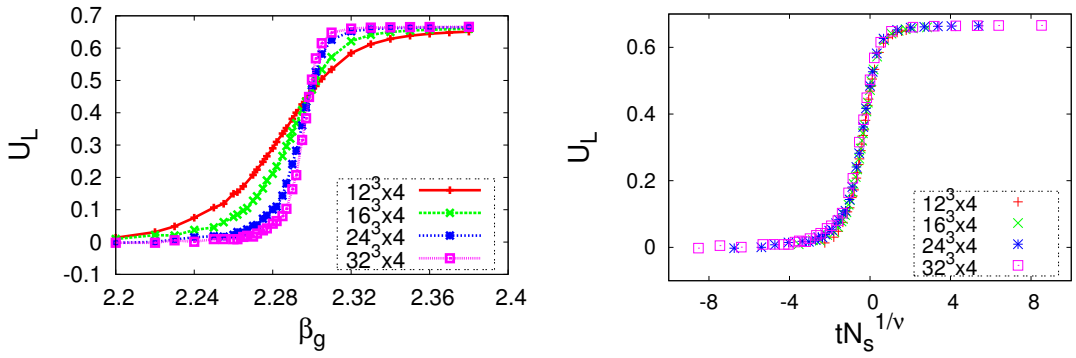

Figure 6.9. (a) Binder cumulant around transition point for different N_s (b) scaling of the Binder cumulant with $t = (\frac{\beta_g - \beta_{gc}}{\beta_{gc}})$, when $\kappa = 0.058865$, $\lambda = 0.005$ for SU(2)+Higgs respectively.

[38, 42, 65, 66, 70]. The CD transition was found to be crossover except for $\kappa = 0$. In ref. [66] , the average value of the Polyakov loop on $12^3 \times 4$ was found to vary with β_g which is consistent with critical 3D Ising behavior and found to be in the universality class of the Ising model. This was interpreted as due to the influence of the critical point at $\kappa = 0$. When we repeated these calculations, close to the critical point the average of the Polyakov loop did not fit any critical behavior. Moreover critical behavior can only be ascertained by scaling of observables with lattice size. In order to establish that there is realization/restoration of the Z_2 symmetry and the CD transition is second order, we carry out the finite size scaling studies of the Binder cumulant U_L of the Polyakov loop for the first time [71].

$$U_L = 1 - \frac{\langle P^4 \rangle}{3\langle P^2 \rangle^2} \tag{6.4.2}$$

In Fig. 6.9(a) the Binder cumulant around transition point is shown for different spatial volumes. The value of the Binder cumulant at the crossing point corresponds to the universality class of the $3D$-Ising model. Further the scaling of the Binder cumulant, shown in Fig. 6.9(b). where $t = (\frac{\beta_g - \beta_{gc}}{\beta_{gc}})$. The scaling of the Binder cumulant a value for the critical exponent $\nu \sim 0.62998$ which is also consistent with the same universality class. These results clearly show that the CD transition is second order even for finite but small κ.

Conventionally it is thought that the CD transition is true second order only for $\kappa = 0$. We believe that the origin of this second order CD transition for finite but non-zero κ is because the statistically dominant fluctuations respect the Z_2 symmetry.

6.5 Phase diagram related to Z_N symmetry for $N_\tau = 4$

We have studied the Z_2 symmetry for other values of λ. Changing the λ changes the range of κ for which the Z_2 symmetry is realized. Our results suggest that with increase in λ the largest value of κ for which we observe the Z_2 symmetry slightly increases. This suggests that there will be a line in the Higgs symmetric phase (i.e. thick green line) which separates the region where the Z_2 symmetry is realized from the region where the symmetry is explicitly broken. In Fig. 6.10, we schematically show the Z_2 symmetry on

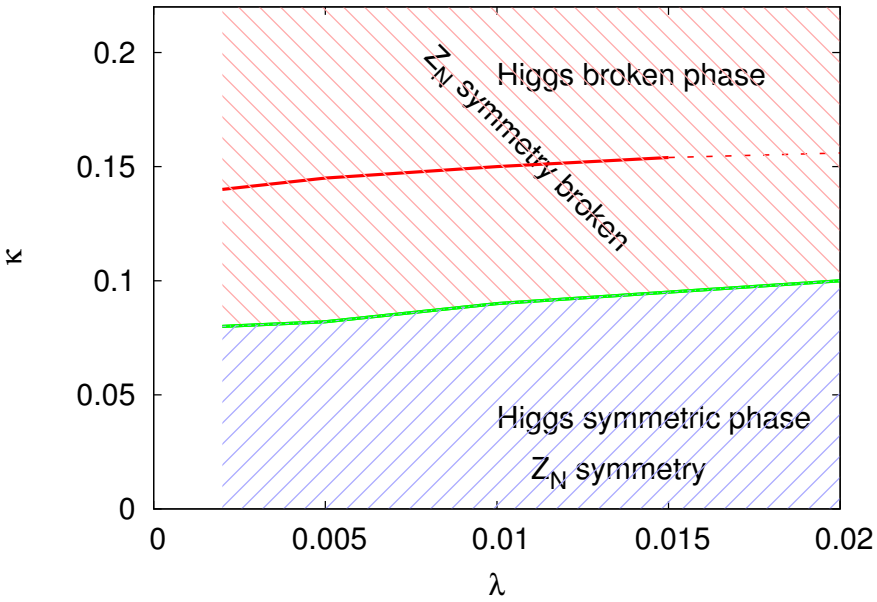

Figure 6.10. Higgs phase diagram showing Z_N symmetry for $16^3 \times 4$ lattice with $\beta_g = 2.30$ for SU(2)+Higgs theory.

the $\lambda - \kappa$ plane, for $N_\tau = 4$. In Fig. 6.10, the red line (solid and dashed) is the Higgs transition line. The area above this line corresponds to the Higgs phase and below this line corresponds to the Higgs symmetric phase. The Higgs symmetric phase and Higgs broken phase are separated by a first order phase transition line (i.e. thick red line) for lower λ values which turns to second order at some critical value of λ_c and crossover for higher values of λ. The Z_2 symmetry is explicitly broken in parts of Higgs symmetric regime below the Higgs transition line and all over the regions of Higgs broken phase. The

region above the green line in the above figure is the regime where Z_2 symmetry explicitly broken. The restoration of Z_2 symmetry corresponds to a second order CD transition which is observed from the finite size scaling behavior of the Binder cumulant. We expect similar type of Z_N symmetry phase diagram for higher N. Since the explicit symmetry breaking of Z_2 for $N_\tau = 4$ is different than $N_\tau = 2$. This suggest that the interaction between the gauge and Higgs fields changes with N_τ. So it is desirable to extend these studies to larger N_τ. Larger N_τ lattices are closer to continuum so the results are more reliable. Along this line, in our follow up work we carry out simulations for $N = 2$. In the next chapter we describe our results for N_τ dependence of the explicit symmetry breaking and the CD transition. We compare our results to perturbative calculations and lattice QCD studies.

7 N_τ dependence of Z_N symmetry and CD transition: Simulations-II

The strength of the explicit breaking of the Z_2 symmetry in SU(2)+Higgs theory depends on the parameters of the theory and also on N_τ. Previous studies have found that the corresponding CD transition for $N_\tau = 2$ is a crossover for non-zero κ. In our previous studies for $N_\tau = 4$ this transition turns out to be second order in parts of the $\lambda - \kappa$ plane, for finite non-zero κ. Clearly the Z_2 symmetry and the nature of the CD transition depend on N_τ. It is likely that the results for $N_\tau = 4$ will change with further increase in N_τ. This suggests that a careful continuum limit study of the aspects of Z_2 symmetry is necessary for this theory. To simplify the study of N_τ dependence of the Z_2 symmetry, we consider $\lambda = 0$. Further we take the Higgs mass $m_H = 0$. Intuitively an increase in the Higgs mass m_H will only lead to decrease in the explicit symmetry breaking. Our results clearly show that with increase in N_τ the explicit symmetry breaking decreases and vanishes for $N_\tau = 8$. The lattice action for this choice of parameters is given by setting the scaled parameters $\lambda = 0$ and $\kappa = 0.125$.

$$S[U,\Phi] = \beta_g \sum_p \left(1 - \frac{1}{4}\mathrm{Tr}(U_p + U_p^\dagger)\right) - \frac{1}{8}\sum_{\mu,n} \mathrm{ReTr}\left[(\Phi^\dagger_{n+\mu} U_{n,\mu} \Phi_n)\right] + \frac{1}{2}\sum_n \mathrm{Tr}\left(\Phi^\dagger_n \Phi_n\right). \tag{7.0.1}$$

With $\lambda = 0$ the partition function is easier to simulate. The Higgs update procedure for this case is pure heat bath algorithm. In the pseudo-heat bath there is an accept/reject component which is not required here.

The CD transition is studied for three values of temporal lattice points $N_\tau = 2, 4$ and 8 [16]. For $N_\tau = 2$, we consider three spatial volumes, $N_s = 8, 10$ and 12. For $N_\tau = 4$ we consider $N_s = 16, 20$ and 24 and for $N_\tau = 8$, we consider $N_s = 32, 40$ and 48. The reason for this choice of N_s and N_τ is to make sure the physical volume is same. For each volume and each run, we analyze $100,000$ configurations. The Polyakov loop, susceptibility and Binder cumulant are computed for various values of β_g to locate the transition point. We also compute the volume average of $\Phi^\dagger\Phi$ and the interaction term $Ka^4 = \frac{1}{8}\sum_{\mu,\nu}\mathrm{Re}(\Phi^\dagger_{n+\mu}U_{n,\mu}\Phi_n)$. It is important to note that even though the Φ field is massless at the tree level, the fluctuations are finite. This is because the interaction with the gauge fields generate a non-zero finite mass for the Φ field. In the following sections, we describe our simulation results.

7.1 The CD transition for $N_\tau = 2$ and 4

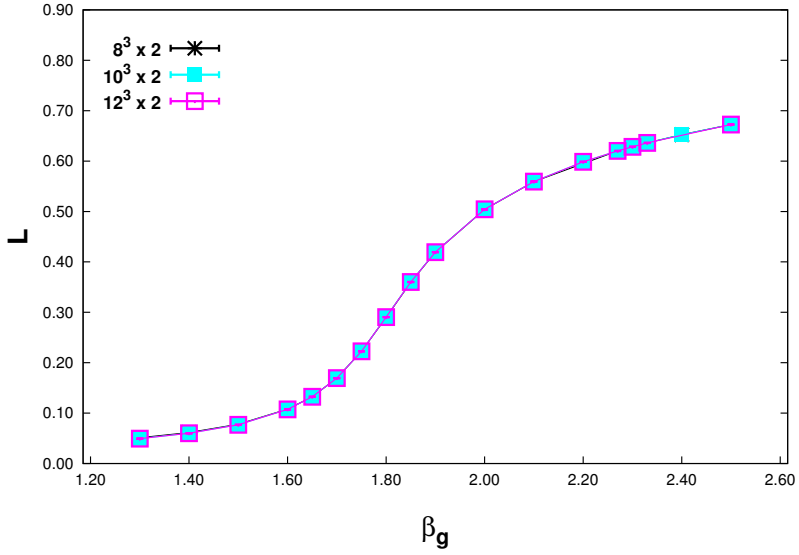

Figure 7.1. The Polyakov loop average vs β_g for $N_\tau = 2$

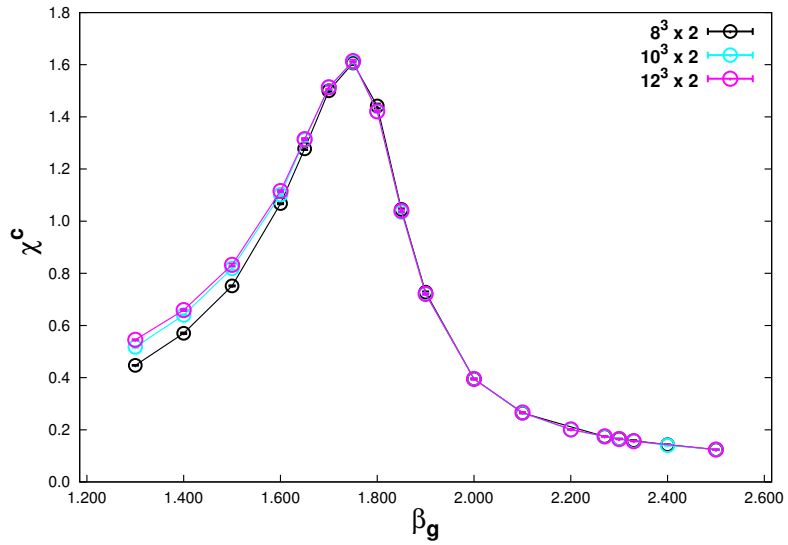

Figure 7.2. The Susceptibility vs β_g for $N_\tau = 2$

The Polyakov loop avg (L) vs β_g for $N_\tau = 2$ is shown in Fig. 7.1. L grows with β_g with a sharp increase around the transition. The Polyakov loop susceptibility is also sharply peaked as shown in Fig. 7.2 around the transition point. However both L and the susceptibility of the Polyakov loop $\left\langle |P^2| \right\rangle$ - $\langle |P| \rangle^2$ do not show any volume dependence near the transition.

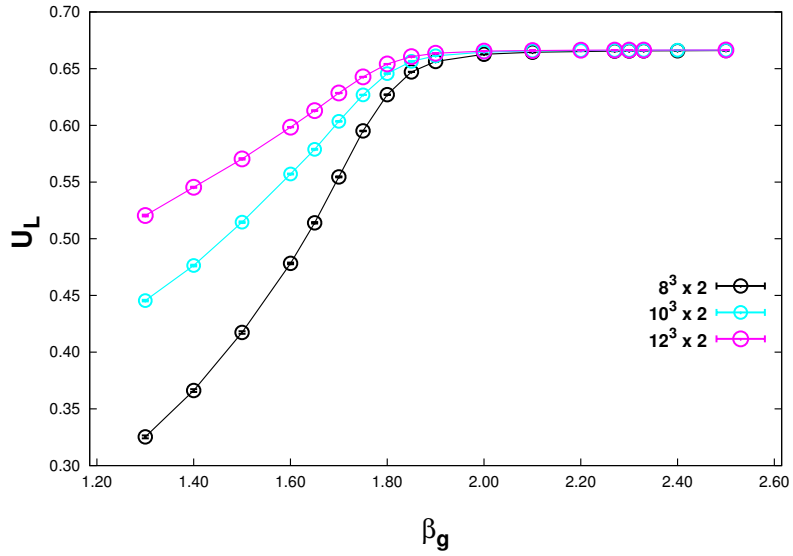

Figure 7.3. U_L vs β_g for different volumes for $N_\tau = 2$

The Binder cumulant U_L for $N_\tau = 2$ is show in Fig. 7.3. The Binder cumulant has a sharp variation near transition. The volume dependence is exactly opposite of what is expected in a second order transition where the Binder cumulant curves for different spatial volume intersect at the transition point.

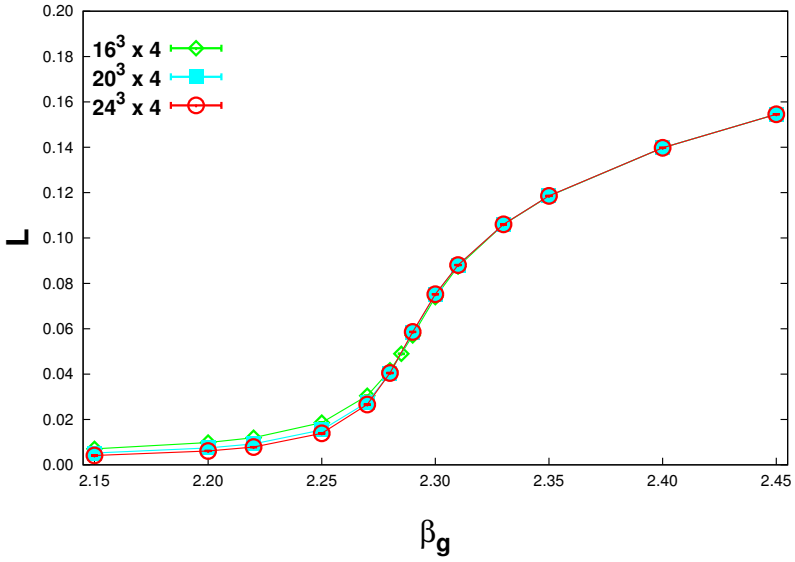

Figure 7.4. The Polyakov loop average vs β_g for $N_\tau = 4$

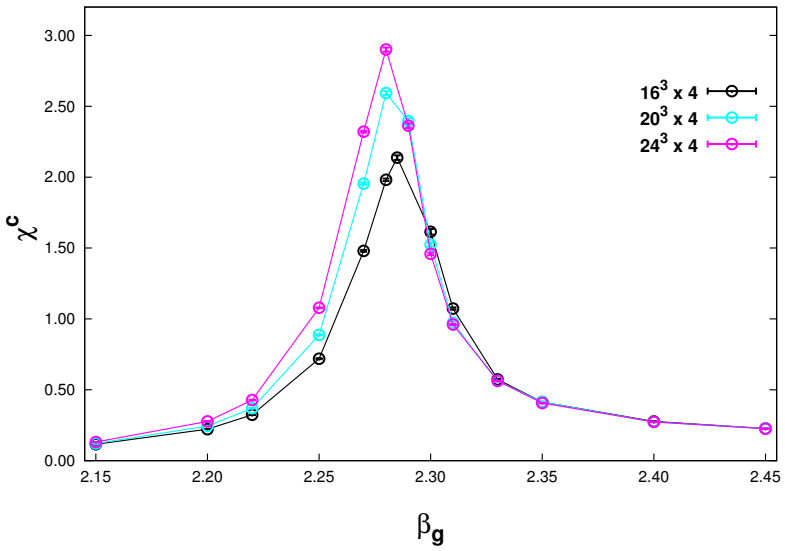

Figure 7.5. The Susceptibility vs β_g for $N_\tau = 4$

For $N_\tau = 4$, the avg of the Polyakov loop L vs β_g is shown in Fig. 7.4. In this case also the Polyakov loop average varies sharply with β_g. The $1-$ loop $\beta-$function temperature dependence of L is found to be consistent with the power law, $L \sim (T - T_c)^{1/3}$. But very close to the transition point the power law breaks down. In any case, this is supposed to be for very large lattices. Near the transition point the L has small volume dependence, but unlike in the case of a second order phase transition.

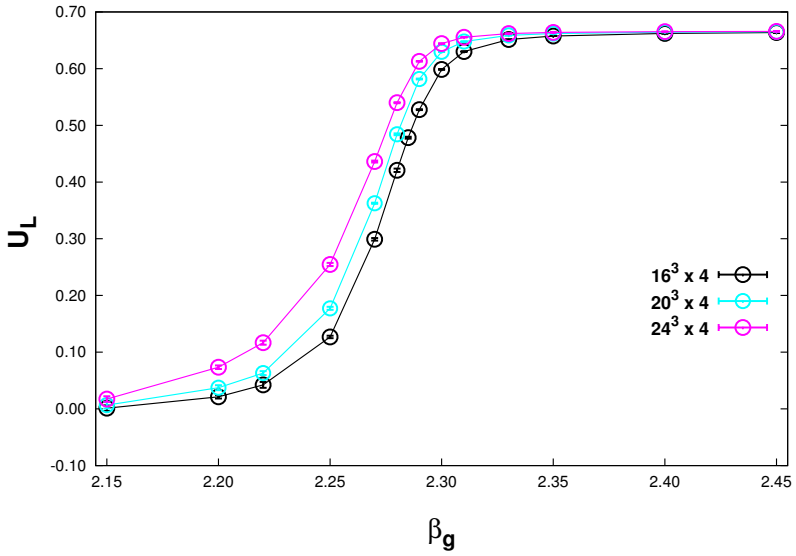

Figure 7.6. U_L vs β_g for different volumes for $N_\tau = 4$

The volume dependence is more prominent in the plot of susceptibility in Fig. 7.5. Like in the previous case the Binder cumulant curves for different volume do not intersect at any β_g value, as seen in Fig. 7.6. In the absence of any finite size scaling, the sharp variation of the Polyakov loop around $\beta_{gc} \sim 1.8$, ($N_\tau = 2$) and $\beta_{gc} \sim 2.29$, ($N_\tau = 4$) only suggest a cross-over for the CD transition. In both cases the correlation length does not grow with volume.

7.2 The CD transition for $N_\tau = 8$

The behavior of the Polyakov loop for $N_\tau = 8$ is completely different from that of $N_\tau = 2$ and 4. The Polyakov loop avg L around the transition point β_{gc} behaves almost like the magnetization in the Ising model. The results for L vs β_g for different volumes are shown in Fig. 7.7(a). In this case, L clearly shows volume dependence. The volume dependence of the susceptibility χ^c of the Polyakov loop around the transition point is shown in Fig. 7.8(a).

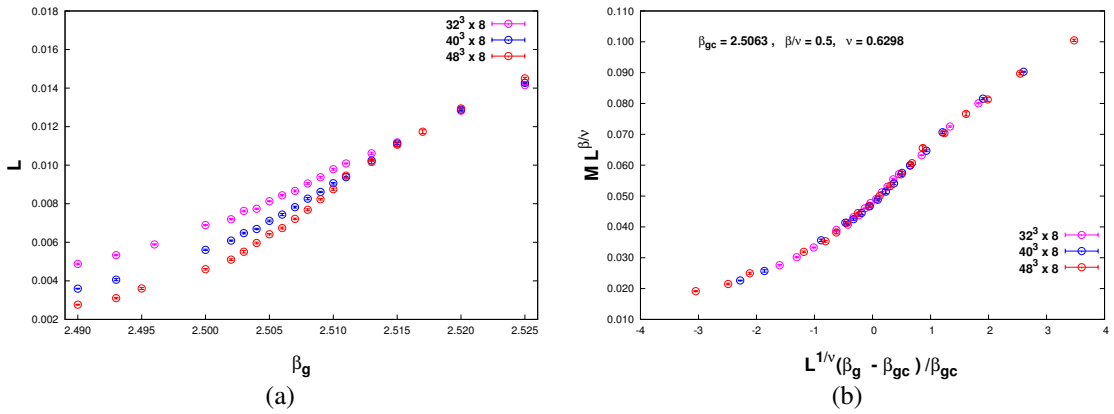

Figure 7.7. $N_\tau = 8$. (a) The Polyakov loop vs β_g for different volumes, and (b) Scaled Polyakov loop vs β_g for different volumes.

In Figs. 7.7(b) and 7.8(b), we show magnetization and susceptibility vs $(L^{1/\nu}(\beta_g - \beta_{gc})/\beta_{gc})$, respectively. We see that both the quantities collapse to single curves. We find the value of the exponent, γ/ν, by studying the finite size scaling (FSS) of the location of the maxima of the χ^c's similar to as in [72]. However instead of using Reweighting method to determine χ^c_{max}, we use the cubic spline Interpolation method to generate a few hundred points close to $\beta_{g\chi max}$ for every jackknife sample since we have a reasonable amount of data near the peak for each volume. The scaling behavior of χ^c_{max} as a function of spatial volume, L, are shown in Fig. 7.10(a). We obtain $\gamma/\nu = 1.97(4)$.

The Binder cumulant for $N_\tau = 8$ is shown in Fig. 7.9(a). While the $U_L(\beta_g)$ for different volumes do not intersect for $N_\tau = 2$ and 4, they do for $N_\tau = 8$ in a narrow

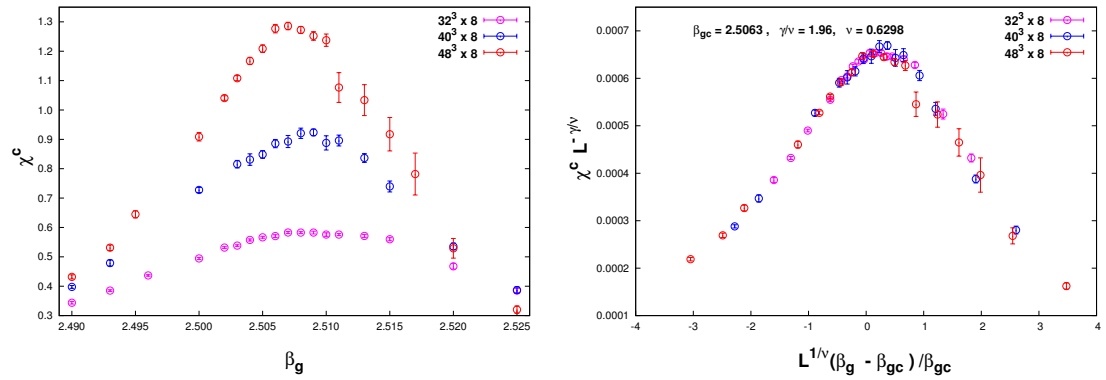

(a) (b)

Figure 7.8. $N_\tau = 8$. (a) Susceptibility vs β_g for different volumes, and (b) Scaled Susceptibility vs β_g for different volumes.

region around the transition point. To determine β_{gc} and corresponding value of Binder cumulant, we use the following finite size behavior of U_L in the vicinity of the critical point,

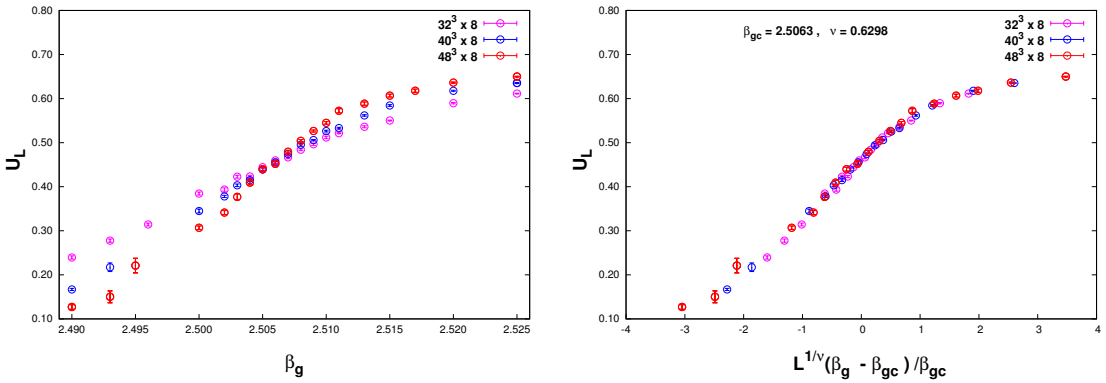

(a) (b)

Figure 7.9. $N_\tau = 8$. (a) The Binder cumulant U_L vs β_g for different volumes, and (b) Scaled U_L vs β_g for different volumes.

$$U_L \approx a_0 + a_1\,(\beta_g - \beta_{gc})/\beta_{gc}\,L^{1/\nu} + a_2\,L^{-\omega} + \cdots\,. \tag{7.2.1}$$

By following the same procedure as in [73], we can write

$$\beta_{gc}{}^{\text{eff}} = \beta_{gc}\,(1 - \alpha\epsilon)\,, \quad \text{where } \epsilon = L^{-1/\nu-\omega}\frac{1-b^{-\omega}}{b^{1/\nu}-1}\,, \quad b = \frac{L'}{L}\,, \quad b > 1. \tag{7.2.2}$$

The crossing point of the straight lines of two different spatial volumes pro-

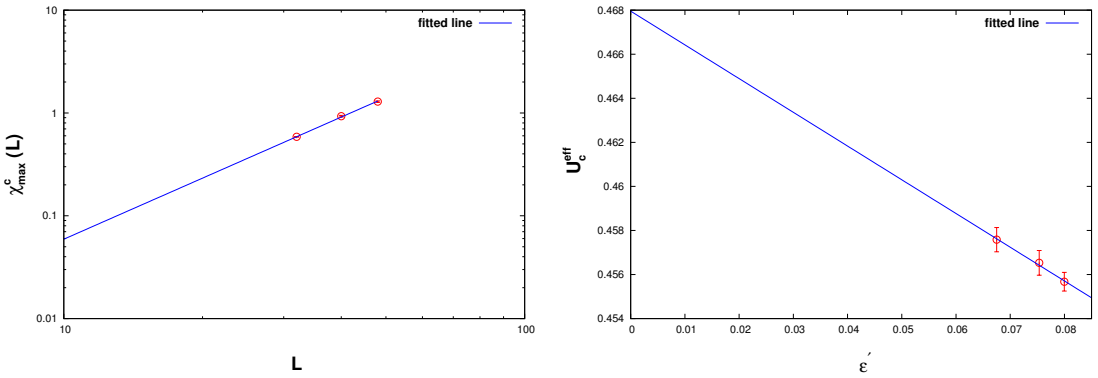

(a) (b)

Figure 7.10. $N_\tau = 8$. (a) The values of χ^c_{max} as a function of L for $L = 32, 40$ and 48. The slope of fitted line provides the value of γ/ν. (b) The values of $U_c^{\rm eff}$ obtained from the crossing points of Binder cumulant between two different volumes as a function of ϵ'. The intercept provides the value of U_c.

vides ${\beta_{gc}}^{\rm eff}$. By using the 3D Ising values of $\nu = 0.6298$ and $\omega = 0.825$, we obtain β_{gc} in the limit $\epsilon \to 0$ as $\beta_{gc} = 2.5063(4)$. Fig. 7.9(b) shows that U_L vs $(L^{1/\nu}(\beta_g - \beta_{gc})/\beta_{gc})$ for different volumes collapse to a single curve. To obtain infinite volume Binder cumulant, U_c, we use the following relation

$$U_c^{\rm eff} = U_c\,(1 + \alpha'\epsilon')\ , \quad \text{where } \epsilon' = L^{-\omega}\frac{1 - b^{-\omega-1/\nu}}{1 - b^{-1/\nu}} \tag{7.2.3}$$

In Fig. 7.10(b), we show $U_c^{\rm eff}$ vs ϵ'. In the limit $\epsilon' \to 0$, we obtain $U_c = 0.468(4)$. To determine the exponent β/ν, we find magnetization at β_{gc} for each volume using Cubic Spline Interpolation. Using $\langle|P|\rangle|_{\beta_{gc}} \sim L^{\beta/\nu}$, we get $\beta/\nu = 0.53(3)$. The above values of β/ν, γ/ν and $U_L(\beta_{gc})$ from our computations are close to the 3D Ising values. These results seem to show that the CD transition transition for $N_\tau = 8$ is a second order phase transition.

Large N_τ, continuum limit study of Z_N symmetry in SU(N)+Higgs theory is necessary as, if not for $N_\tau = 8$ studies we would have concluded that the CD transition in the theory massless Higgs coupled to SU(2) gauge fields is a crossover.

7.3 N_τ dependence of explicit Z_2 breaking

The different N_τ studies clearly show that the nature of the CD transition depends on N_τ. The change in the nature of the CD transition from $N_\tau = 8$ to $N_\tau = 4, 2$ is similar to that of the Ising transition when the external field is increased. So it is possible that the explicit breaking of the Z_2 symmetry decrease with increase in N_τ.

To check this, we compute the histogram of the Polyakov loop near the transition point for $N_\tau = 2, 4, 6$ and 8. For $N_\tau = 2$ and 4, no Z_2 symmetry is observed in the distribution of the Polyakov loop. On the deconfinement side and close to the transition

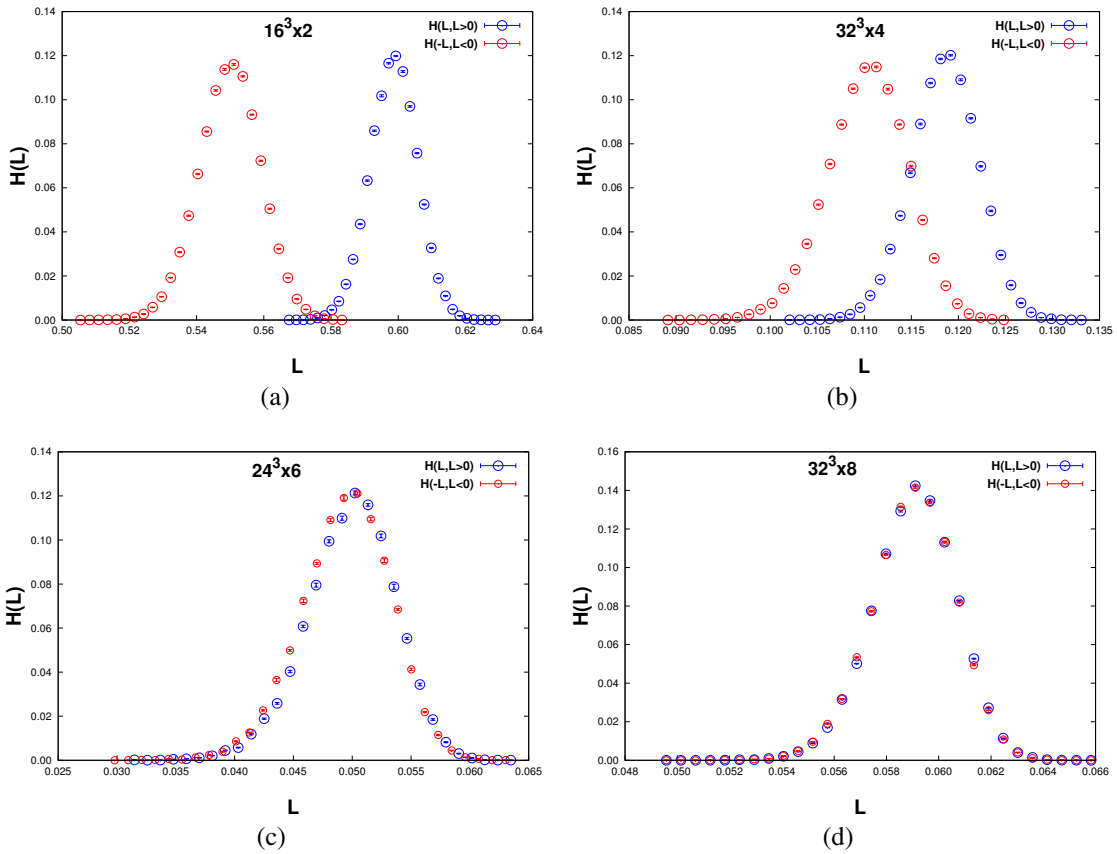

Figure 7.11. $H(L)$ vs $|L|$. $H(L)$ is normalized to 2. (a) $16^3 \times 2$ lattice with $\beta_g = 2.2$, (b) $32^3 \times 4$ lattice with $\beta_g = 2.35$, (c) $24^3 \times 6$ lattice with $\beta_g = 2.50$, and (d) $32^3 \times 8$ lattice with $\beta_g = 3.20$

.

point, the histograms always show one peak located on the positive real axis. Away from the transition point and inside the deconfinement phase, locally stable states are observed

for which the Polyakov loop is negative. In Fig. 7.11(a) the histogram of the Polyakov loop $H(L)$ vs $|L|$ for $\beta_g = 2.2$ is shown for $N_\tau = 2$. $H(L)$ is normalized to 2. There is no Z_2 symmetry either between the locations or the widths of the peaks. So the behavior of the Polyakov loop such as thermal average, fluctuations, correlation length etc. are found to be different for these two states. The distribution for $N_\tau = 4$ is similar to $N_\tau = 2$. However, for $N_\tau = 6$, the Polyakov loop $H(L)$ vs $|L|$ for $\beta_g = 2.50$ the two peaks are approaching towards each other though they are not same. For $N_\tau = 8$ the Polyakov loop distribution for the two Z_2 sectors, shown in Fig. 7.11(d), agree with each other. Though 10^6 measurements are used to compute all the data points in Fig. 7.11(d), each individual point in the figure is the average over $(H(L) * 10^6)$ configurations in a small bin. For example, the peaks of the histogram result from about $\sim 1.5 \times 10^4$ configurations. It is interesting to see that $H(L)$ for $+L$ and $(-L)$ agree even with such small statistics. All physical observables which depend on the temporal gauge field such as gauge action and interaction term have same average when computed for the two Z_2 sector. These results suggest the effective realization of the Z_2 symmetry for $N_\tau = 8$.

7.4 Interaction between gauge and Higgs field

It is important to show that the realization of the Z_2 symmetry is not due to decoupling between the gauge and the Higgs fields. In Fig. 7.12, we plot the Monte Carlo history of

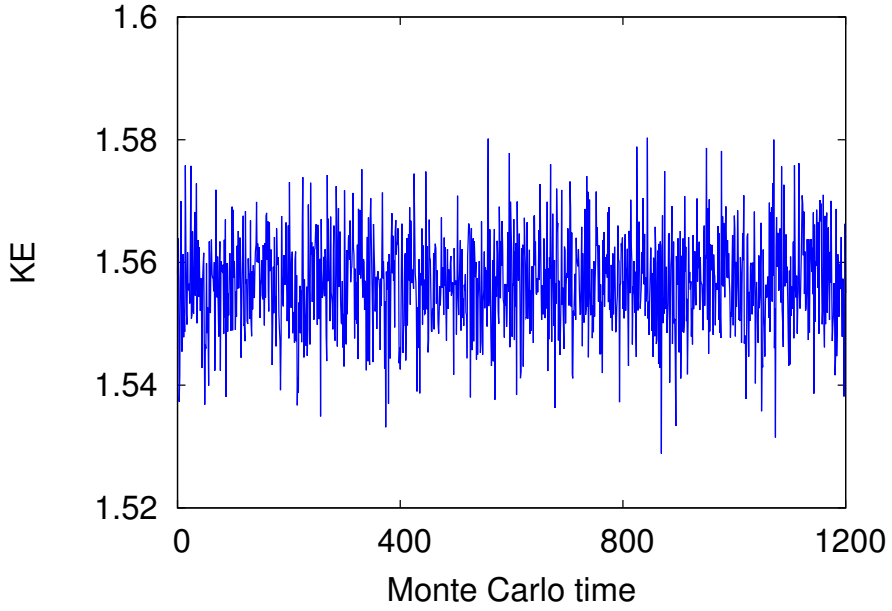

Figure 7.12. Monte Carlo history of $\sum_n \Phi^\dagger_{n+\mu} U_{n,\mu} \Phi_n$ for $32^3 \times 8$ lattice with $\lambda = 0$, $\kappa = 0.125$ and $\beta_g = 2.508$ in SU(2)+Higgs theory.

the gauge Higgs interaction term $KE = \sum_n \Phi^\dagger_{n+\mu} U_{n,\mu} \Phi_n$. The plot is for $\lambda = 0$, $\kappa = 0.125$ and $\beta_g = 2.508$ parameters of the SU(2)+Higgs theory. Non-zero value of the interaction term show that the Higgs and gauge fields are not decoupled. The Z_2 symmetry supposed to exist when Higgs and gauge fields are decoupled, but our simulation results show that even with finite non-zero gauge Higgs interaction the realization of Z_2 symmetry happens.

We also have checked that the realization of Z_2 symmetry for higher N_τ is not because of the increase in Higgs mass as cut-off increases. For this we try to calculate the Higgs mass on a zero temperature lattice. Due to time constraint a reliable computation of the Higgs mass vs N_τ could not be done. On the other hand if the Higgs mass increases with N_τ average of the interaction, i.e κ term, in the action should decrease with N_τ. In Fig. 7.13 we show the κ term vs β_g in a given physical volume, for $N_\tau = 4, 6$ and 8. The

β_g range for each N_τ is around $\beta_{gc}(N_\tau)$. We observe that the interaction in a given physical volume increases with N_τ in Fig. 7.13. From $N_\tau = 4$ to 6, the interaction increases by a factor of ~ 5 and , from $N_\tau = 6$ to 8, it increases by a factor of ~ 3. The interaction between the Higgs and gauge fields are non-zero which implies that the realization of the Z_2 symmetry is not due to the vanishing or small interaction. In our simulations, we find that fluctuations of the Higgs field play an important role. Z_2 flip of the gauge fields are always accompanied by realignment ($\Phi \rightarrow \Phi'$) of the Higgs configuration. As soon as the Higgs fluctuations are frozen/fixed, the explicit breaking of Z_2 reappears. The possible

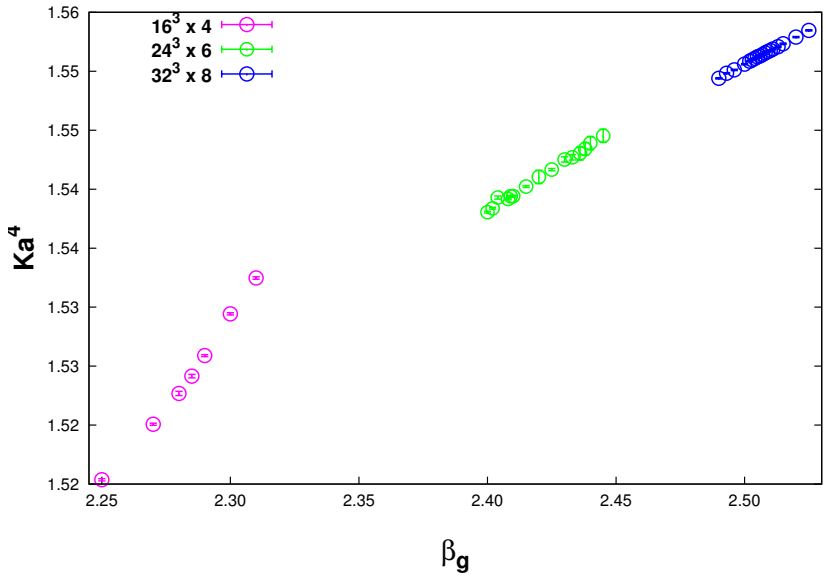

Figure 7.13. The avg. of $Ka^4 = \frac{1}{8}\sum_{\mu,\nu} \mathrm{Re}(\Phi^\dagger_{n+\mu} U_{n,\mu} \Phi_n)$ for different N_τ near transition point.

reason, why the Z_2 realization happens for $N_\tau = 8$ and not for $N_\tau = 2$ and 4 is because for $N_\tau = 8$ the phase space of Φ field is larger. With the increase in the phase space, it is more likely that for a given Φ there exists a Φ' which can compensate for the increase in action due to Z_2 rotation of the gauge fields. We numerically find that the likelihood of finding such a Φ' increases with N_τ. It is important to note that the Z_2 symmetry in our simulations only implies that a Φ' exists for every statistically significant Φ. It is obvious that there will be Φ configurations for which there will not be any Φ' even in the limit of $N_\tau \rightarrow \infty$. This happens when the Higgs field acquires a condensate. In this case for large fraction of Φ from the thermal ensemble there are no corresponding Φ'.

7.5 Phase diagram of Z_2 breaking for higher N_τ

We find from our N_τ studies that explicit breaking of Z_N symmetry depends on N_τ. For $\lambda = 0, \kappa = 0.125$, the explicit breaking vanishes for $N_\tau = 8$. It is important to study how the phase diagram of Z_2 symmetry breaking changes with N_τ. So we attempt to extend the previous study of $N_\tau = 8$ for $m_H a = 0, \lambda = 0$ to other parts of the $\lambda - \kappa$ plane.

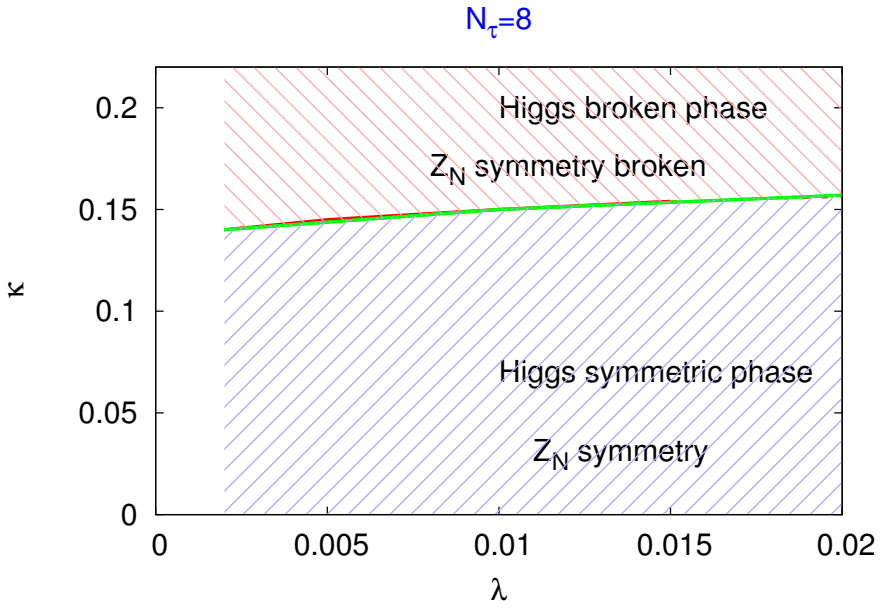

Figure 7.14. Higgs phase diagram showing Z_N symmetry restoration in all over the region of Higgs symmetric phase for $N_\tau = 8$ with $\beta_g = 2.30$ for SU(2)+Higgs theory.

We compute the distribution of the Polyakov loop $H(L)$ for different point on the $\lambda - \kappa$ plane. We find that the Z_2 symmetry is realized in all of the symmetric phase for λ values $0 - 0.02$ as shown in Fig. 7.14. In the Higgs phase the Z_2 symmetry is found to be explicitly broken. In comparision to Fig. 6.10, the red and blue lines merge for $N_\tau = 8$. For the same range of λ for $N_\tau = 4$ the Z_2 symmetry is restored only in parts of the region of Higgs symmetric phase. Note that larger N_τ studies have smaller cut-off corrections. Therefore, Z_2 symmetry phase diagram for $N_\tau = 8$ is more reliable than that for $N_\tau = 4$. It will be interesting to see if there is any change in the Z_2 symmetry phase diagram for $N_\tau > 8$.

8 Discussions and Conclusions

In this thesis, we have studied the Z_N symmetry and the confinement deconfinement transition in the SU(N)+Higgs theory using lattice Monte Carlo simulations. Most of our simulations are for SU(2)+Higgs, though we have also considered $N = 3$ for lattices with smaller temporal sites.

In SU(N)+Higgs theories the presence of the Higgs field leads to the explicit breaking of Z_N symmetry at the level of the action. The strength of the explicit symmetry breaking depends on the fluctuations, so implicitly on the parameters λ, κ of the theory and the cut-off. So we focused on the study of Z_N symmetry and CD transition on the $\lambda-\kappa$ plane for the different number of temporal lattice sites. For $N_\tau = 4$ we find that the explicit symmetry breaking varies with λ and κ. On the other hand, given a (λ, κ) the strength does not vary much with the CD transition parameter β_g. The patterns of explicit symmetry breaking observed in $N = 2$ and $N = 3$ are very similar. The explicit breaking of Z_N symmetry has a clear pattern on any trajectory on the $\lambda - \kappa$ plane along which κ and the Higgs condensate decrease. We observe that for larger values of κ which also corresponds to the larger value of the Higgs condensate, the explicit symmetry breaking is so large that the distributions of the Polyakov loop have only one peak in deconfined phases. The large explicit symmetry breaking causes the meta-stable states to become unstable. Further, as κ and the Higgs condensate decrease multiple peaks in the distributions do appear. It is possible that for some other trajectories in the Higgs phase there are no meta-stable states associated with the Z_N symmetry. As the trajectory crosses the Higgs transition point κ_c

the explicit symmetry breaking drops sharply.

In our simulations for $N_\tau = 4$, away from the transition point, the nature of the confinement-deconfinement transition is found to be almost indistinguishable from the pure SU(N) gauge theory. For $N = 3$ we find a first order transition at critical $\beta_g = \beta_{gc}$. For $N = 2$, finite size scaling studies of various observables and the Binder cumulant confirm that the transition is second order. For $\beta_g > \beta_{gc}$, in the distributions of the Polyakov loop, there are N peaks of almost equal heights. These correspond to the N, Z_N states in the deconfinement. In our computations all physical observables such as the gauge action, interaction $\kappa-$term etc. are found to be same for all the Z_N states. As a consequence, the free energies of the different Z_N states have same free energy. All these results seem to suggest that the explicit breaking of the Z_N symmetry is vanishingly small even for non-zero κ values. It has been argued previously that in a lattice theory of SU(N)+Higgs with frozen radial mode of the Higgs, the presence of Higgs field does not change the pure gauge CD transition for small coupling between the gauge and Higgs fields [43]. The presence of Higgs field only modifies the critical "temperature" for the CD transition. However, these studies are basically strong coupling results, without the continuum limit.

The value of κ for which the symmetry is effectively restored/realized in theory depends on λ. For larger λ this restoration of the Z_N symmetry occurs at a higher value of κ. As we do not observe much variation in the explicit symmetry breaking of Z_N by varying β, these results suggest that there is a line that divides the $\lambda - \kappa$ plane into the region where Z_N symmetry is explicitly broken and region where the Z_N symmetry is almost restored/realized. In other words, there is a strip on the $\lambda - \kappa$ plane in the Higgs symmetric phase where the Z_N symmetry is effectively realized. In contrast, previously, for $N = 2$ the CD transition was found to be a crossover for all non-zero κ values. Clearly this shows that the nature of the CD transition and the explicit symmetry breaking depend on N_τ. To understand the role of N_τ, we study the CD transition and Z_2 symmetry for N_τ up to 8. At first we considered vanishing Higgs mass ($\kappa = .125$) and Higgs quartic

coupling ($\lambda = 0$). We found strong cut-off effects. For $N_\tau = 2$ and 4, the CD transition turns out to be a crossover. The Polyakov loop varies sharply around the transition point, but no volume dependence was observed. Previously for $12^3 \times 4$ lattice sharp variation of the Polyakov loop was thought be a critical behavior. When repeated the calculations, we find no sign of any finite size scaling, i.e singular behavior. For $N_\tau = 8$, the temperature dependence, susceptibility and the Binder cumulant of the Polyakov loop show volume dependence and singular behavior suggesting a second order CD transition. Our results for the critical exponents are found to be consistent with the 3D Ising universality class. The singular behavior of the Polyakov loop for $N_\tau = 8$ is accompanied by the effective realization of the Z_2 symmetry. Z_2 symmetric peaks were observed in the histogram of the Polyakov loop in the deconfined phase near the transition point. Thermal averages such as the fluctuations of the Polyakov loop, the interaction term between the gauge and the Higgs field, the gauge action, etc. were all found to be same for the two deconfined states related by the Z_2 symmetry.

The $N_\tau = 8$ study was repeated for other values of (λ, κ). For small λ up to $\lambda = 0.02$ the Z_2 symmetry is found to be realized/restored in the entire Higgs symmetric phase. In the region of Higgs phase, we did not see any change in the explicit breaking up to $N_\tau = 8$. However, we cannot be sure that the $N_\tau = 8$, Z_N symmetry phase diagram in the $\lambda - \kappa$ plane will not evolve with further increase in N_τ. Since the pattern of explicit symmetry breaking between $N = 2$ and $N = 3$ were similar for $N_\tau = 4$, we expect that the Z_N symmetry for $N \geq 3$ will also be realized/restored in the Higgs symmetric phase for large enough N_τ.

We have tried to understand the physics behind the restoration/realization of the Z_N symmetry for non-zero κ. It is possible that for small enough κ the Higgs mass will be larger than the inverse of the lattice spacing. In this case, the interaction term will vanish as the nearest neighbor site Φ fields will be uncorrelated. The κ values we simulated were beyond this range, as we observed finite non-zero interaction between the

gauge and the Higgs field. We also checked that the decrease in the explicit symmetry breaking with N_τ is not due to the gradual decoupling of the Higgs field. For this, we computed the interaction term in physical units using 1−loop beta-function. We find that the interaction in a given physical volume increases with N_τ. From $N_\tau = 4$ to 6, the interaction increases by a factor of ~ 5 and, from $N_\tau = 6$ to 8, it increases by a factor of ~ 3.

The Higgs fluctuations instead of decoupling played an important role in the Z_N symmetry realization/restoration. In our simulations, a Z_2 flip of the gauge fields is always accompanied by a realignment ($\Phi \to \Phi'$) of the Higgs configuration. As soon as the Higgs fluctuations are frozen/fixed, the explicit breaking of Z_2 reappears. We believe that the reason the Z_2 realization happens for higher N_τ but not for smaller $N\tau$ is because of the increase in the phase space of the Φ field with N_τ. With the increase in the phase space, it is more likely that for a given Φ there exists a Φ' which can compensate for the increase in the action due to the Z_2 rotation of the gauge fields. We find numerically that the likelihood of finding a Φ' for a given Φ increases with N_τ. It is important to note that the Z_2 symmetry in our simulations only implies that a Φ' exists for every statistically significant Φ. It is obvious that there will be Φ configurations for which there will not be any corresponding Φ'. However, contribution to the partition function of these Φ configurations is statistically insignificant for the parameters for which Z_2 symmetry is realized/restored. In the Higgs broken phase, the explicit symmetry breaking is significant, because the statistically important Φ configurations do not have corresponding Φ' which can compensate for the change in action due to the Z_2 rotation of the gauge fields.

Our results for Z_2 symmetry for higher N_τ simulations do not agree with the previous perturbative, mean field and non-perturbative studies which are only for small N_τ s. In these studies, the Z_N symmetry is realized only for $\kappa = 0$, i.e infinite Higgs mass. In contrast, our results suggest that the Z_N symmetry is realized in the whole of Higgs symmetric phase, at least for small λ. Note that adding more Higgs fields to our theory

will not change the status of the Z_N symmetry. For small Higgs quartic couplings, the Z_N symmetry will still be realized in the Higgs symmetric phase, when all the fields melt. The perturbative calculations, on the other hand, suggest that putting more Higgs field increases the explicit symmetry breaking. For $N = 2$, in the massless case, for 4 Higgs doublet fields the meta-stable state disappears. We believe that the discrepancy between our non-perturbative results and perturbative calculations is because, in the later only the zero mode of the Polyakov loop (or gauge fields) couple with the matter fields. Going beyond the Gaussian fluctuations, in which the higher modes of the Polyakov loop will couple with matter fields, likely the 1−loop results will be modified. In previous Monte Carlo studies the value of N_τ used were $2, 4$. These values were too small to observe Z_N symmetry restoration observed in our study. Moreover, these studies looked at only the average of the Polyakov loop. Even for $N_\tau = 4$ previous studies observed critical like behavior which was explained as due to the pure gauge transition at $\kappa = 0$. Later in our study we found this critical behaviour was not consistent with finite size scaling.

The Higgs symmetric phase is realized only at high temperatures. For such conditions, in case the gauge fields happen to be in the deconfined phase, then there will be Z_N domain walls in the medium. For $N \geq 3$ these domain walls will be connected to strings [74–76]. The realization of the Z_N symmetry makes these domain walls long lived, possibly making them relevant for the evolution of the system. If there is no Z_N symmetry these domain walls tend to decay quickly [77]. It will be interesting to see if these domain walls play any role above the electroweak symmetry breaking. Realization of Z_N symmetry in the large density regime of QCD, where there is a possibility of a phase of diquarks (in the fundamental representation) interacting with the gauge fields, will lead to domain walls.

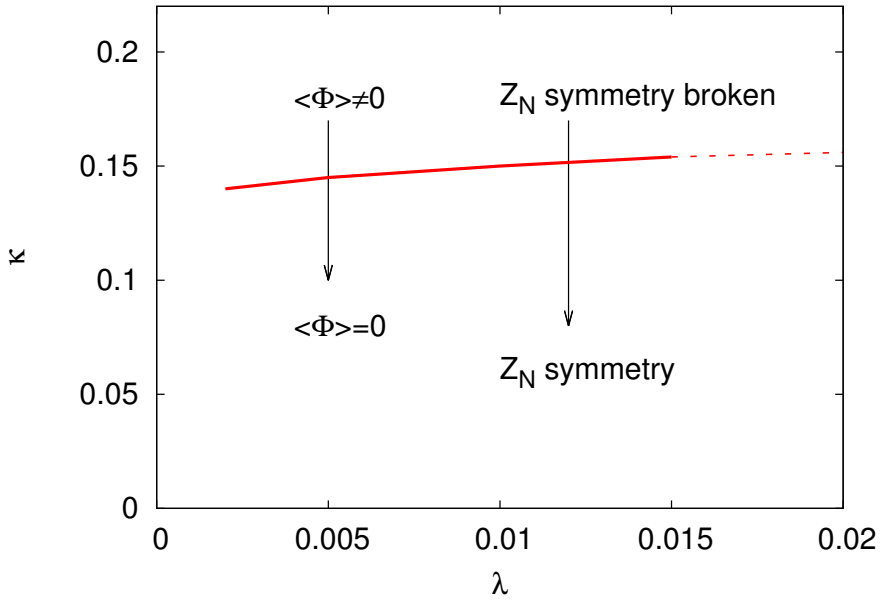

Figure 8.1. Higgs phase diagram showing Higgs condensate acts like an external symmetry breaking field.

8.0.1 Future plans

We observe that decrease in κ leads to decrease in the strength of the explicit symmetry breaking. At the same time with decrease in κ, it is expected that the condensate decreases. This suggests that the Higgs condensate plays the role of the Z_N symmetry breaking field as in Fig. 8.1. However, more work is needed to relate the Higgs condensate to the effective field for the Z_N symmetry. In this work, we have used the Higgs transition point to infer the values of the Higgs condensate. Since the Higgs field is not gauge invariant the Higgs condensate is not well defined [78]. However, the gauge fixed Higgs condensate is found to behave like an order parameter for the Higgs transition [67]. We plan to calculate the Higgs condensate by appropriately choosing a gauge which will make the Higgs condensate well defined and find out the connection between the Higgs condensate and the explicit symmetry field for Z_N.

Our results clearly show that the interaction between the gauge and Higgs field depends on N_τ, at least the aspects which control the Z_N symmetry and the CD transition.

We have done extensive studies for $N = 2$. We plan to carry out similar detail study for $N \geq 3$ in future. We believe that the large cut-off effects on the Z_N symmetry in Higgs theory seen here in SU(N)+Higgs theory will likely be present also in QCD. So at present we are planning to extend the studies to QCD, also to theories where fermions and bosons both present as in the Standard model.

Bibliography

[1] B. Svetitsky, *Symmetry Aspects of Finite Temperature Confinement Transitions*, *Phys. Rept.* **132** (1986) 1–53.

[2] B. Svetitsky and L. G. Yaffe, *Critical Behavior at Finite Temperature Confinement Transitions*, *Nucl. Phys.* **B210** (1982) 423–447.

[3] J. Kuti, J. Polonyi, and K. Szlachanyi, *Monte Carlo Study of SU(2) Gauge Theory at Finite Temperature*, *Phys. Lett.* **98B** (1981) 199.

[4] L. D. McLerran and B. Svetitsky, *A Monte Carlo Study of SU(2) Yang-Mills Theory at Finite Temperature*, *Phys. Lett.* **98B** (1981) 195.

[5] F. Karsch, C. Schmidt, and S. Stickan, *Common features of deconfining and chiral critical points in QCD and the three state Potts model in an external field*, *Comput. Phys. Commun.* **147** (2002) 451–454, arXiv:hep-lat/0111059 [hep-lat].

[6] N. Weiss, *The Wilson Line in Finite Temperature Gauge Theories*, *Phys. Rev.* **D25** (1982) 2667.

[7] V. M. Belyaev, I. I. Kogan, G. W. Semenoff, and N. Weiss, *Z(N) domains in gauge theories with fermions at high temperature*, *Phys. Lett.* **B277** (1992) 331–336.

[8] F. Karsch, E. Laermann, A. Peikert, C. Schmidt, and S. Stickan, *Flavor and quark mass dependence of QCD thermodynamics*, *Nucl. Phys. Proc. Suppl.* **94** (2001) 411–414, arXiv:hep-lat/0010040 [hep-lat]. [,411(2000)].

[9] F. Karsch, E. Laermann, and C. Schmidt, *The Chiral critical point in three-flavor QCD*, *Phys. Lett.* **B520** (2001) 41–49, arXiv:hep-lat/0107020 [hep-lat].

[10] M. Biswal, S. Digal, and P. S. Saumia, *Dynamical Restoration of Z_N Symmetry in $SU(N)$ + Higgs Theories*, *Nucl. Phys.* **B910** (2016) 30–39, arXiv:1511.08295 [hep-lat].

[11] M. Creutz, *Monte Carlo Study of Quantized SU(2) Gauge Theory*, *Phys. Rev.* **D21** (1980) 2308–2315.

[12] N. Cabibbo and E. Marinari, *A New Method for Updating SU(N) Matrices in Computer Simulations of Gauge Theories*, *Phys. Lett.* **119B** (1982) 387–390.

[13] B. Bunk, *Monte Carlo methods and results for the electro-weak phase transition*, *Nucl. Phys. Proc. Suppl.* **42** (1995) 566–568.

[14] C. Whitmer, *Over-relaxation methods for Monte Carlo simulations of quadratic and multiquadratic actions*, *Phys. Rev.* **D29** (1984) 306–311.

[15] F. Green and F. Karsch, *Mean Field Analysis of SU(N) Deconfining Transitions in the Presence of Dynamical Quarks*, *Nucl. Phys.* **B238** (1984) 297–306.

[16] M. Biswal, M. Deka, S. Digal, and P. S. Saumia, *Confinement-deconfinement transition in $SU(2)$ Higgs theory*, *Phys. Rev.* **D96** no. 1, (2017) 014503, arXiv:1610.08265 [hep-lat].

[17] R. Hagedorn, *Statistical thermodynamics of strong interactions at high-energies*, *Nuovo Cim. Suppl.* **3** (1965) 147–186.

[18] S. Sarkar, H. Satz, and B. Sinha, *The physics of the quark-gluon plasma*, *Lect. Notes Phys.* **785** (2010) pp.1–369.

[19] H. Satz, *The Quark-Gluon Plasma: A Short Introduction*, *Nucl. Phys.* **A862-863** (2011) 4–12, arXiv:1101.3937 [hep-ph].

[20] H. Bohr and H. B. Nielsen, *Hadron Production from a Boiling Quark Soup*, *Nucl. Phys.* **B128** (1977) 275–293.

[21] F. Karsch, *Lattice QCD at high temperature and density*, *Lect. Notes Phys.* **583** (2002) 209–249, arXiv:hep-lat/0106019 [hep-lat].

[22] A. Nakamura, *Quarks and Gluons at Finite Temperature and Density*, *Phys. Lett.* **149B** (1984) 391.

[23] U. M. Heller and F. Karsch, *Finite Temperature SU(2) Lattice Gauge Theory With Dynamical Fermions*, *Nucl. Phys.* **B258** (1985) 29–45.

[24] U. M. Heller, *Deconfinement in SU(2) Gauge Theory With Fermions of Intermediate Mass*, *Phys. Lett.* **163B** (1985) 203–206.

[25] J. B. Kogut, J. Polonyi, H. W. Wyld, and D. K. Sinclair, *Thermodynamics of SU(2) Gauge Theory With Dynamical Light Fermions*, *Phys. Rev.* **D31** (1985) 3307.

[26] J. B. Kogut, J. Polonyi, H. W. Wyld, and D. K. Sinclair, *On the Thermodynamics and Scaling Behavior of SU(2) Gauge Theory With Fermion Feedback*, *Nucl. Phys.* **B265** (1986) 293–302.

[27] O. Philipsen, *The QCD equation of state from the lattice* , *Prog. Part. Nucl. Phys.* **70** (2013) 55–107, arXiv:hep-lat/1207.5999 [hep-lat].

[28] R. Gupta, *Equation of State from Lattice QCD Calculations* , *Nucl. Phys. A.* **862-863** (2011) 111–117, arXiv:hep-lat/1104.0267 [hep-lat].

[29] S. Borsanyi, G. Endrodi, Z. Fodor, A. Jakovac, S. D. Katz, S. Krieg, C. Ratti, and K. K. Szabo, *The QCD equation of state with dynamical quarks* , *JHEP* **1011** (2010) 1–32, arXiv:hep-lat/1007.2580 [hep-lat].

[30] A. Bazavov and *et al.* [HotQCD Collaboration], *Equation of state in (2+1)-flavor QCD* , *Phys. Rev. D* **90** (2014) 094503(1–25), arXiv:hep-lat/1407.6387 [hep-lat].

[31] S. Sharma, *QCD Thermodynamics on the Lattice* , *Adv. High Energy Phys.* **2013** (2013) 1–26, arXiv:hep-lat/1403.2102 [hep-lat].

[32] T. Celik, J. Engels, and H. Satz, *The Order of the Deconfinement Transition in SU(3) Yang-Mills Theory*, *Phys. Lett.* **125B** (1983) 411–414.

[33] J. B. Kogut, M. Stone, H. W. Wyld, W. R. Gibbs, J. Shigemitsu, S. H. Shenker, and D. K. Sinclair, *Deconfinement and Chiral Symmetry Restoration at Finite Temperatures in SU(2) and SU(3) Gauge Theories*, *Phys. Rev. Lett.* **50** (1983) 393.

[34] L. G. Yaffe and B. Svetitsky, *First Order Phase Transition in the SU(3) Gauge Theory at Finite Temperature*, *Phys. Rev.* **D26** (1982) 963.

[35] T. Banks and A. Ukawa, *Deconfining and Chiral Phase Transitions in Quantum Chromodynamics at Finite Temperature*, *Nucl. Phys.* **B225** (1983) 145–155.

[36] J. Polonyi and K. Szlachanyi, *Phase Transition from Strong Coupling Expansion*, *Phys. Lett.* **110B** (1982) 395–398.

[37] N. Weiss, *The Effective Potential for the Order Parameter of Gauge Theories at Finite Temperature*, *Phys. Rev.* **D24** (1981) 475.

[38] P. H. Damgaard and U. M. Heller, *The Fundamental SU(2) Higgs Model at Finite Temperature*, *Nucl. Phys.* **B294** (1987) 253.

[39] M. Deka, S. Digal, and A. P. Mishra, *Meta-stable States in Quark-Gluon Plasma*, *Phys. Rev.* **D85** (2012) 114505, arXiv:1009.0739 [hep-lat].

[40] S. Digal, E. Laermann, and H. Satz, *Interplay between chiral transition and deconfinement*, *Nucl. Phys.* **A702** (2002) 159–163.

[41] R. D. Pisarski and F. Wilczek, *Remarks on the Chiral Phase Transition in Chromodynamics*, *Phys. Rev.* **D29** (1984) 338–341.

[42] P. H. Damgaard and U. M. Heller, *Deconfinement in the Fundamental SU(2) Higgs Model*, *Phys. Lett.* **B171** (1986) 442–448.

[43] E. H. Fradkin and S. H. Shenker, *Phase Diagrams of Lattice Gauge Theories with Higgs Fields*, *Phys. Rev.* **D19** (1979) 3682–3697.

[44] F. Zantow, O. Kaczmarek, F. Karsch, and P. Petreczky, *A New order parameter with renormalized Polyakov loops* , *C01-08-26.5 Proceedings* (2001) 1–2, arXiv:hep-lat/0110106 [hep-lat].

[45] *M. E. Peskin and D. V. Schroeder, in An Introduction to Quantum Field Theory (book)*, .

[46] D. J. Gross, R. D. Pisarski, and L. G. Yaffe, *QCD and Instantons at Finite Temperature*, *Rev. Mod. Phys.* **53** (1981) 43.

[47] L. D. McLerran and B. Svetitsky, *Quark Liberation at High Temperature: A Monte Carlo Study of SU(2) Gauge Theory*, *Phys. Rev.* **D24** (1981) 450.

[48] A. M. Polyakov, *Thermal Properties of Gauge Fields and Quark Liberation*, *Phys. Lett.* **72B** (1978) 477–480.

[49] L. Susskind, *Lattice Models of Quark Confinement at High Temperature*, *Phys. Rev.* **D20** (1979) 2610–2618.

[50] G. 't Hooft, *On the Phase Transition Towards Permanent Quark Confinement*, *Nucl. Phys.* **B138** (1978) 1–25.

[51] G. 't Hooft, *A Property of Electric and Magnetic Flux in Nonabelian Gauge Theories*, *Nucl. Phys.* **B153** (1979) 141–160.

[52] T. Bhattacharya, A. Gocksch, C. Korthals Altes, and R. D. Pisarski, *Interface tension in an SU(N) gauge theory at high temperature*, *Phys. Rev. Lett.* **66** (1991) 998–1000.

[53] R. Jackiw, *Functional evaluation of the effective potential*, *Phys. Rev.* **D9** (1974) 1686.

[54] *Eugene P. Wigner, in Group Theory, Academic Press Inc. New York, 1959 (book)* , .

[55] *Joseph I. Kapusta and Charles Gale, in Finite-Temperature Field Theory: Principles and Applications (book)*, .

[56] F. Green, *Strong Coupling Expansions for the String Tension at Finite Temperature*, *Nucl. Phys.* **B215** (1983) 83–108.

[57] F. Green and S. Samuel, *Chiral Models: Their Implication for Gauge Theories and Large N*, *Nucl. Phys.* **B190** (1981) 113–150.

[58] J. B. Kogut, M. Snow, and M. Stone, *Mean Field and Monte Carlo Studies of SU(N) Chiral Models in Three-dimensions*, *Nucl. Phys.* **B200** (1982) 211–231.

[59] J. Carlsson, *Integrals over SU(N)*, arXiv:0802.3409 [hep-lat].

[60] K. Kajantie, M. Laine, K. Rummukainen, and M. E. Shaposhnikov, *The Electroweak phase transition: A Nonperturbative analysis*, *Nucl. Phys.* **B466** (1996) 189–258, arXiv:hep-lat/9510020 [hep-lat].

[61] A. D. Kennedy and B. J. Pendleton, *Improved Heat Bath Method for Monte Carlo Calculations in Lattice Gauge Theories*, *Phys. Lett.* **156B** (1985) 393–399.

[62] W. K. Hastings, *Monte Carlo Sampling Methods Using Markov Chains and Their Applications*, *Biometrika* **57** (1970) 97–109.

[63] *The MIMD Lattice Computation (MILC) Collaboration*, http://www.physics.utah.edu/ detar/milc/.

[64] J. Jersak, C. B. Lang, T. Neuhaus, and G. Vones, *Properties of Phase Transitions of the Lattice SU(2) Higgs Model*, *Phys. Rev.* **D32** (1985) 2761.

[65] H. G. Evertz, J. Jersak, and K. Kanaya, *FINITE TEMPERATURE SU(2) HIGGS MODEL ON A LATTICE*, *Nucl. Phys.* **B285** (1987) 229–252.

[66] P. H. Damgaard and U. M. Heller, *Search for Symmetry Restoration in the Fundamental SU(2) Higgs Model*, *Nucl. Phys.* **B304** (1988) 63–76.

[67] P. H. Damgaard and U. M. Heller, *Higgs and Confinement Phases in the Fundamental SU(2) Higgs Model: Mean Field Analysis*, *Phys. Lett.* **164B** (1985) 121–126.

[68] G. Boyd, J. Engels, F. Karsch, E. Laermann, C. Legeland, M. Lutgemeier, and B. Petersson, *Thermodynamics of SU(3) lattice gauge theory*, *Nucl. Phys.* **B469** (1996) 419–444, arXiv:hep-lat/9602007 [hep-lat].

[69] G. Boyd, J. Engels, F. Karsch, E. Laermann, C. Legeland, M. Lutgemeier, and B. Petersson, *Equation of state for the SU(3) gauge theory*, *Phys. Rev. Lett.* **75** (1995) 4169–4172, arXiv:hep-lat/9506025 [hep-lat].

[70] T. Munehisa and Y. Munehisa, *Monte Carlo Study of an SU(2) Lattice Gauge Higgs Theory*, *Z. Phys.* **C32** (1986) 531.

[71] K. Binder, *Finite size scaling analysis of Ising model block distribution functions*, *Z. Phys.* **B43** (1981) 119–140.

[72] K. Kanaya and S. Kaya, *Critical exponents of a three dimensional O(4) spin model*, *Phys. Rev.* **D51** (1995) 2404–2410, arXiv:hep-lat/9409001 [hep-lat].

[73] J. Fingberg, U. M. Heller, and F. Karsch, *Scaling and asymptotic scaling in the SU(2) gauge theory*, *Nucl. Phys.* **B392** (1993) 493–517, arXiv:hep-lat/9208012 [hep-lat].

[74] A. P. Balachandran and S. Digal, *Topological string defect formation during the chiral phase transition*, *Int. J. Mod. Phys.* **A17** (2002) 1149–1158, arXiv:hep-ph/0108086 [hep-ph].

[75] U. S. Gupta, R. K. Mohapatra, A. M. Srivastava, and V. K. Tiwari, *Simulation of Z(3) walls and string production via bubble nucleation in a quark-hadron transition*, *Phys. Rev.* **D82** (2010) 074020, arXiv:1007.5001 [hep-ph].

[76] U. S. Gupta, R. K. Mohapatra, A. M. Srivastava, and V. K. Tiwari, *Effects of Quarks on the Formation and Evolution of Z(3) Walls and Strings in Relativistic Heavy-Ion Collisions*, *Phys. Rev.* **D86** (2012) 125016, arXiv:1111.5402 [hep-ph].

[77] J. Ignatius, K. Kajantie, and K. Rummukainen, *Cosmological QCD Z(3) phase transition in the 10-TeV temperature range?*, *Phys. Rev. Lett.* **68** (1992) 737–740.

[78] S. Elitzur, *Impossibility of Spontaneously Breaking Local Symmetries*, *Phys. Rev.* **D12** (1975) 3978–3982.